SAICAR acts as a master metabolite in cancer cell growth, survival, and proliferation

by
Kirstie Elizabeth Keller

A dissertation submitted to Johns Hopkins University in conformity with the requirements for the degree of Doctor of Philosophy

Baltimore, Maryland
June 2014

ABSTRACT

Cancer cells must reprogram their metabolic networks to adapt to stress conditions, which are commonly found in a tumor microenvironment. To accomplish this, cancer cells alter expression and regulation of many target proteins. Among these, the glycolytic enzyme pyruvate kinase M2 (PKM2) has been implicated as essential for cancer cell growth and survival in stress conditions. As with other pyruvate kinases, PKM2 catalyzes the final step of glycolysis, dephosphorylating phosphoenol pyruvate (PEP) to generate pyruvate and ATP. PKM2 is differentially expressed in highly proliferating tissues including cancer cells, and has intrinsically lower activity than other pyruvate kinases. However, the role of PKM2 and its function in cancer cells remains poorly understood.

In this study, we have identified a novel protein-metabolite interaction between PKM2 and the cellular metabolite succinyl-aminoimidazole carboxamide-ribosyl-5-phosphate (SAICAR) that promotes cancer cell growth. We found that SAICAR, a de novo purine nucleotide biosynthesis intermediate, accumulates in an oscillatory manner in glucose deprived cancer cells, but not in normal cells. SAICAR activates PKM2 both in vitro and in vivo, and induces metabolic reprogramming by augmenting the Warburg effect. Additionally, accumulation of SAICAR promotes long-term cancer cell survival in glucose-limited conditions, in a PKM2-dependent manner. The activation of PKM2 by

SAICAR demonstrates that cancer cells coordinate a delicate balance between metabolic pathways to optimize their survival in stress conditions.

Recent literature has shown that PKM2 is capable of acting as a protein kinase, and phosphorylation of its targets promotes long-term cellular adaptation. However, the mechanism and extent of this novel function is not fully understood. In this study, we also identified SAICAR as an activator of PKM2 protein kinase function. SAICAR binding renders PKM2 an efficient protein kinase both in vitro and in vivo. Additionally, we identified that PKM2-SAICAR phosphorylates over 100 cellular proteins, many of which are involved in cell proliferation and survival. Of these, we found that PKM2-SAICAR phosphorylates and activates Erk1/2, forming a positive feedback loop that is necessary for long term proliferative signaling.

Taken together, our study demonstrates that cancer cells utilize the PKM2-SAICAR interaction to couple metabolic status with long-term proliferation and survival.

Readers:

Advisor: Young-Sam Lee, Ph.D

Second Reader: Beverly Wendland, Ph.D

ACKNOWLEGDMENTS

Throughout my academic career, I have had many wonderful people provide me with generous help and support.

First, I would like to thank my thesis advisor, Dr. Young-Sam Lee. His guidance and expertise has allowed me to pursue the many different avenues brought forth by my research project. His willingness to utilize any technique and his rigorous approach to science was inspiring as a young scientist. He always asked me to think harder and reach higher.

Next, I would like to thank my thesis committee members: Beverly Wendland, Anne Le, and Samer Hattar. I appreciate their advice on both the direction of my project and on my future career. Additionally, Beverly has provided me with an incredible amount of support both personally and professionally, and I am very lucky to have her as a mentor. I would also like to thank the past and present members of the Lee lab: Mary Thomas, Sabrina Schatzman, Tiffany Coupet, Zainab Doctor, Zach Dwyer, Candace Hu, as well as the countless wonderful rotation students. Mary and Sabrina were not just fellow lab members; they were also great friends.

Johns Hopkins and the CMDB program have provided me with an incredible learning environment and the collaborative nature of everyone in the department has been wonderful. Although there are many people in the department that merit my thanks, Joan Miller is beyond deserving. She is wonderful both inside and out, and she truly holds this department together. I

also need to thank the members of the Bio East wing. It has been incredibly fun to have so many great scientists in the same place and to enjoy these friendships during my time here. I especially need to thank Bob Johnston, for his wonderful advice, help, and humor. Also, I want to give a big thanks to my classmates, who are all wonderful scientists, people, and friends.

I also would like to thank the amazing friends I have made during my years at Johns Hopkins. My friends have commiserated with me during my failures, celebrated my successes, and provided me with so much support. Finally, I would like to express my deepest gratitude to my family, for being there for me through everything. I cannot thank them enough for being my support system throughout my life. Without them, I would not be standing here today.

TABLE OF CONTENTS

INDEX OF FIGURES AND TABLES

CHAPTER 1

Introduction

Cancer Cell Reprogramming

Metabolic reprogramming occurs in most cancer cells, regardless of origin or type (1-4, 9). Specifically, cancer cells uptake more glucose than normal cells and metabolize glucose through oxygen-independent lactate fermentation, also known as aerobic glycolysis. (6). This process is deemed the Warburg effect and has been shown to be necessary for the growth, proliferation and survival of tumors (1-4, 9). Surprisingly, most cancer cells rely upon aerobic glycolysis as the method of energy production, which produces much less energy than oxidative phosphorylation per glucose molecule consumed (3, 9, 13). It has been suggested that aerobic glycolysis leads to an increase in the production of anabolic products, such as nucleotides, fatty acids, and amino acids, and generates lactate and protons. (3, 9). These anabolic products can be utilized for the production of vital cellular components such as DNA, proteins, and lipids, which may give cancer cells a competitive advantage (3). However, cells need sufficient amounts of energy for growth and proliferation using these cellular building blocks. When cancer cells are in nutrient-rich conditions, they can compensate for an energy deficit by uptaking more glucose (15, 16). However, as a tumor progresses, cancer cells transition into both nutrient-limited and oxygen-limited conditions. To proliferate and survive, cancer cells must balance energy production and anabolic processes. Currently, the molecular mechanism for the metabolic reprogramming of cancer cells in not fully understood and its

contribution to cancer cell growth and survival at the molecular level remains unclear.

Pyruvate Kinase M2 is expressed in cancer

Several proteins have been implicated as important for metabolic reprogramming in cancer and are necessary for the Warburg effect, including pyruvate kinase muscle form 2 (PKM2) (10). PKM2 is one of four pyruvate kinases (PKM1, PKL, PKR) found in mammals, which all catalyze the final step of glycolysis from phosphoenolpyruvate (PEP) to pyruvate, while generating ATP from ADP (Figure 1-1A) (7). It is believed that cells express a specific isoform of pyruvate kinase dependent on the metabolic needs of the tissue. PKM2 is expressed in some differentiated tissues, such as the lung and pancreatic islets, as well as cells with high rates of nucleic acid synthesis including highly proliferating normal cells, fetal cells, and malignant cancer cells (10). The other isoforms, PKM1, PKR, and PKL, are expressed solely in normal somatic tissues. Specifically, PKR is expressed in red blood cells, PKL is the predominant form in the liver, and PKM1 is expressed in most adult tissues, including the brain and muscle.

A single gene encodes PKM1 and PKM2 (PKM), and the same is true with PKL and PKR (PKLR). The PKM gene consists of 12 exons and 11 introns (Figure 1-1B). To produce each PKM isoform, an hnRNP-dependent splicing event occurs, choosing either exon 9 (PKM1) or exon 10 (PKM2) to be expressed

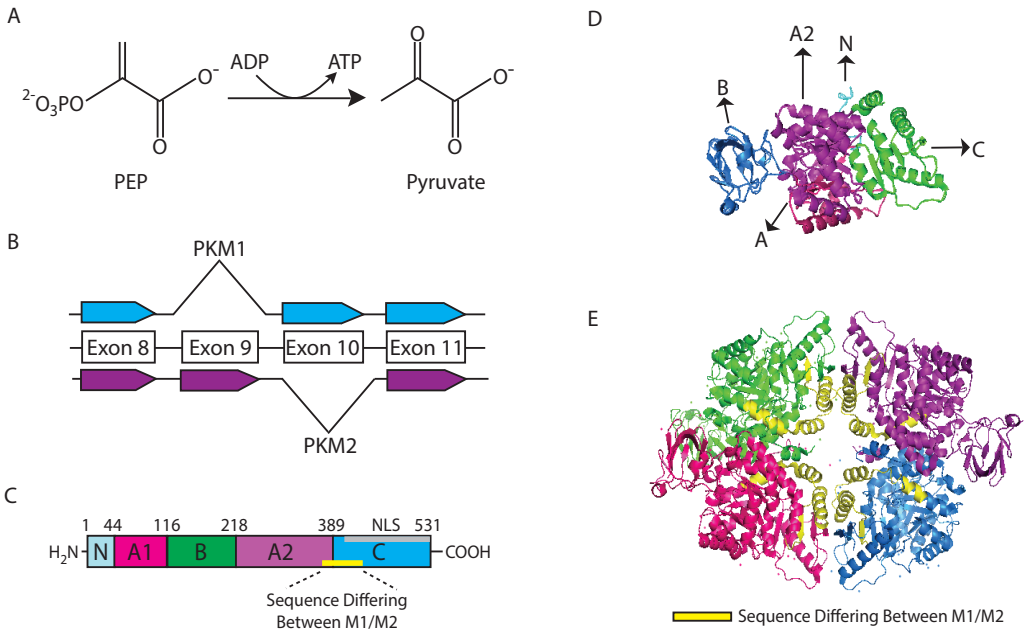

Figure 1-1. PKM2 is a typical pyruvate kinase. A) Pyruvate kinases catalyze the reaction from phosphonel pyruvate (PEP) to pyruvate and ADP to ATP. B) Schematic representation of mRNA transcript after splicing of PKM1 and PKM2. PKM1 contain exons 1-8, 10, and 11. PKM2 contains exons 1-9 and 11. C) Diagram representing the linear protein structure of PKM1/2. PKM1/2 contains several protein domains, and differ between aa 378-434 (depicted in yellow). D) Crystal structure of one subunit of PKM2. Structure is color matched to protein domain diagram (PBD 4FXJ). E) Structure of PKM2 homotetramer. Sequence differing between PKM1 and PKM2 is highlighted in yellow; the four subunits are labeled using different colors (PBD 4FXJ).

differentially (Figure 1B). Despite the altered exon choice, PKM1 and PKM2 differ at the protein level by only 23 amino acids at their carboxyl terminus out of 531 total residues and are 95% identical (Figure 1C). Structurally, PKM1 and PKM2 exist in a homotetramer, as a dimer of dimers, and theoretically can transition between homodimer and homotetramer. Both PKM1 and PKM2 consist of several domains on each of the four subunits: A, B, A2, and C (Figure 1-1C-D). The cleft between the A and B domain forms the active site (Figure 1-1D-E). The A domain binds with another PK subunit to form a homodimer (aa 378-434; figure 1-1C-E). The tetramer is then form by contacts between the C domains. Interestingly, crystallographic studies show that most of the residue differences between PKM2 and PKM1 lie within the dimer-dimer interface of the PKM1/2 homotetramer (Figure 1-1D, 21). Additionally, the C domain houses a putative nuclear localization sequence (NLS), which is buried upon tetramerization (Figure 1-1C, 21).

PKM2 expression is known to be upregulated in a number of cancers. EGFR activation was shown to trigger a signaling pathway that leads to PKM2 overexpression, through PLCg1-dependent PKCe ubiquitinylation and NF-kb activation. NF-kb interacts with HIF1a and together, they bind together to the PKM promoter and then lead to increased transcription. The increased expression of PKM2 correlated with increased glucose consumption, glycolytic flux, and lactate production (43). The data linking PKM2 expression with cancer

cell proliferative signaling and metabolic flux implicates PKM2 as important for both the Warburg effect and tumorigenesis (43).

PKM2 has distinct biochemical properties

Although PKM1 and PKM2 are highly similar in sequence and structure, these two proteins have distinct properties. Biochemically, PKM2 is intrinsically much less active than its splice variant PKM1 (Figure 1-2A). PKM1 has a 100-fold lower Michaelis-Menten constant (K_m) for its substrate PEP when compared to PKM2 (Figure 1-2A, 10 uM and 1 mM for M1 and M2, respectively) and the rate of turnover (k_{cat}) is approximately four times higher than that of PKM2 (7, 26). Additionally, the quaternary structure of PKM2 is much more dynamic than that of PKM1 or the other pyruvate kinases PKL and PKR. As previously mentioned, pyruvate kinases exist as primarily as homotetramers; this form is considered to be an active pyruvate kinase. Unlike PKM1 and other pyruvate kinases, PKM2 transitions between a homodimer and homotetramer in vitro and *in vivo* (Figure 1-2C, 27, 28). The homodimeric form is often found in cancer cells, and its prevalence often correlates with the progression of cancer from benign to malignant (28, 29).

In addition to biochemical and quaternary structure differences, PKM2 activity is regulated by cellular metabolites and post-translational modifications (25, 30). The upstream glycolytic intermediate fructose 1-6 bisphosphate (FBP) binds to PKM2 at lysine 433 and increases its affinity for the substrate PEP to

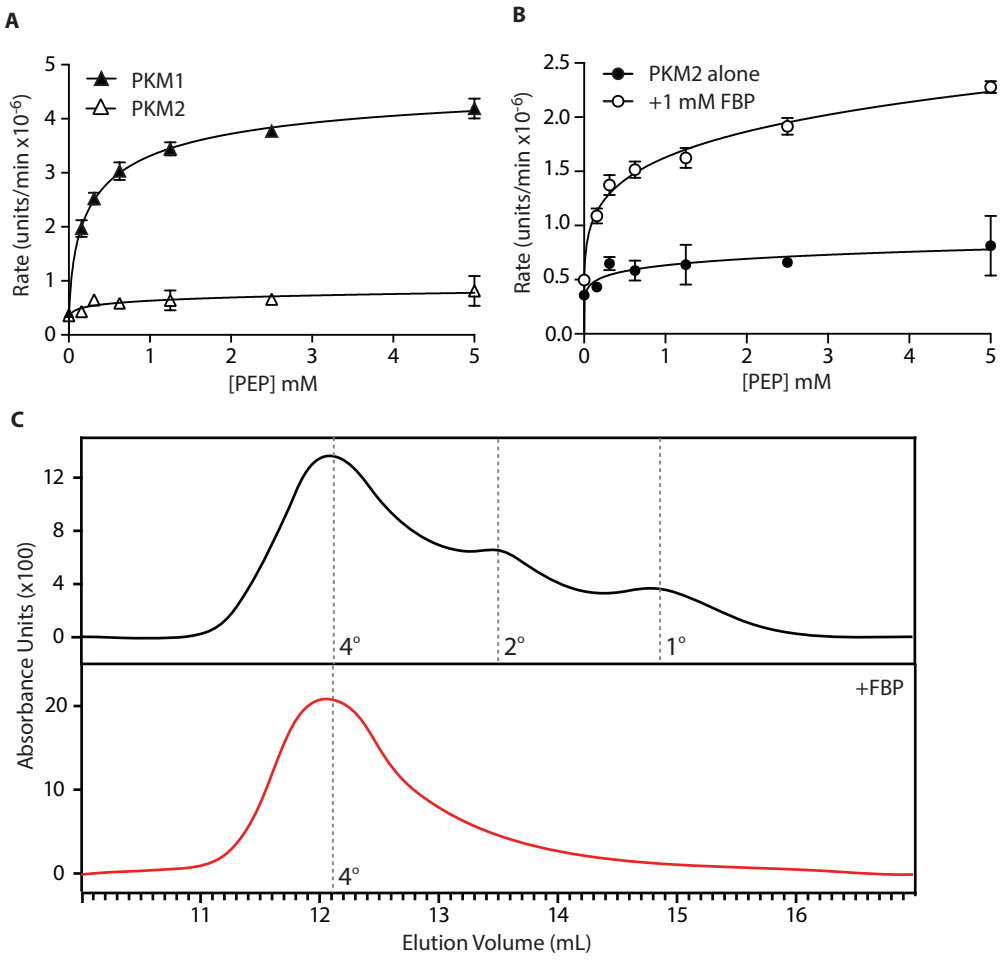

Figure 1-2. PKM2 activity and structure is allosterically regulated. A) PKM1 is more active than PKM2 intrinsically. In an LDH-NADH coupled activity assay, PKM1 has a lower K_m for substrate and higher k_{cat} than that of PKM2. B) FBP activates PKM2 approximately 2-fold. C) Gel filtration analysis of PKM2 quaternary structure. PKM2 exists as a tetramer, dimer, and monomer (labeled 4, 2, 1, respectively). Upon addition of the allosteric activator FBP, PKM2 quaternary structure shifts to a tetramer.

micromolar level, while prompting the quaternary structure change from homodimer to homotetramer (Figure 1-1B-C, 25). Activation of PKM2 and stabilization of the tetramer by FBP is reversible through phosphorylation at tyrosine 105 by oncogenic fibroblast growth factor receptor under hypoxic conditions (30). Serine was also found to be a natural ligand and allosteric activator of PKM2, binding to PKM2 at histidine 464 and lowering the Km for PEP by 2.3 fold (38). The activation of PKM2 by serine was found to operate in a rheostat manner, and allows cells to coordinate serine biosynthesis needed for cell proliferation and energy production by PKM2 (38). Furthermore, PKM2 is acetylated at lysine 305, which occurs only upon stimulation with high glucose. This acetylation event decreases PKM2 activity, promotes an interaction with HSC70, and leads to degradation of PKM2 by chaperone-mediated autophagy (44).

As PKM2 is thought to be a nearly inactive pyruvate kinase, many have suggested that cancer cells use the M2 isoform to divert more glycolytic intermediates to biosynthetic processes, such as the pentose phosphate pathway (PPP), to promote cell growth and proliferation (Figure 1-3). In normal cells, PKM1 is expressed and highly active, allowing flux to proceed through glycolysis into the TCA cycle and ultimately generate energy. Cancer cells however, express PKM2. The inactivity of PKM2 causes a bottleneck in glycolysis and feeds intermediates into the PPP, generating precursor molecules to produce

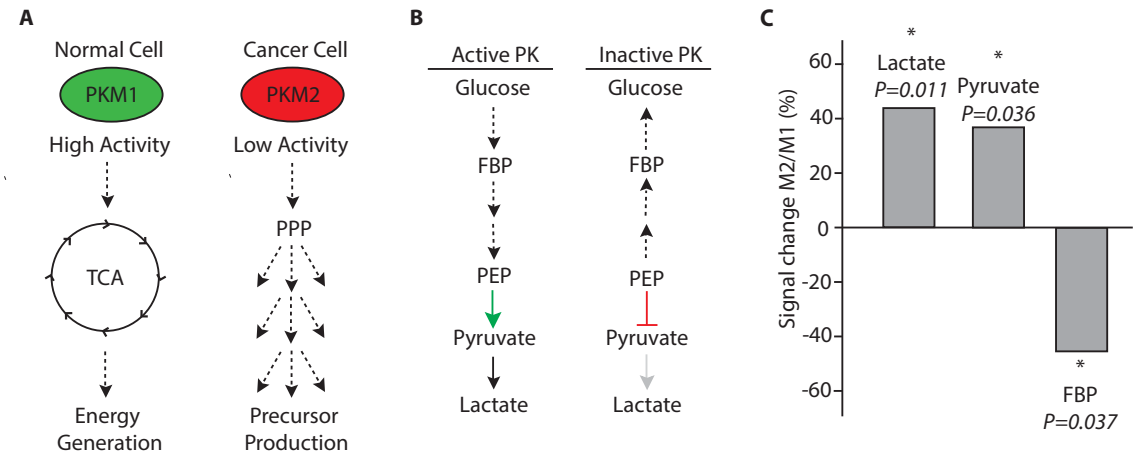

Figure 1-3. The role of PKM2 in cancer cells is unclear. A) Schematic diagram representing a common model in the field that PKM1 is highly active and promotes glycolytic flux, through the TCA cycle, and ultimately energy generation. PKM2 is inactive and promotes flux through the pentose phosphate pathway (PPP) to generate precursor molecules. B) Diagram representing the proposed flux in a scenario where pyruvate kinase activity is altered. C) Figure adapted from Christofk et al. 2008. Mass spectrometry signal ratio of lactate, pyruvate, and FBP production in cells expressing PKM2 or PKM1

proteins, fats, and nucleotides (Figure 1-3). Although this model can explain some aspects of PKM2 in cancer cell metabolism, several key aspects from available data have not been factored in. In the commonly proposed bottleneck model, upstream metabolites in the glycolytic pathway are expected to increase, while downstream intermediates, including pyruvate and lactate, would decrease. However, metabolites analyzed from H1299 cells expressing PKM2 showed an increased production of both pyruvate and lactate, in comparison to H1299 cells expressing PKM1 (Figure 1-3) (3). Additionally, upstream metabolites, including FBP, were decreased in these cells (Figure 1-3) (3). These data contradict the bottleneck model, suggesting that the role of PKM2 in cancer cells is still unclear. Furthermore, cells in nutrient limited conditions, such as a those found in a tumor microenvironment, would become rapidly energy depleted without an active pyruvate kinase, as a great deal of energy is required for the production of anabolic intermediates. Again, the bottleneck model is not supported by data.

In addition, the expectation of the model is that pyruvate kinase activity is directly correlative to cancer cell growth and proliferation. In contrast to this model, replacing PKM2 in cancer cells with any other pyruvate kinase isoform drastically reduces cancer cell survival in stress conditions (hypoxia (4) or glucose-depletion (8)) and suppresses tumorigenecity (4). Thus, pyruvate kinase activity and cancer cell growth are not simply inversely correlated. These findings suggest that unidentified subtle differences between the tumor-specific isoform PKM2 and its normal cell counterparts are essential for tumor growth and

survival in stress conditions (4). The molecular mechanism defining the role of PKM2 in tumor growth in stress conditions is still unclear.

PKM2 acts as a protein kinase

A new role for PKM2 in cancer cells has been identified that appears to be important for growth and proliferation (38-41). Surprisingly, PKM2 has been shown to act as a protein kinase in addition to its known function as a pyruvate kinase. Unlike other protein kinases, studies have shown that PKM2 uses PEP as the phosphate donor rather than the traditional use of ATP. ADP acts as a competitive inhibitor for protein substrate binding, suggesting that ADP and the protein substrates bind the same site (38). Additionally, the quaternary structure of PKM2 appears to play an important role in its activity as a protein kinase. As previously mentioned, PKM2 can exist as both a homodimer and a homotetramer. Gel filtration chromatography experiments suggest that the PKM2 dimer acts as a protein kinase, while the tetramer is an active pyruvate kinase (38). FBP, although an activator of pyruvate kinase activity, does not affect protein kinase activity substantially (38). Furthermore, the PKM2 mutant R399E exists primarily as a dimer and was found to be a very active protein kinase (38).

Several proteins have been identified as PKM2 substrates. Nearly a decade ago, it was suggested that PKM2 phosphorylates histone H1 at a lysine residue, but no functional consequences were identified and the low likelihood of phosphorylation at a lysine residue made the work controversial (41). A serine-

threonine phosphorylated PKM2 was found to phosphorylate prothymosin a, a protein involved in the immune response, but again no functional outputs were identified (42). In an indirect study, PKM2 was suggested to phosphorylate the catalytic histidine of phosphoglycerate mutase, as the authors found that PEP was the phosphate donor. However, PKM2 was never confirmed to be the protein kinase involved (43).

In more recent years, the targets of PKM2 have become more defined and the functional outputs were clearly identified. PKM2 phosphorylates the transcription factor stat3 at tyrosine 705 (Y705), thereby activating the transcription of MEK5 and potentially other genes regulated by STAT3 (38). The upregulation of MEK5 contributes to increased cell proliferation in cancer, presumably through ERK5 signaling (38). PKM2 has also been shown to bind to the phospho-tyrosine 333 (pY333) form of beta-catenin upon stimulation of epithelial growth factor receptor (EGFR) (40). The binding of PKM2 and beta-catenin is required to recruit both to the promoters of specific gene targets, and leads to increased expression of c-Myc, GLUT1, and LDHA (39). Although not proven, PKM2 protein kinase activity is suspected to be involved in the transcriptional activation of these genes (40).

Additionally, PKM2 has been shown to directly phosphorylate histone H3 at threonine 11 (pT11). Phosphorylation of histone H3 at T11 is necessary for the removal of the histone deacetylase HDAC3 from gene promoters, H3 acetylation at lysine 9 (H3K9), and the expression of both the cell cycle regulator

cyclin D1 and proliferation factor c-Myc (40). Thus, pT11 H3 directly promotes cancer cell growth and proliferation and this occurs through the action of PKM2 as a protein kinase (40).

PKM2 localization

Although PKM2 typically resides in the cytoplasm, some protein substrates, such as histone H3, exist solely in the nucleus. Recent findings have shown that upon activation of EGFR, PKM2 localizes the nucleus where it is able phosphorylate nuclear protein targets (Figure 1-4) (41). Additionally, only dimeric PKM2 was found in the nucleus, and has been shown to act as a robust protein kinase when used for *in vitro* studies (40). In support of this finding, the mutant R399E, which exists predominantly as a dimer, was found to be constitutively nuclear regardless of condition and acts as an effective protein kinase (40). To enter the nucleus, Erk1/2 binds directly to PKM2 at isoleucine 429 and leucine 431, and subsequently phosphorylates PKM2 serine 37 (Figure 1-4) (39). Phosphorylated S37 PKM2 binds to peptidyl-proline isomerase PIN1 and leads to cis-trans isomerization. The isomerization exposes a previously inaccessible NLS, which promotes binding to importin a5 and nuclear localization (Figure 4). Further support for this mechanism was found when a phosphorylation deficient mutant (PKM2 S37A) was unable to enter the nucleus and downstream targets were no longer activated. The phospho-mimic mutant PKM2 S37D mutant was constitutively nuclear and was able to bind and activate gene targets.

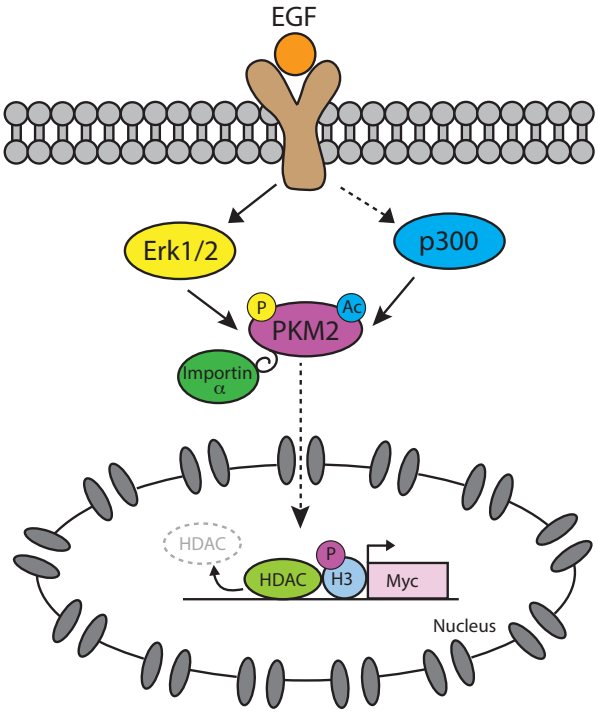

Figure 1-4. Schematic diagram illustrating the proposed entrance of PKM2 into the cell nucleus. Upon EGF binding to its cognate receptor, Erk1/2 becomes activated and phosphorylates PKM2. Additionally, through a separate pathway, p300 also is activated, and acetylates PKM2. Both modifications are necessary for PKM2 to enter the nucleus, through its interaction with importins. Upon nuclear entry, PKM2 can act as a protein kinase and phosphorylate histone H3, promoting release of an HDAC and expression of the oncogene Myc.

Upon EGF addition, Erk1/2 becomes activated and phosphorylates PKM2 at serine 37. Acetylase p300 also becomes activated and acetylates PKM2 at lysine 433. Both marks are proposed to recruit PIN1, which binds and initiates a cis-trans isomerization and exposure of the nuclear localization signal. The signal is recognized and PKM2 is transported into the nucleus with Importin alpha. PKM2, once inside the nucleus can act as a protein kinase and activate a number of protein targets; H3 phosphorylation is depicted in Figure 1-4. H3T11 phosphorylation leads to removal of the HDAC and subsequent expression of genes, such as Myc.

Another recent study revealed that PKM2 is able to enter the nucleus upon acetylation, as well as phosphorylation. The p300 acetyltransferase acetylates PKM2 at lysine 433, the residue responsible for the binding of allosteric activator FBP (Figure 1-4) (44). Acetylation promotes nuclear localization, presumably by interfering with FBP binding, which stabilizes the tetrameric form of PKM2. Conditions supporting cell growth, including cell cycle activation, EGF addition, and oncoprotein overexpression, enhanced acetylation of PKM2. Acetylation of PKM2 was also found to enhance the protein kinase activity of PKM2 in vitro, and an acetylation-mimic of PKM2 (K433Q) was found to act as protein kinase. Furthermore, acetylation of PKM2 is enriched in human breast cancers, providing more support that PKM2 nuclear localization and protein kinase activity is important for tumorigenesis (43).

PKM2 has an unclear role in tumorigenesis

PKM2 is overexpressed in a number of cancer cell types and tissues and has been thought to have a large role in tumorigenesis. Low PKM2 pyruvate kinase activity is thought to lead to increased anabolic products and cell proliferation. However, this bottleneck model is contradicted by many pieces of data, as outlined above. Additionally, PKM2 acts as a protein kinase and has been shown to activate transcription of downstream proliferative signaling genes. Recombinant PKM2 purified from *E. coli* was unable to phosphorylate protein targets in vitro, suggesting that there is another factor required for this activity that is hereto unknown. Recent data suggest that acetylation of PKM2 transforms PKM2 into a protein kinase in vitro, however little structural analysis was performed and the basis for this activity is unclear (44).

A controversy about the requirement of PKM2 for tumorigenesis has been persistent within the field. According to recent data, all tumor cells do not require PKM2. In fact, in the Brca1-loss driven mouse model, PKM2 deletion accelerated tumor formation, and leads to heterogeneous PKM1 expression (45). Additionally, the authors found that PKM2 expression is variable within human cancers and that those cancers with PKM2 possess point mutations in this gene (45). The authors conjecture that these data imply that inactive PKM2 is required for tumor growth and formation, while active pyruvate kinases are not necessary (45). Although the data certainly support this hypothesis, studies by numerous other groups produce some doubt that this finding may be context specific.

Regardless of the controversy, PKM2 and its regulation are far from being completely understood; much of the mystery is still waiting to be uncovered.

Thesis Overview

Despite the many findings describing PKM2 activity and its role in cancer cell metabolism, how cells circumvent the energy deficit associated with a deficient pyruvate kinase activity remains unknown. Additionally, the molecular mechanism behind PKM2 protein kinase activity is still poorly understood.

In the second chapter of this study, we show that a novel interaction exists between PKM2 and the de novo purine biosynthesis intermediate SAICAR. We found that SAICAR co-purifies with PKM2 in glucose depleted cancer cells and activates PKM2 isozyme-specifically both in vitro and in vivo. SAICAR accumulates in a physiologically relevant manner in glucose-depleted cancer cells, but does not accumulate in normal cells. Using cells with modified SAICAR metabolism, we found that cellular SAICAR concentration correlates with PKM2 activity, as well as with glucose uptake and lactate production, two components of the Warburg effect. Increased cellular SAICAR protect cells from cell death in glucose depleted cancer cells, and in a PKM2-dependent manner.

This chapter provides insight into the mechanism by which cancer cells coordinate metabolic pathways in response to external stimuli. Additionally, identifying the interaction between catabolic and anabolic pathways could elucidate the major differences in cancer and normal cell metabolism, which would prove valuable in creating therapeutics that specifically target cancer cells. Furthermore, the methodology described in this chapter can be used to identify

many other metabolite-protein interactions that are previously unrecognized in both normal cells and cancer cells (32-34).

In the third chapter of this study, we show that cellular SAICAR concentration increases upon EGFR activation. SAICAR induces the protein kinase activity of PKM2 both in vitro and in vivo, and promotes nuclear localization of PKM2. PKM2-SAICAR phosphorylates over 100 cellular proteins, many of which are involved in proliferative signaling pathways. Of these, we found that Erk1 is directly phosphorylated by PKM2-SAICAR in the activation loop at threonine 202. Phosphorylation of T202 leads to partial activation of Erk1. Phosphorylation of PKM2 by Erk1/2 rendered PKM2 hypersensitive to SAICAR, leading to a positive feedback loop between PKM2-SAICAR and MAPK signaling. Finally, we found that the mutual phosphorylation of PKM2 and Erk1/2 is necessary for sustained proliferative signaling.

This chapter identifies a molecular mechanism by which PKM2 becomes an active protein kinase, and emphasizes that the scope of PKM2's activity in cancer cells was not fully appreciated previously. Additionally, our findings show that cancer cells couple metabolic status with cell proliferation and growth signaling. Furthermore, this study offers new evidence that allosteric ligands are capable of altering protein function, rather than just activity, suggesting that there are potentially many other metabolite-protein interactions that are not yet known.

In chapter four of this study, we found that cellular SAICAR concentration increases upon addition of a number of growth factors (BDNF, GDNF, HGF, IGF,

TGF, VEGF), but not in conditions inducing differentiation or cell death (Retinoic Acid or TNF). We found that regulation of the protein level of the SAICAR synthetase PAICS is likely responsible for increased cellular SAICAR production. Cellular SAICAR level correlates with PAICS protein level, Erk1/2 phosphorylation, PKM2 nuclear localization, histone H3T11 phosphorylation, and cell proliferation. Furthermore, we found that growth factors that lead to cellular SAICAR increases also stabilize PAICS protein level, potentially through phosphorylation, but not through translation.

The appendices of this thesis provide results found in several preliminary studies. In the first study, we utilized a high throughput screen to find compounds that inhibit or activate the enzymatic activity of the SAICAR cleavage enzyme ADSL activity. However, upon further investigation, we found that some potential hits of the screen were likely due to non-specific interactions. The second study examines the relationship between SAICAR and GLUT1 localization. We found that GLUT1 localization differs in the presence versus the absence of cellular SAICAR. In the third appendix, we found evidence for a PKM2 stimulating factor of unknown identity. The factor was identified in yeast extracts and we attempted to purify the compound utilizing many biochemical techniques. Finally, we examined the effect of various ligands and mutations of the quaternary structure of PKM2. Among the mutants, we found that the R399V mutation was predominantly a dimer, similar to the published R399E mutant. This mutant is hypersensitive to SAICAR, implying that SAICAR may bind to the

dimer. Although SAICAR does not significantly affect the overall quaternary structure of PKM2, activation of PKM2 by SAICAR is specific to the dimer. The preliminary findings of this thesis provide the groundwork for future studies on the role of SAICAR and PKM2 in many cellular processes, as well as for the biochemical and biophysical bases for the activation of PKM2 by SAICAR.

REFERENCES

1. Koppenol WH, Bounds PL, Dang CV. Otto Warburg's contributions to current concepts of cancer metabolism. Nat Rev Cancer. 2011;11(5):325-37.

2. Hanahan D, Weinberg RA. Hallmarks of cancer: the next generation. Cell. 2011;144(5):646-74.

3. Vander Heiden MG, Cantley LC, Thompson CB. Understanding the Warburg effect: the metabolic requirements of cell proliferation. Science. 2009;324(5930):1029-33. PMCID: 2849637.

4. Cairns RA, Harris IS, Mak TW. Regulation of cancer cell metabolism. Nat Rev Cancer. 2011;11(2):85-95.

5. Macintyre AN, Rathmell JC. PKM2 and the Tricky Balance of Growth and Energy in Cancer. Mol Cell. 2011;42(6):713-4.

6. Lardinois D, Weder W, Hany TF, Kamel EM, Korom S, Seifert B, et al. Staging of non-small-cell lung cancer with integrated positron-emission tomography and computed tomography. N Engl J Med. 2003;348(25):2500-7.

7. Gambhir SS. Molecular imaging of cancer with positron emission tomography. Nat Rev Cancer. 2002;2(9):683-93.

8. Tennant DA, Duran RV, Gottlieb E. Targeting metabolic transformation for cancer therapy. Nat Rev Cancer. 2010;10(4):267-77.

9. Hsu PP, Sabatini DM. Cancer cell metabolism: Warburg and beyond. Cell. 2008;134(5):703-7.

10. Christofk HR, Vander Heiden MG, Harris MH, Ramanathan A, Gerszten RE, Wei R, et al. The M2 splice isoform of pyruvate kinase is important for cancer metabolism and tumour growth. Nature. 2008;452(7184):230-3.

11. Rolfes RJ. Regulation of purine nucleotide biosynthesis: in yeast and beyond. Biochem Soc Trans. 2006;34(Pt 5):786-90.

12. Zikanova M, Krijt J, Hartmannova H, Kmoch S. Preparation of 5-amino-4-imidazole-N-succinocarboxamide ribotide, 5-amino-4-imidazole-N-succinocarboxamide riboside and succinyladenosine, compounds usable in diagnosis and research of adenylosuccinate lyase deficiency. J Inherit Metab Dis. 2005;28(4):493-9.

13. Salway JG. Metabolism at a glance. 3rd Edition ed. Malden, MA: Blackwell Publishing, Inc.; 2004.

14. Mazurek S, Eigenbrodt E. The tumor metabolome. Anticancer Res. 2003;23(2A):1149-54.

15. Pedersen PL. Warburg, me and Hexokinase 2: Multiple discoveries of key molecular events underlying one of cancers' most common phenotypes, the "Warburg Effect", i.e., elevated glycolysis in the presence of oxygen. J Bioenerg Biomembr. 2007;39(3):211-22.

16. Kim JW, Dang CV. Cancer's molecular sweet tooth and the Warburg effect. Cancer Res. 2006;66(18):8927-30.

17. Gupta V, Bamezai RN. Human pyruvate kinase M2: a multifunctional protein. Protein Sci. 2010;19(11):2031-44. PMCID: 3005776.

18. Chen M, Zhang J, Manley JL. Turning on a fuel switch of cancer: hnRNP proteins regulate alternative splicing of pyruvate kinase mRNA. Cancer Res. 2010;70(22):8977-80. PMCID: 2982937.

19. Clower CV, Chatterjee D, Wang Z, Cantley LC, Vander Heiden MG, Krainer AR. The alternative splicing repressors hnRNP A1/A2 and PTB influence pyruvate kinase isoform expression and cell metabolism. Proc Natl Acad Sci U S A. 2010;107(5):1894-9. PMCID: 2838216.

20. David CJ, Chen M, Assanah M, Canoll P, Manley JL. HnRNP proteins controlled by c-Myc deregulate pyruvate kinase mRNA splicing in cancer. Nature. 2010;463(7279):364-8. PMCID: 2950088.

21. Dombrauckas JD, Santarsiero BD, Mesecar AD. Structural basis for tumor pyruvate kinase M2 allosteric regulation and catalysis. Biochemistry. 2005;44(27):9417-29.

22. Chen J, Xie J, Jiang Z, Wang B, Wang Y, Hu X. Shikonin and its analogs inhibit cancer cell glycolysis by targeting tumor pyruvate kinase-M2. Oncogene. 2011.

23. Spoden GA, Mazurek S, Morandell D, Bacher N, Ausserlechner MJ, Jansen-Durr P, et al. Isotype-specific inhibitors of the glycolytic key regulator pyruvate kinase subtype M2 moderately decelerate tumor cell proliferation. Int J Cancer. 2008;123(2):312-21.

24. Spoden GA, Rostek U, Lechner S, Mitterberger M, Mazurek S, Zwerschke W. Pyruvate kinase isoenzyme M2 is a glycolytic sensor differentially regulating cell proliferation, cell size and apoptotic cell death dependent on glucose supply. Exp Cell Res. 2009;315(16):2765-74.

25. Spivey HO, Flory W, Peczon BD, Chandler JP, Koeppe RE. Kinetics of the activation of rat liver pyruvate kinase by fructose 1,6-diphosphate and methods for characterizing hysteretic transitions. Biochem J. 1974;141(1):119-25. PMCID: 1168056.

26. Mazurek S. Pyruvate kinase type M2: A key regulator of the metabolic budget system in tumor cells. Int J Biochem Cell Biol. 2011;43(7):969-80. PMCID: 3118193

27. Mazurek S, Zwerschke W, Jansen-Durr P, Eigenbrodt E. Effects of the human papilloma virus HPV-16 E7 oncoprotein on glycolysis and glutaminolysis: role of pyruvate kinase type M2 and the glycolytic-enzyme complex. Biochem J. 2001;356(Pt 1):247-56. PMCID: 1221834.

28. Zwerschke W, Mazurek S, Massimi P, Banks L, Eigenbrodt E, Jansen-Durr P. Modulation of type M2 pyruvate kinase activity by the human papillomavirus type 16 E7 oncoprotein. Proc Natl Acad Sci U S A. 1999;96(4):1291-6. PMCID: 15456.

29. Landt S, Jeschke S, Koeninger A, Thomas A, Heusner T, Korlach S, et al. Tumor-specific correlation of tumor M2 pyruvate kinase in pre-invasive, invasive and recurrent cervical cancer. Anticancer Res. 2010;30(2):375-81.

30. Christofk HR, Vander Heiden MG, Wu N, Asara JM, Cantley LC. Pyruvate kinase M2 is a phosphotyrosine-binding protein. Nature. 2008;452(7184):181-6.

31. Schmidt TG, Skerra A. The Strep-tag system for one-step purification and high-affinity detection or capturing of proteins. Nat Protoc. 2007;2(6):1528-35.

32. Lee YS, Bergson P, He WS, Mrksich M, Tang WJ. Discovery of a small molecule that inhibits the interaction of anthrax edema factor with its cellular activator, calmodulin. Chem Biol. 2004;11(8):1139-46.

33. Lee YS, Huang K, Quiocho FA, O'Shea EK. Molecular basis of cyclin-CDK-CKI regulation by reversible binding of an inositol pyrophosphate. Nat Chem Biol. 2008;4(1):25-32. PMCID: 2367112.

34. Lee YS, Mulugu S, York JD, O'Shea EK. Regulation of a cyclin-CDK-CDK inhibitor complex by inositol pyrophosphates. Science. 2007;316(5821):109-12. PMCID: 2211727.

35. Passonneu JV. Enzymatic Analysis: A Practical Guide: Humana Press; 1993.

36. Berg JM TJ, Stryer L. Biochemistry. Sixth Ed. ed: W.H. Freeman; 2006.

37. Dang CV. PKM2 tyrosine phosphorylation and glutamine metabolism signal a different view of the Warburg effect. Sci Signal. 2009;2(97):pe75.

38. Chaneton B, Hilleton P, Zheng L, Martin A, Maddocks O, Chokkathukalam A, Coyle J, Jankevics A, Holding F, Vousden K, Frezza C, O'Reilly M, and Gottlieb E. Serine is a natural ligand and allosteric activator of PKM2. Nature. 2012. 15;491(7424):458-62. doi: 10.1038

39. Yang W, Zheng Y, Ji H, Chen X, Guo F, Lyssiotis CA, Aldape K, Cantley LC, and Lu Z. Erk1/2-dependent phosphorylation and nuclear translocation of PKM2 promotes the Warburg effect. Nat Cell Bio. 2012. 14(12):1295-304 doi: 10.1038/ncb2629

40. Yang W, Xia Y, Zheng Y, Liang J, Huang W, Gao X, Aldape K, and Lu Z. Nuclear PKM2 regulates B-catenin transactivation upon EGFR activation. Nature. 2011. 1;480(7375):118-22 doi: 10.1038/nature10598

41. Ignacak J and Stachurska M. The dual activity of pyruvate kinase type M2 from chromatin extracts of neoplasmic cells. Comp. Biochem. Physiol. B Biochem. Mol. Biol., 134 (2003), pp. 425-433

42. Diaz-Jullien C, Moreira D, Sarandeses C, Covelo G, Barbeito P, and Freire M. The M2-type isoenzyme of pyruvate kinase phosphorylates prothymosin a in proliferating lymphocytes. Biochem. Biophys. Acta, 1814 (2011), pp. 355-365

43. Yang W, Xia Y, Cao Y, Zheng Y, Bu W, Zhang L, You M, Hoh M, Cote G, aldpae K, Li Y, Verma I, Chaio P, Lu Z. EGFR-induced and PKCe monoubiquitylation-dependent NF-KB activation upregulates PKM2 expression and promotes tumorigenesis. Mol Cell. 2012 771-784 doi:10.1016/j.molcel.2012/09.028

44. Lv L, Xu Y, Zhao D, Li F, Wang W, Saski N, Jiang Y, Zhou X, Li T, Guan K, Lei Q, Xiong Y. Mitogenic and Oncogenic Stimulation of K433 Acetlyation Promotes PKM2 Portein Kinase Activity and Nuclear Localization. Mol Cell. 2013 52;3 340-352 doi:10.016/j.molcel.2013.09.004

45. Irsaelson W, Dayton T, Davidson S, Fiske B, Hosios A, Bellinger G, Li J, Yu Y, Saski M, Horner J, Burga, L, Xie J, Jurczak M, DePinho A, Cantley L, Vander Heiden M. PKM2 Isoform Specific Deletion Reveals a Differential Requirement for Pyruvate Kinase in Tumor Cells. Cell. 2013 115; 2 397-409 doi:10.1016/j.cell.2013.09.025

CHAPTER 2

SAICAR Stimulates Pyruvate Kinase Isoform M2 and Promotes Cancer Cell Survival in Glucose-Limited Conditions

*This chapter was previously published in *Science* (Keller et al, 2012). Figures 2-5 to 2-7 were generated by the co-author Irene Tan and Figures 2-2 and 2-3 were generated by Young-Sam Lee. All other results presented in this chapter represent original work. For this dissertation, modifications to the text and figures were made.

ABSTRACT

Pyruvate kinase isoform M2 (PKM2) plays an important role in the growth and metabolic reprogramming of cancer cells in stress conditions. Here, we report that SAICAR (succinylaminoimidazolecarboxamide ribose-5'-phosphate, an intermediate of the *de novo* purine nucleotide synthesis pathway) specifically stimulates PKM2. Upon glucose starvation, cellular SAICAR concentration increases in an oscillatory manner and stimulates PKM2 activity in cancer cells. Changes in SAICAR levels in cancer cells alter cellular energy level, glucose uptake, and lactate production. The SAICAR-PKM2 interaction also promotes cancer cell survival in glucose-limited conditions. SAICAR accumulation is not observed in normal adult epithelial cells or lung fibroblasts regardless of glucose conditions. This allosteric regulation may explain how cancer cells coordinate different metabolic pathways to optimize their growth in the nutrient-limited conditions commonly observed in the tumor microenvironment.

INTRODUCTION

An emerging hallmark of cancer cells is metabolic reprogramming, which includes elevated glucose uptake and oxygen-independent lactate fermentation known as the Warburg effect (1-3). This reprogramming is necessary for the growth and survival of tumors (4) in stress conditions and in xenografts. However, the molecular basis for this event and its role in cancer growth has remained unclear.

Several proteins, including PKM2, play important roles in the metabolic reprogramming and growth of cancer cells (4-6). PKM2 is one of four pyruvate kinases (PKs) found in mammals (7). It is highly expressed in fetal cells and cancer cells, whereas the other isoforms (PKM1, PKR, and PKL) are expressed in normal somatic tissues. Replacement of PKM2 in cancer cells with any other PK isoform drastically reduces cancer cell survival in stress conditions (hypoxia (4) or glucose-depletion (8)) and suppresses tumorigenicity (4). This suggests that subtle differences between this tumor-specific isoform and its normal cell counterparts are essential for tumor growth (4).

Biochemically, PKM2 is less active than its splice variant PKM1 due to its higher Michaelis-Menten constant (K_m) for phosphoenolpyruvate [PEP, (7)]. It has been hypothesized that the PKM2 isoform allows cancer cells to divert more glycolytic intermediates to biosynthetic processes like the pentose phosphate pathway to promote cell growth (2, 9). Although this model explains many

aspects of PKM2's role in cancer cell metabolism and growth, new data suggest that this may not be the entire story. For example, knocking down PKM2 without supplying additional PK limits cell growth (4), indicating that the relationship between PK activity and cell growth is not a simple inverse correlation. Similar results were seen with inhibitors specifically targeting PKM2 (8). It has been suggested that PKM2 can balance both cell growth and energy generation in cancer, but the mechanism remains unclear (10).

We speculated that this delicate balance of cell growth and energy generation may be explained by assuming that there is an allosteric regulator of PKM2 coordinating the PK activity (and thus energy generation) in response to the cell's metabolic demands. PKM2 is activated by the upstream glycolytic intermediate fructose-1,6-bisphosphate [FBP; (7)]. However, other PK isoforms (PKL and PKR) also activated by FBP cannot replace PKM2 for cancer cell growth in stress conditions (4, 7).

RESULTS

To identify unrecognized metabolites that interact with PKM2 in a glucose-dependent manner, we extracted cellular metabolites from A549 human lung cancer cells treated with high (25 mM) or no glucose media (for 0.5 hrs). Metabolites binding to recombinant PKM2 were then identified using liquid-chromatography mass spectrometry (LC-MS, **Fig. 2-1A**). When metabolite extracts from cells grown in glucose-rich conditions were used, peaks corresponding to known PKM2-binding metabolites (FBP and pyruvate) could be identified. When metabolites from glucose-depleted cells were used, a metabolite peak (m/z in positive ion mode: 455.0817) was found (* in **Fig. 2-1A**). This compound was identified as SAICAR (succinylaminoimidazolecarboxamide ribose-5'-phosphate, **Fig. 2-1B**), a purine nucleotide biosynthesis intermediate, based on its mass (calc. exact mass, $[M\times H]^+$: 455.0815) and its fragmentation pattern (**Fig. 2-2**). There were several peaks other than SAICAR, but none were specific to PKM2 as they also co-eluted with PKM1.

To test whether SAICAR affects PKM2's function, we synthesized SAICAR (*11*) (**Fig. 2-3**) and tested its effect on PKM2 using a lactate dehydrogenase (LDH)-coupled method. SAICAR activates PKM2 with an effective concentration at the half-maximal effect (EC_{50}) of 0.3 ± 0.1 mM (**Fig. 2-1C**). Increasing the incubation time (to 3 hours) did not alter the EC_{50}. SAICAR did not affect other PKs tested (**Fig. 2-1** and **2-4**). SAICAR-binding increased the catalytic turnover number (k_{cat}) of PKM2 by 2-3-fold while reducing the K_m for PEP from ~2 mM to

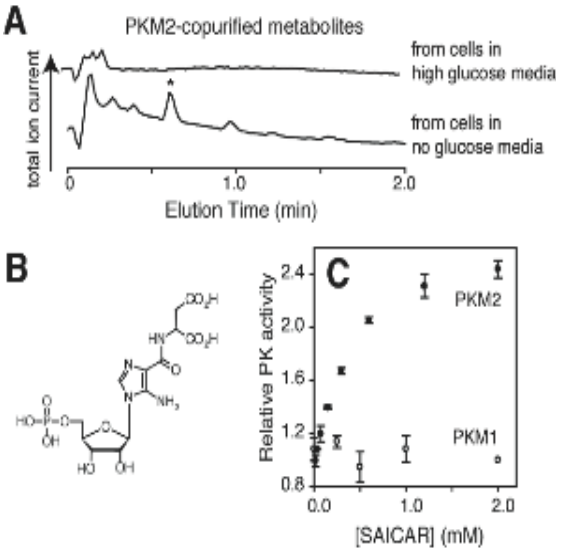

Figure 2-1. Identification of SAICAR as a regulator of PKM2. (**A**) LC-MS total ion current chromatographs of PKM2-copurified metabolites from glucose-rich (top) and glucose-free cells (bottom). A metabolite further characterized (**Fig. 2-2**) is noted with an asterisk (*). A549 cells were incubated in fresh DMEM (10% dialyzed FBS) containing either 25 mM or no glucose for 30 min, and metabolites extracted. Extracted metabolites were mixed with recombinant human PKM2 for 30 min at 37°C, cooled on ice, and subjected to a gel-filtration chromatography (exclusion limit: 10 kDa) at 4°C. Metabolites that co-purified with PKM2 were subjected to LC-MS analysis [C_{18}, electron-spray ionization (ESI), positive mode]. (**B**) Structure of SAICAR. (**C**) Effect of enzymatically synthesized SAICAR (**Fig. 2-3**) on PK activities of (•) PKM2 and (o) PKM1. Avg.± s.d. (n=3).

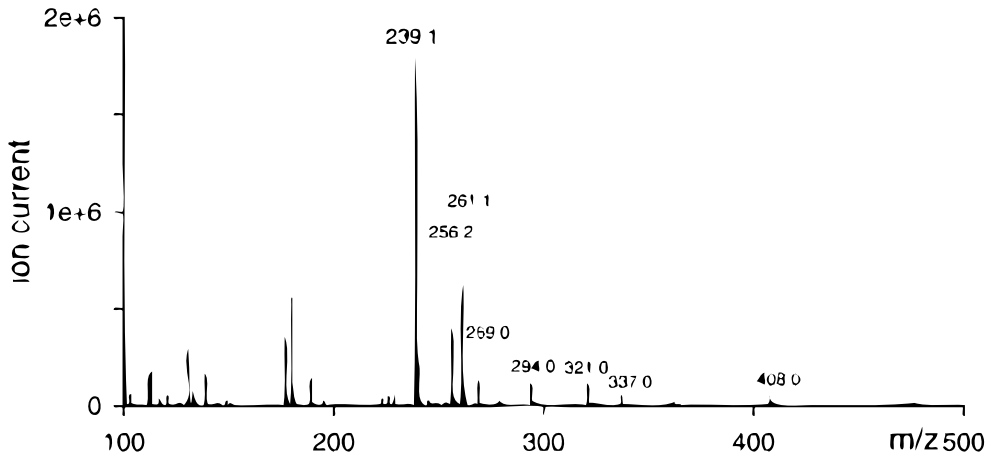

Figure 2-2. MS/MS (positive ion mode) analysis of the metabolite from glucose-starved cancer cells bound to PKM2. Peaks corresponding to decarboxylated SAICAR (408.0), SAICAR minus $C_4H_6O_4$ (337.0), and further loss of phosphate (239.1) are noticeable. LCQ Ion trap mass spectrometer was used.

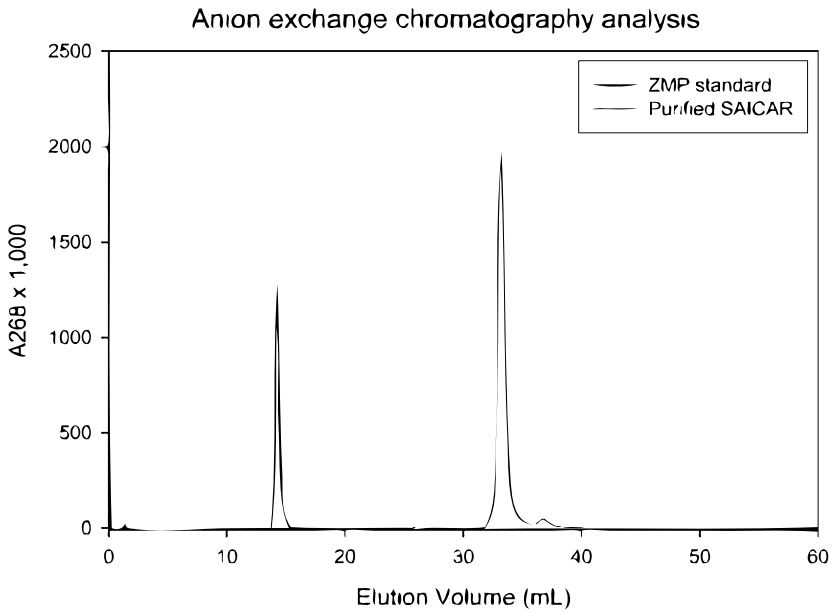

Figure 2-3. Analytical anion exchange chromatograph of starting material AICAR (black line) and enzymatically synthesized SAICAR (red line).

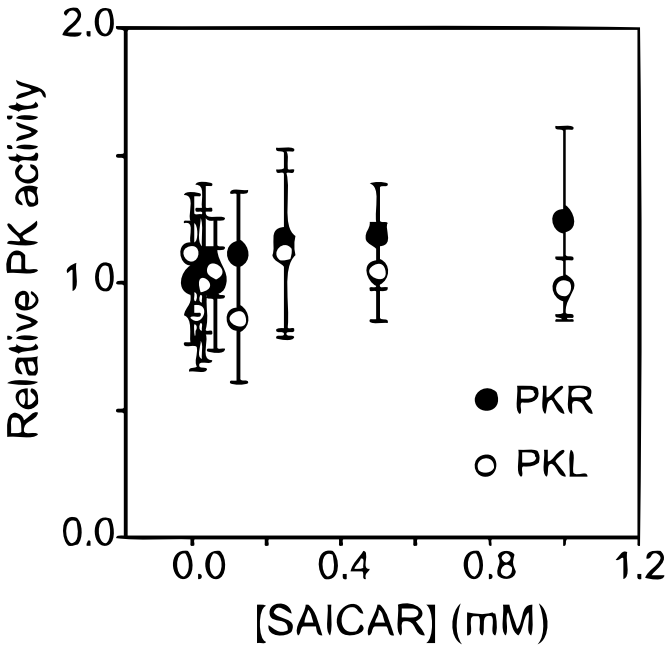

Figure 2-4. SAICAR has no effect on PKR or PKL. Effect of SAICAR on recombinant PKR or PKL was measured using a lactate dehydrogenase coupled assay as described. Avg. ± s.d. (n = 3).

~0.1 mM. SAICAR did not affect the K_m for ADP. Overall, the binding of SAICAR rendered PKM2's pyruvate kinase activity similar to that of PKM1.

When effects of other compounds related to SAICAR were tested (**Fig. 2-5**), succinyl-AMP stimulated PKM2, but the EC_{50} value several-fold higher than that of SAICAR (1.5 ± 0.4 mM vs. 0.3 ± 0.1 mM). None of the other tested compounds affected PKM2 activity significantly. SAICAR did not affect LDH activity (**Fig. 2-6**). The stimulation of PKM2 by SAICAR and by FBP was not additive (**Fig. 2-7**). Although this could be consistent with a competitive binding between FBP and SAICAR for an identical binding site, the study of mutant PKM2 proteins discussed later argues against this possibility.

To assess the physiological significance of this interaction, we measured SAICAR concentrations in several cell lines by LC-MS. In all human cancer cells tested (HeLa cervical cancer, A549, U87 glioblastoma, and H1299 non-small cell lung cancer cells), cellular levels of SAICAR were elevated upon glucose starvation from 0.02-0.1 to 0.3–0.7 mM (**Fig. 2-9A-C)**. The concentration of SAICAR is similar to that measured in glucose-rich leukemia cells [40uM, (12)]. The increase in cellular SAICAR level is oscillatory in HeLa (**Fig. 2-9A**) and H1299 cells (**Fig 2-8**). Pyruvate, lactate, and the ATP/ADP ratio also changed in a manner similar to the oscillation of SAICAR levels (**Fig 2-9A** and **2-8**). SAICAR accumulation of HeLa cells was observable even after a 12-hour incubation in glucose-free media. At a fixed time point (30 min), cellular SAICAR levels in HeLa cells increased as extracellular glucose concentration decreased [**Fig 2-9B**;

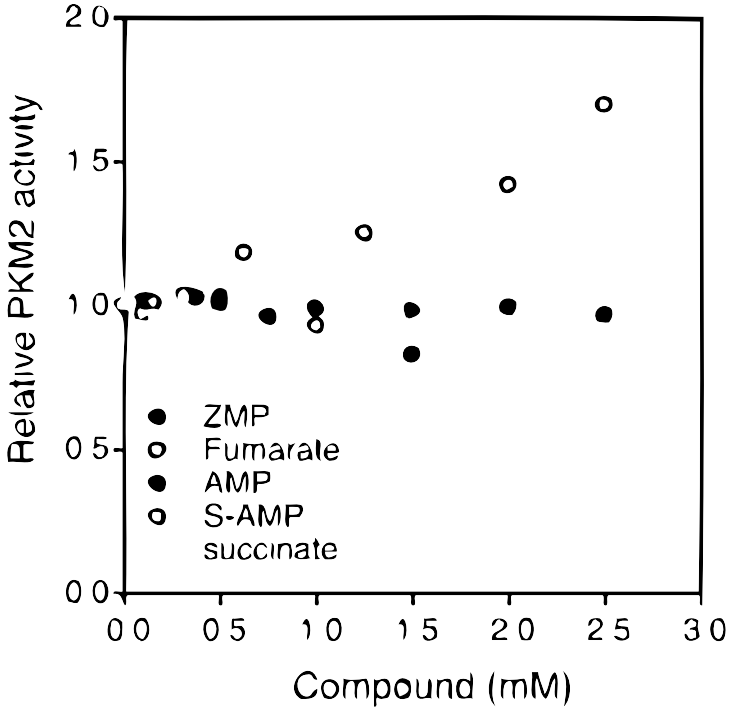

Figure 2-5. Effects of succinyl-AMP (S-AMP, yellow symbols), AMP (red), fumarate (empty), succinate (green), and ZMP (black) on PKM2.

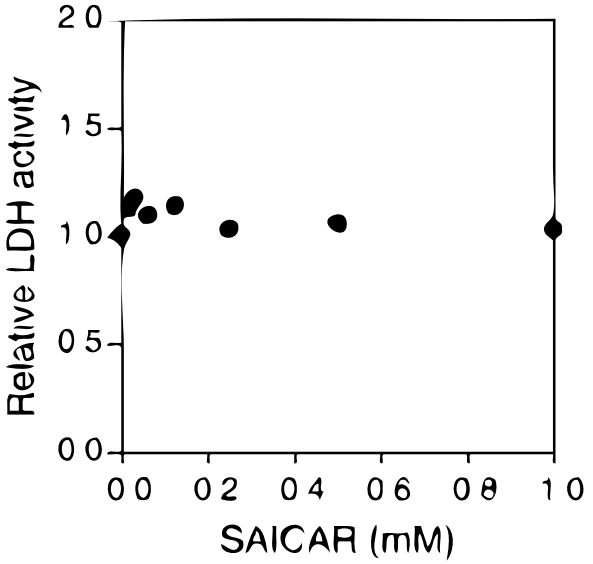

Figure 2-6. Effect of SAICAR on rabbit muscle lactate dehydrogenase (LDH). Effect of SAICAR on commercial rabbit muscle LDH was measured by monitoring NADH consumption using pyruvate as a substrate.

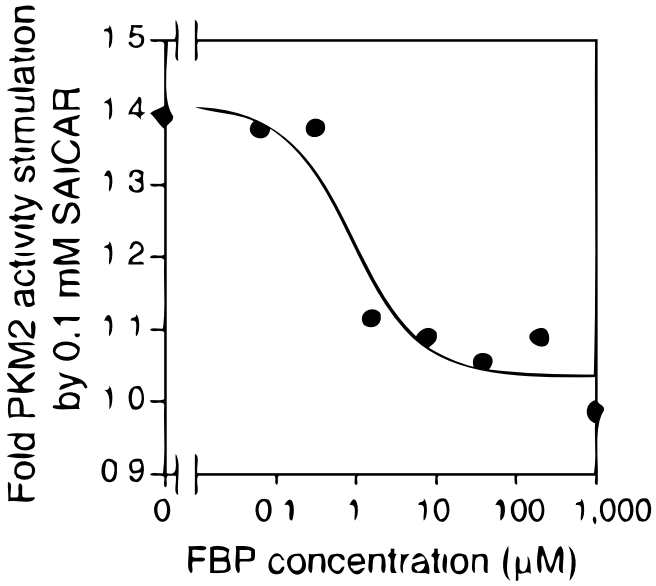

Figure 2-7. SAICAR-mediated PKM2 stimulation is not additive to the FBP-mediated PKM2 stimulation. Effect of SAICAR (0.1 mM) on the activity of PKM2 pre-incubated with various concentrations of FBP was measured. FBP-bound PKM2 is not activated further by the addition of SAICAR.

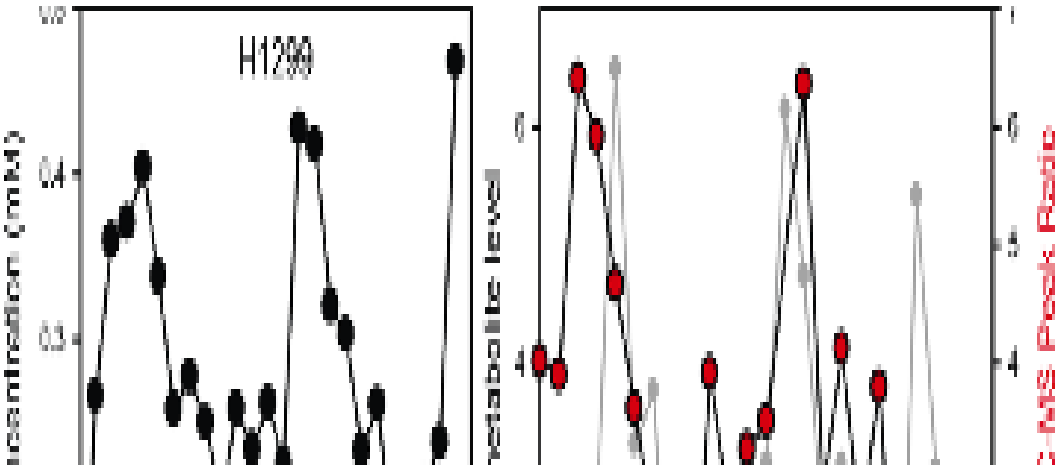

Figure 2-8. Oscillation of SAICAR and other metabolites in (left) H1299 cells and (right) HeLa cells in glucose-free media. (Left) SAICAR concentration of H1299 cells plotted against incubation time in glucose-free media. (Right) SAICAR concentration change of HeLa cells is shown in gray line and symbol while the ratio of ATP and ADP LC-MS peak areas (red circles) are overlaid to show the correlation between these two parameters.

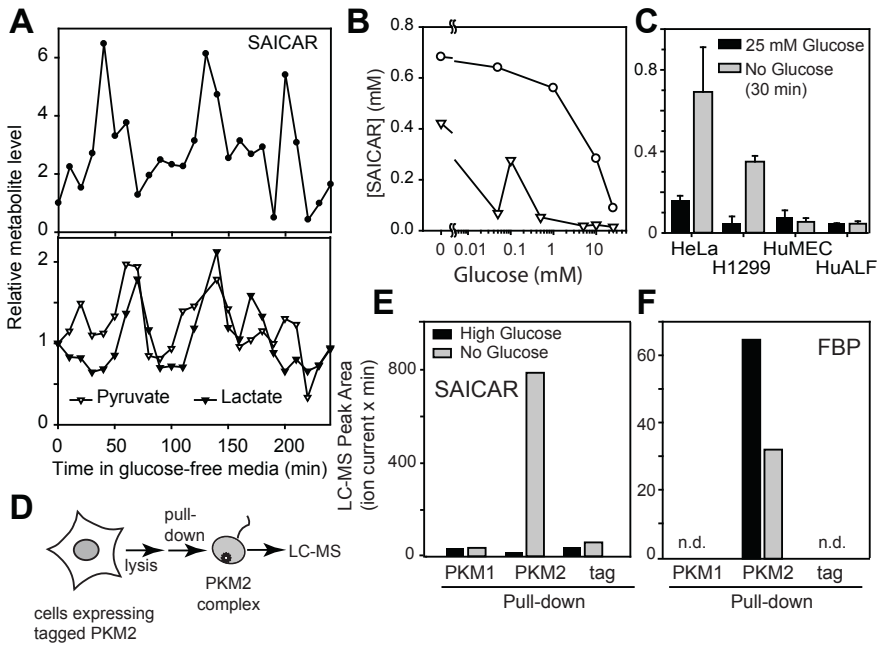

Figure 2-9. SAICAR binds to PKM2 in glucose-depleted cancer cells. (**A**) Cellular concentration of SAICAR in HeLa cells in response to glucose-depletion. HeLa cells were incubated in glucose-free media, and changes in SAICAR, pyruvate, and lacate concentration were measured using LC-MS. (**B**) Effect of extracellular glucose concentration on cellular SAICAR amount in (o) HeLa and (∇) NIH 3T3 cells after incubating with various glucose concentrations. (**C**) Effect of cell type. HeLa, H1299, HuMEC, and HuALF were incubated in 25 mM (filled box) or in no glucose media (gray box) for 30 min and used for the analysis of SAICAR level. Avg.± s.d. (n = 3). Other cancer cell lines tested also showed glucose-depletion dependent increase of cellular SAICAR level. (**D**) LC-MS peak area of SAICAR co-purified with PKM1, PKM2, or StrepII tag from H1299 cells incubated for 30 min in fresh 25 mM or no glucose media. (**E**) Amount of FBP that co-purified with the protein of interest analyzed as in (**D**).

physiological blood glucose level in healthy patients: 4-7 mM (13)]. In NIH 3T3 mouse embryonic fibroblast cells, an increase in SAICAR level was observed only when extracellular glucose concentrations were far below the physiological range. In normal human mammary epithelial (HuMEC) and in adult lung fibroblast (HuALF) cells, SAICAR accumulation was not observed even in glucose-free media (**Fig. 2-9C**). In all cells tested, FBP levels were gradually decreased upon glucose depletion (**Fig. 2-10**). These results suggest that the cellular concentration of SAICAR increases to a level sufficient to stimulate PKM2 in glucose-deprived cancer cells. It also suggests that SAICAR accumulation in glucose-depleted conditions may be limited to highly proliferating cells, perhaps because these cells use the *de novo* nucleotide synthesis pathway more than normal cells. However, other proliferating normal cells expressing PKM2 may also use this regulatory mechanism.

To determine if the PKM2-SAICAR interaction also occurs in cancer cells, we used an approach similar to the global metabolite-protein interaction mapping in yeast (14). HeLa cells were transfected with plasmids coding StrepII-tagged PKM2 or PKM1. These proteins were affinity purified. Metabolites co-purified with these proteins were then analyzed by LC-MS (**Fig. 2-9D**). Co-purification of SAICAR with PKM2 was observed when PKM2 was purified from glucose-depleted cells. SAICAR was not enriched with PKM1 (**Fig 2-9E**). FBP co-purified with PKM2 from glucose-rich cells as expected. These results suggest that the isozyme-specific PKM2-SAICAR interaction occurs in cells.

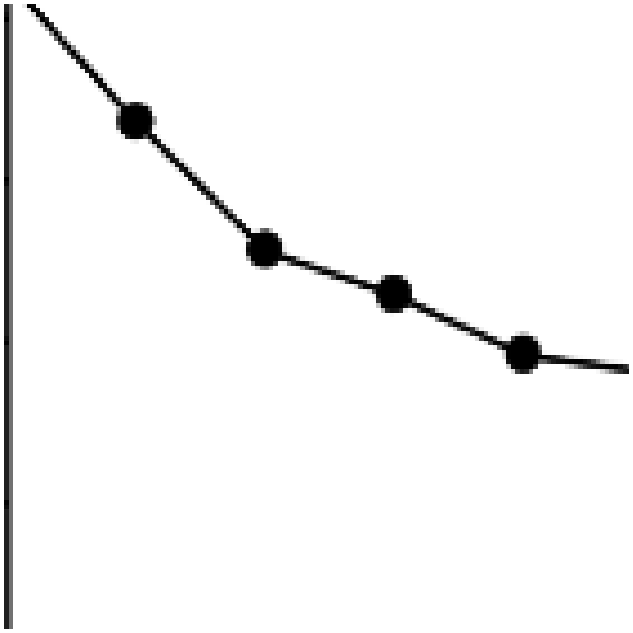

Figure 2-10. Cellular level of FBP upon glucose depletion in HeLa cells.

Data were collected and analyzed as in Fig. 2-1A.

We then examined the effect of SAICAR on the pyruvate kinase activity of PKM2 in cancer cells. We prepared HeLa and H1299 cells stably transfected with shRNA vectors targeting expression of the SAICAR synthase PAICS and the SAICAR cleavage enzyme ADSL (adenylosuccinate lyase; **Fig 2-11A**). In cells where PAICS is knocked down (*paics-kd*), cellular SAICAR concentration was not inducible while *adsl-kd* cells have constitutively elevated SAICAR levels (**Fig. 2-11B**). Depletion of glucose for 30 min further increased cellular levels of SAICAR in *adsl-kd* cells. Prolonged (>12 hrs) glucose depletion eventually led to a decrease in cellular SAICAR levels in *adsl-kd* cells (**Fig 2-12**). In *paics-kd adsl-kd* double-knockdown cells, no increase in SAICAR levels was observed. When PK activity in cell extracts was measured, the PK activity was higher in *adsl-kd* cells (**Fig 2-13**). Addition of SAICAR to the cell extract elevated pyruvate kinase activity of control-kd (cells transfected with scrambled shRNA) and *paics-kd* cell extracts, and only slightly in *adsl-kd* cell extracts (**Fig 2-13**). These results support our hypothesis that elevated cellular level of SAICAR stimulates PKM2.

Next, we measured whether SAICAR affects cancer metabolism. The glucose consumption rate of *paics-kd* cells was reduced in comparison with control-kd and *adsl-kd* cells (**Fig. 2-11C**). The lactate fermentation rate of *adsl-kd* cells was increased in comparison with control-kd and *paics-kd* cells (**Fig. 2-11D**). Similar results were obtained using LC-MS analysis of cellular metabolites (**Fig 2-14**). Both *adsl-kd* and *paics-kd* cells showed increased glutamine

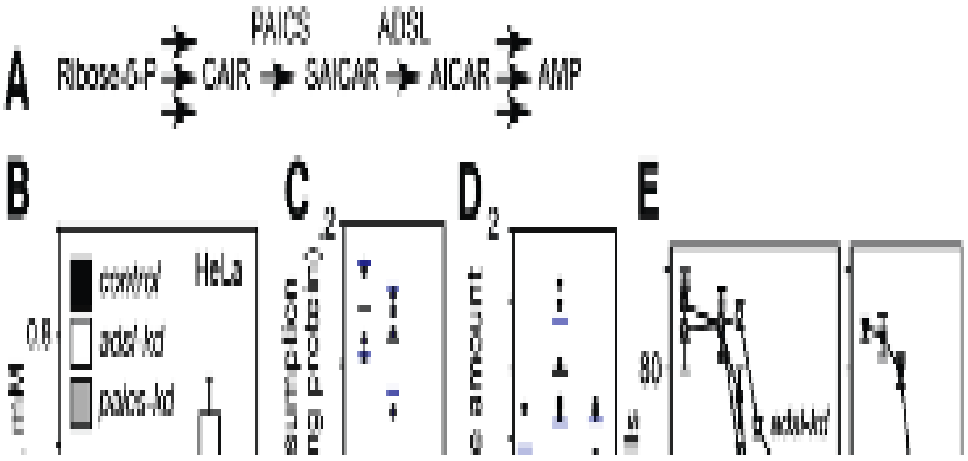

Figure 2-11. SAICAR level affects glucose metabolism, cancer cell survival, and proliferation. (**A**) A schematic diagram showing in the synthesis and metabolism of SAICAR. (**B**) Cellular levels of SAICAR in HeLa control-kd (black box), *adsl-kd* (open box), and *paics-kd* (gray box) before and after 30 min incubation in glucose-free media. Avg.±s.d. (n = 3). (**C** and **D**) Effect of SAICAR on (**C**) glucose uptake and (**D**) lactate fermentation. The amount of glucose or lactate in the media was measured using enzymatic assays and LC-MS analysis, respectively (normalized with total cellular protein concentration). Black and blue bars note Avg. and SD, respectively. (**E**) Survival of HeLa control-kd (control; cells transfected with random shRNA vector), *adsl-kd*, *paics-kd*, and *paics-kd adsl-kd* cells in glucose-free media was measured using a Trypan blue exclusion method. Avg ± s.d. (n=3, where over 50 cells were counted to calculate % live cells in each measurement).

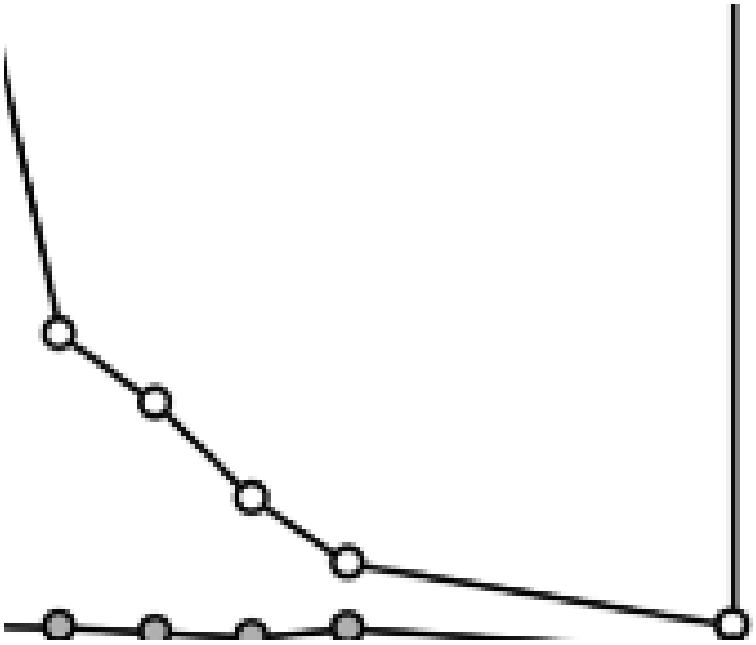

Figure 2-12. Cellular level of SAICAR in *adsl-kd* (open circles) and in *paics-kd* (grey circles) HeLa cells after prolonged incubation in glucose-free media.

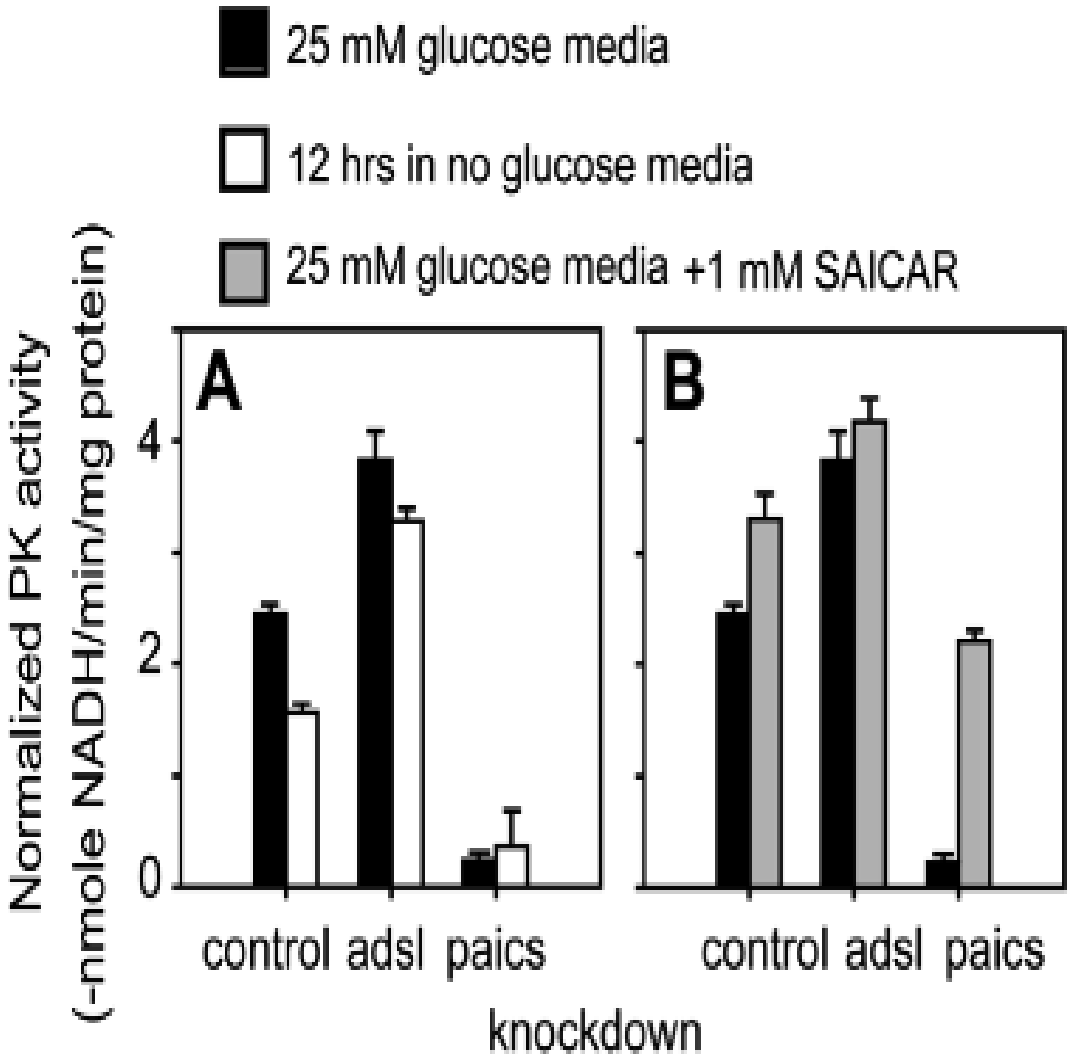

Figure 2-13. Pyruvate kinase activity in cell extracts. (A) Cells grown in 25 mM glucose media (black boxes) or treated with no glucose media for 12 hours (open boxes) were lysed on ice. PK activity was measured and normalized against total protein amounts. (B) To the extract of cells grown in 25 mM glucose media (black boxes; from A), SAICAR was added to final concentration of 1 mM. The mixture was incubated at 4°C for 1hr followed by PK activity measurements (gray boxes). Avg.± s.d (n=3).

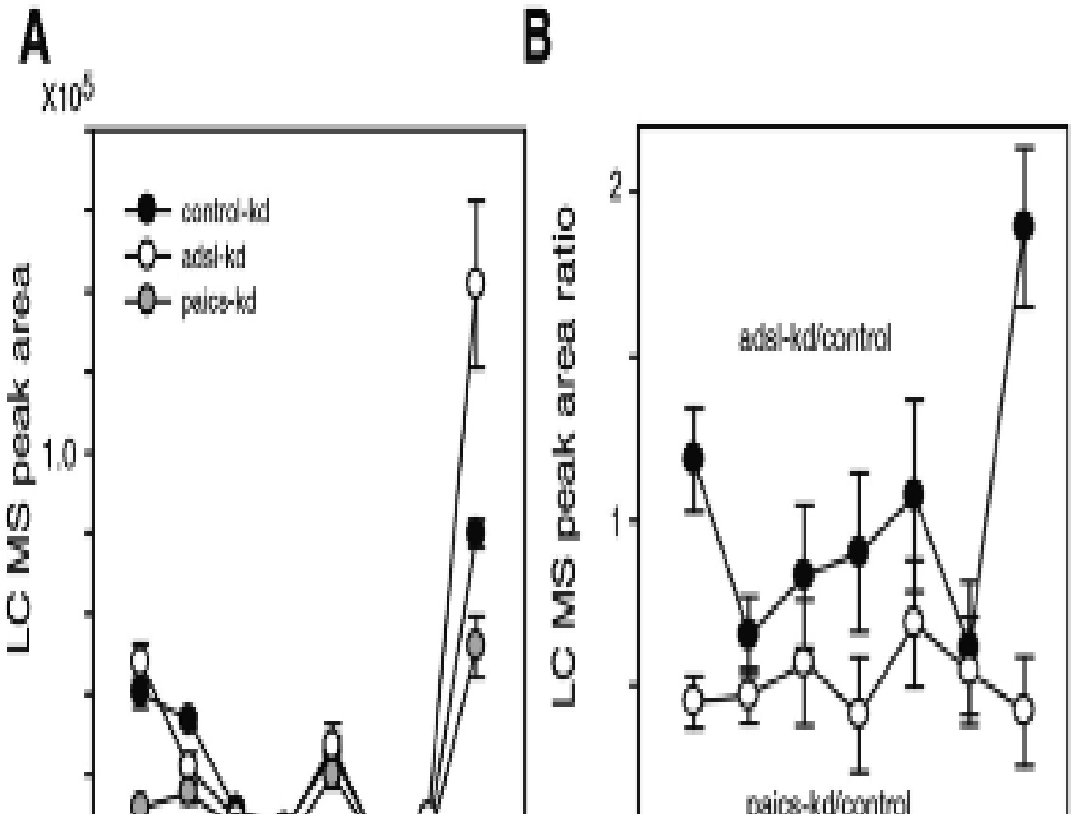

Figure 2-14. Effect of SAICAR on cellular levels of glycolytic intermediates. (A) LC-MS peak area of (black circles) control-kd, (open circles) adsl-kd, and (gray circles) paics-kd cells. Avg.± s.d. (n=3). (B) Ratio of glycolytic intermediate LC-MS peak areas as compared to controls; all cells were grown in high glucose media. These glycolytic intermediates represent the overall general state of cell metabolism in normal oxygen and glucose conditions.

Figure 2-15. Amount of glutamine in media after 30 min incubation with equal number of cells. Adherent cells in 96-well plates were incubated for 30 min in glucose-free media (4 mM glutamine) at 37°C. Amount of glutamine (m/z: 145.042) remaining in media after the incubation were measured using LC-MS as described in the method. Amount of glutamate (m/z: 146.046) was measured and is ~1% of the glutamine signal.

consumption (**Fig 2-15**). These results show that commonly observed metabolic phenotypes of cancer cells are either directly or indirectly affected by SAICAR levels. In addition, in a glucose-limited condition (30 min), *adsl-kd* cells had more ATP than the control-kd or *paics-kd* cells (**Fig. 2-16** and **2-17**), suggesting that the cellular metabolism of SAICAR-overproducing cells is altered in glucose-limiting conditions.

Because metabolic flux and cellular energy balance were altered by the changes in SAICAR concentration, we investigated whether SAICAR affected cancer cell survival in a glucose-dependent manner (**Fig. 2-11E**). In glucose-limited conditions, cells with higher SAICAR concentrations (*adsl-kd* cells or cells overexpressing PAICS, **Fig 2-18**) survived better, while *paics-kd* cells died earlier than control-kd cells (**Fig. 2-11E**). Double knockdown of PAICS and ADSL (*paics-kd adsl-kd*) had an effect similar to the PAICS knockdown alone. These results indicate that SAICAR promotes cancer cell survival in glucose-limited conditions.

To confirm the necessity of the PKM2-SAICAR interaction for increased cell survival in glucose-limited conditions, we searched for a PKM2 mutant that is insensitive to SAICAR while retaining its other properties. Because PKM1 (only 23 amino acids different from PKM2) is insensitive to SAICAR (**Fig 2-1**), we prepared several PKM2 mutants where PKM2-specific residues were mutated to their corresponding PKM1 counterparts. The Q393K mutant was SAICAR-insensitive (**Fig. 2-20A**) and retained wild-type basal activity (**Fig 2-19**). This Q393K mutant was also stimulated by FBP (**Fig. 2-20B**). In contrast, the known

phosphotyrosine–insensitive mutant, K433E [(15); K433 is also the residue contacting FBP (Structure: PDB 3ME3)], was still stimulated by SAICAR (**Fig. 2-20A**).

We used the Q393K mutant to test whether the effect of cancer cell survival in *adsl-kd* cells is due to the PKM2-SAICAR interaction. By a previously described method (4), endogenous PKM2 was knocked down and rescued with plasmid-coded PKM2 or PKM2 Q393K (M2-rescue and Q393K rescue cells, respectively). Western blot analysis showed more than 90 % of endogenous PKM2 expression was knocked down without detectable effects on plasmid-coded PK expression. The PK activity of the Q393K-rescue cells was similar to the level observed in *paics-kd* cells, but the activity was not stimulated by SAICAR (**Fig. 2-18B**). The PKM2-rescue cells behaved similarly to the cells with endogenous PKM2 in both glucose rich and glucose-limited conditions (**Fig. 2-20C).** The expression level of PKM2 was similar in untransfected and in Q393K-rescue cells. Q393K-rescue cells behaved nearly identical to cells with endogenous PKM2 in glucose-rich conditions. However, knockdown of ADSL in Q393K-rescue cells no longer promoted cell survival in glucose-limited conditions (**Fig. 2-20D**), indicating that the effect of SAICAR on cell survival in this condition is due to the SAICAR-PKM2 interaction.

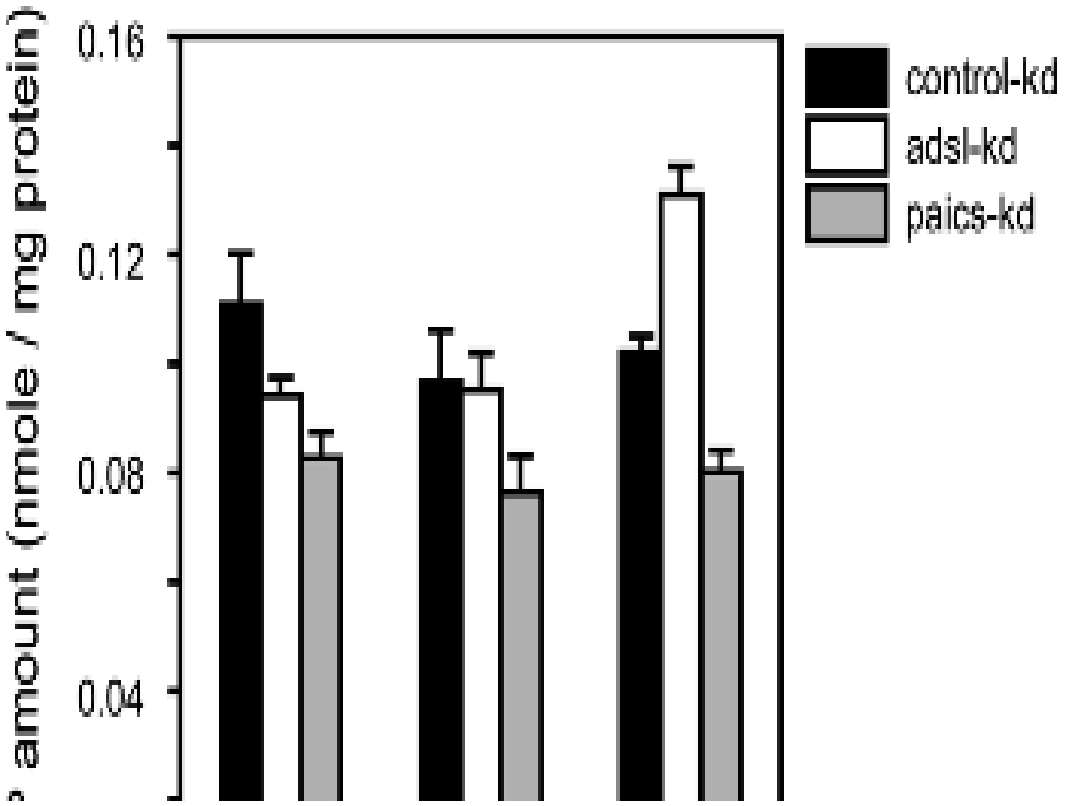

Figure 2-16. Enzymatic analysis of cellular nucleotide levels. Cells were incubated for 30 min in media containing 25, 1, or 0 mM glucose and lysed. ATP amounts in cell extracts were measured using yeast hexokinase and yeast glucose-6-phosphate dehydrogenase in the presence of excess glucose and $NADP^+$ (26). Avg.± s.d. (n=3).

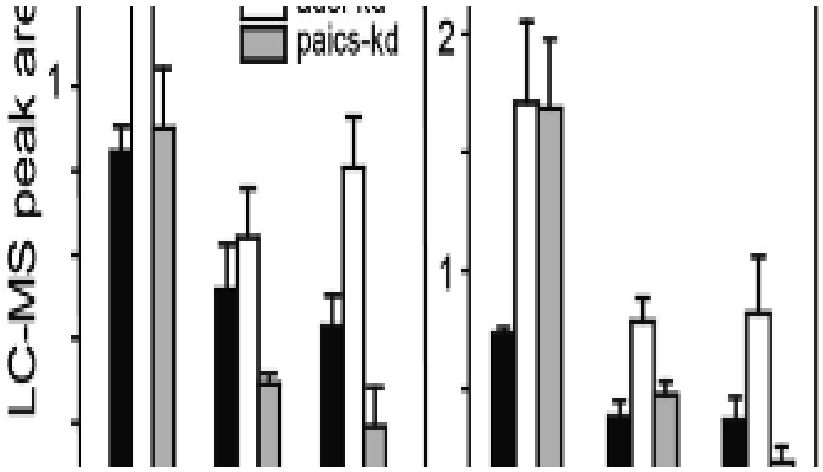

Figure 2-17. Cellular levels of metabolites in control-kd, adsl-kd, and paics-kd cells incubated for 30 min in media containing 1 mM glucose. Avg. ± s.d. (n =3). Due to inherent differences, each nucleotide has a different detection limit in mass spectrometry. Due to this phenomenon, the LC-MS area of one nucleotide may appear much larger or smaller than the area observed in another nucleotide, although the concentrations of both are very similar. For instance, the above data shows a larger peak area for AMP as compared to ATP in all three of the cell types. However, the molar amount of AMP is likely much lower than that of ATP in the cell. The apparent difference is due to the ability of AMP to "fly" better than ATP, thus yielding a higher signal. Therefore, comparison in the concentration one nucleotide between cell types can be monitored, but comparisons between nucleotide concentrations cannot be made using this system.

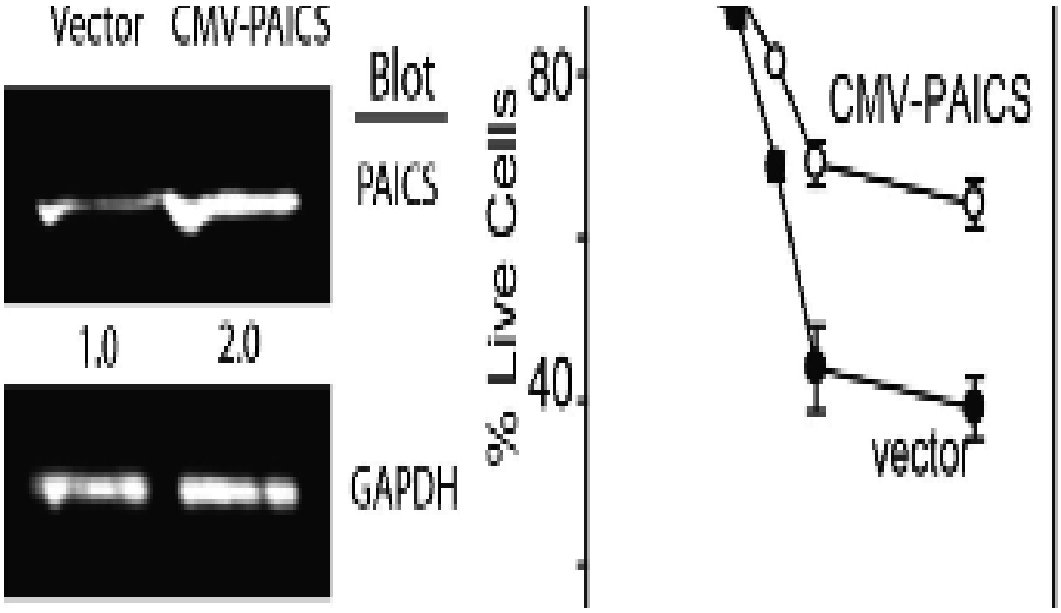

Figure 2-18. Effects of PAICS overexpression on cell survival in glucose-limited conditions. (A) Western analysis of HeLa cells transfected with vector [p31-N-HtS, (*21*)] or with PAICS overexpression vector (CMV-PAICS in p31-N-HtS vector). With CMV-PAICS, the total level of PAICS is elevated ~2-fold. (B) Effect of PAICS overexpression on HeLa cell survival in glucose-free media. Cell survival was measured. Avg. ± s.d. (3 independent measurements of more than 50 cells per measurements).

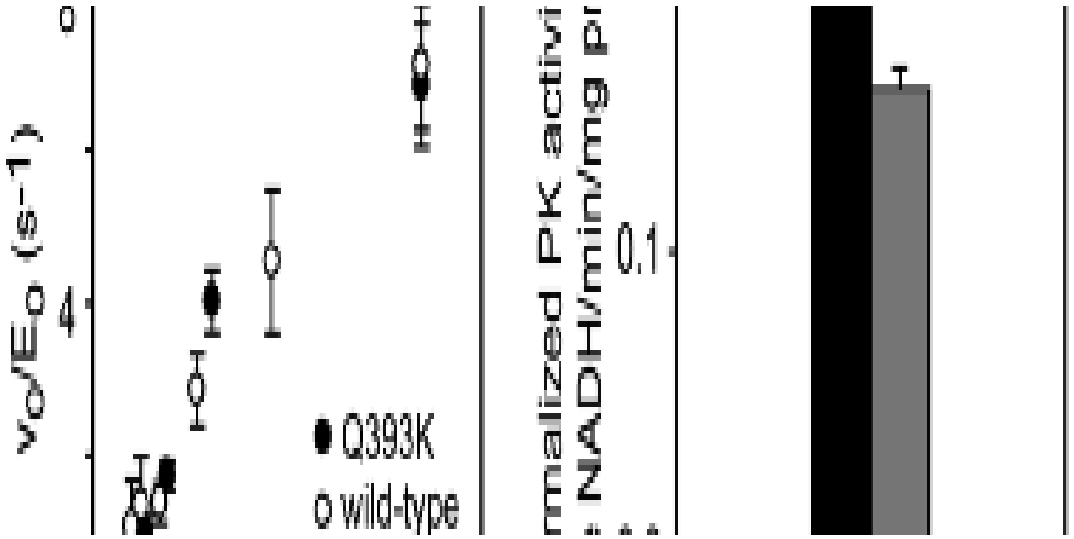

Figure 2-19. Pyruvate kinase activity of the Q393K mutant. (A) Activity of the Q393K mutant (•) was measured by varying the concentration of PEP (1.5 mM ADP, 10 nM enzyme) and comparing with wild-type (wt) PKM2 (o). Avg.±s.d. (n=3). (B) Pyruvate kinase activity of Q393K-rescue cell extract (black box) and the activity after 1 hr incubation with 1 mM SAICAR at 4°C (gray box). The PK activity is similar to that observed in *paics-kd* cells, but cannot be stimulated by incubation with SAICAR.

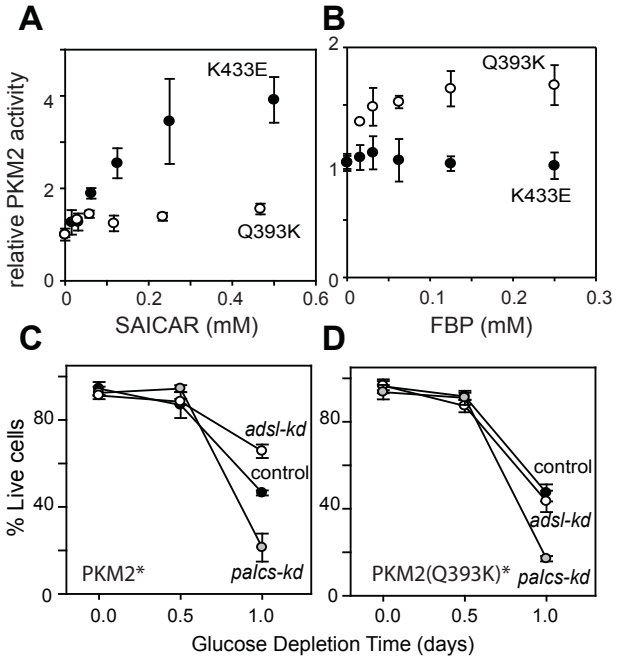

Figure 2-20. SAICAR-PKM2 interaction is responsible for the promotion of cancer cell survival. (**A** and **B**) Identification of a PKM2 mutant insensitive to SAICAR. Effect of (**A**) SAICAR and (**B**) FBP on pyruvate kinase activities of PKM2 Q393K (o) and PKM2 K433E (•) mutants is shown. Avg ± s.d. (n = 3). (**C** and **D**) Cell viability in glucose-depletion conditions was measured in HeLa cells expressing (**C**) PKM2* and (**D**) PKM2* Q393K mutant while endogenous PKM2 expression is knocked down. Avg ± s.d. (n = 3, over 50 cells were counted for each measurement). Control: cells transfected with scrambled shRNA vectors.

DISCUSSION

Based on these results, we conclude that at least some aspects of PKM2's role in tumor biology can be explained by SAICAR-mediated allosteric stimulation. This feature of PKM2 may allow cells to adjust their energy generation in response to nutritional and metabolic demands. When sufficient levels of glucose are provided, diverting glycolytic intermediates to biosynthetic processes like the pentose phosphate pathway can promote cell growth. However, in energy-depleting conditions such as nutrient-limitation, continued diversion of glycolytic intermediates to biosynthetic processes can hamper cells by depleting cellular energy below the minimal level required. The SAICAR-PKM2 interaction described here can be a molecular mechanism for this delicate balance. Ribose-5-phosphate, the starting material of nucleotide biosynthesis, is produced from the pentose phosphate pathway, which diverts glycolytic intermediates away from energy production (16). Connecting PKM2's PK activity with an intermediate of the *de novo* purine nucleotide biosynthesis pathway could give cells fine-tuned control of their metabolism in demanding conditions. SAICAR is produced from l-aspartate, a byproduct of glutaminolysis, which is known to be important in cancer cell metabolism (17), and the cleavage of SAICAR yields fumarate, which contributes to the citric acid cycle in mitochondria (18). SAICAR is therefore positioned to convey cellular metabolic demands to PKM2.

MATERIALS AND METHODS

Plasmids

Plasmids are maintained and propagated in appropriate *E. coli* cells [*ccdB*-survival 2 T1R (Invitrogen) for plasmids containing *ccdB*, DH5a and TOP10 for other purposes]. Plasmids constructed in this study were sequenced from both ends of inserts. Site-directed mutagenesis was done using Quikchange II XL mutagenesis kits (Agilent). Bacterial expression vector for PKM2, which was originally constructed by C. Arrowsmith lab [the Structural Genomics Consortium (SGC) at the University of Toronto] was obtained from Addgene (plasmid 25538). Bacterial expression vector for PKM1 was constructed by amplifying PKM1-specific region from IMAGE:5296639 (OpenBiosystems) and by replacing the corresponding region of the PKM2 expression vector with this PCR product using In-Fusion PCR Cloning kit (Clontech). PKM1 and PKM2 entry vectors were constructed by amplifying genes from these bacterial expression vectors and inserting them into pDONR221 vector (Invitrogen). Entry vector coding PKR (IMAGE:5221697) was from OpenBiosystems. Recombination of Entry vectors and Destination vectors were done using Gateway LR Clonase II enzyme mix (Invitrogen). Plasmids for ADSL expression were obtained from Prof. R. F. Colman (Univ. Delaware; (11)) and from SGC Stockholm (PDBl2J91). Dual-tagging Gateway Destination vectors (21), including p31-N-HtS, were gifts from Dr. Y. Wang (National Institute of Health). Plasmid sets coding shRNAs, in pGFP-V-RS (puromycin-resistant), targeting ADSL and PAICS were purchased

from Origene. Supersilencing shRNA plasmids (neomycin-resistant) targeting PAICS were purchased from Qiagen. Plasmids coding shRNA for PKM1/2 and control shRNA (4) in pLKO.1 vectors were originally constructed by the RNAi Consortium, which were purchased from OpenBiosystems. To replace original puromycin-markers of pLKO.1-based vectors, zeocin-resistance marker was amplified from psiRNA-DUO (Invivogen) and inserted to BamHI/KpnI-sites of pLKO.1 or its derivatives.

Proteins

Protein purities were assessed using SDS-PAGE and either Coomasssie or Sypro-Ruby (Invitrogen) staining. Protein concentrations were determined by measuring absorbance at 280 nm (A_{280}) in denaturing conditions (22). Functional ADSL was prepared as in literature (11). PKM2 and other pyruvate kinases were expressed from BL21 Codonplus RIL (DE3) cells using a procedure modified from the procedure originally developed by the Structural Genomics Consortium (http://www.thesgc.org/structures/details?pdbid=1ZJH/). Pyruvate kinase expression was induced by the addition of isopropyl-β-d-galactopyranoside (IPTG) for 18 hours at 20°C. All purification steps were carried out at 4°C or on ice unless noted otherwise. Cells were centrifuged (5,000g 20 min), and the pellet resuspended with 20 mM HEPES, 150 mM NaCl, 1 mM DTT, and 0.25% CHAPS buffer. Cells were lysed by sonication, and the debris was removed by centrifugation (15,000xg 20 min). All following chromatographic steps were

carried out using an AkTA Purifier 10 (GE Lifesciences) at 4°C. The supernatant was injected into a 5 mL HiTrap Chelating column (GE Lifesciences) charged with zinc chloride and equilibrated in buffer IA (20 mM HEPES, pH 7.4, 500 mM NaCl, 1 mM DTT, 30 mM imidazole, 5 % glycerol). After washing the resin with buffer IA until A_{280} reached baseline, bound proteins were eluted with a linear gradient of buffer IB (20 mM HEPES, pH 7.4, 500 mM NaCl, 1 mM DTT, 5 % glycerol, 250 mM imidazole). Fractions containing desired proteins were combined, concentrated with an Amicon Ultra-15 centrifugal filter, and passed through a HiTrap Desalt (5 mL; GE Lifesciences) column (elution buffer: 20 mM HEPES, 500 mM NaCl, 1 mM magnesium acetate, 5 % glycerol, 1 mM tris(2-carboxyethyl)-phosphine (TCEP)). After concentrating the protein solution and determining the protein concentration (ε_{280}: 30,535$M^{-1}\times cm^{-1}$), 4 molar equivalents ADP were added to the protein solution. Aliquots were stored at -80°C.

Identification of protein-binding metabolite

Cellular metabolites were extracted from adherent A549 cells as in literature (23) with modifications. For the identification of protein-binding metabolites, cellular metabolites extracted using methanol were first filtered through an Amicon Ultra-4 (molecular weight cut off, mwco, 3 kDa; Millipore) at 4 °C to remove macromolecules. This filtrate was dried in vacuum at 25 °C using a Speed-Vac or freeze-dried. Dried materials were dissolved in aqueous 20 mM ammonium acetate, pH 7.0. Recombinant protein (25 uM final concentration) and

cellular metabolites in 1 mL running buffer 1 (20 mM ammonium acetate, pH 7.0, 1 mM DTT, 1 mM magnesium acetate) were incubated at 37°C for 30 min, cooled on ice, and injected to a HiPrep 26/10 Desalt column (GE Lifesciences) equilibrated at 4°C in the running buffer 1 with a flow rate of 3 mL/min using the running buffer 1 as an eluent. The void volume fraction containing protein and protein-bound metabolites were collected, and passed through an Amicon Ultra-4 (mwco 3 kDa) centrifugal filter at 25°C (3,000 g). The filter was then washed with methanol. Combined filtrates were dried in vacuum using a freeze drier or a speed vac. Dried materials were dissolved in minimal amount of solvent (aqueous 0.1 % formic acid for reverse-phase HPLC – mass spectrometry or 20 mM ammonium acetate in methanol for hydrophilic interaction chromatography HPLC – mass spectrometry) and subjected to mass spectrometric analysis as described below.

Pyruvate kinase activity assay

Pyruvate kinase activity was measured using a lactate dehydrogenase (LDH) coupled method. In typical experiments, pyruvate kinase (20 nM) in assay buffer (50 mM HEPES, pH 7.4, 100 mM KCl, 6.2 mM $MgSO_4$, 1 mM DTT) containing ADP (1.5 mM for typical experiments) was incubated for 30 min at 37 °C in the presence of SAICAR or other ligands. To the solution, LDH (final: 5 units/mL; Roche) and then NADH (final concentration 220 μM for typical experiments) were added. The reaction was then initiated by the addition of PEP

(0.15 or 1.5 mM for typical experiments). The decrease of NADH was monitored spectroscopically at 340 nm in quartz cuvettes using a Beckman DU-650I spectrophotometer or in UV-transparent bottom 96-well plates using a Tecan Infinity M2 microplate reader. Rate was determined by dividing the change of ΔA_{340} per minute with the extinction coefficient of NADH at 340 nm (ε_{340}: 6,600 $M^{-1}\times cm^{-1}$).

SAICAR synthesis

Recombinant ADSL was prepared as in literature (11). ADSL activity was measured spectroscopically using S-AMP (Sigma-Aldrich) as substrate (11). SAICAR was synthesized from 5-aminoimidazole-4-carboxamide ribose-5'-phosphate (AICAR; Toronto Research Chemicals) and fumarate. In brief, AICAR powder (free acid form) was dissolved in 50 mM ammonium acetate (pH 7.0) immediately before use. The concentration of AICAR was spectroscopically determined using UV absorbance (ε_{269}: 12,600 $M^{-1}\times cm^{-1}$; (24)). A 2-mL solution containing 20 mM HEPES, pH 7.4, 50 mM KCl, 1 mM DTT, 2 mM EDTA, 50 mM ammonium acetate, 40 mM AICAR, 50 mM disodium fumarate, and 4 μM recombinant ADSL was incubated at 37°C for 4 – 12 hrs. The solution was cooled on ice, diluted with 8 mL 30 mM ammonium acetate and injected to a Mono Q 5/50 GL column (GE Life Sciences) equilibrated in 30 mM ammonium acetate (flow rate: 0.40 mL/min at 4°C). The column was washed with 30 mM ammonium acetate until A_{269} reached baseline, and bound materials were eluted

with a linear gradient of 3 N ammonium acetate over 3 hours. Fractions containing SAICAR, which was eluted when conductance was ~ 65 – 80 mS/cm^2, were pooled, dried extensively in vacuum at 25 °C using a rotary evaporator, and dissolved in water. Dissolved solution was stored at 4 °C for at least several weeks without any evidence of degradation. ESI-TOF (positive mode, water with 0.1 % formic acid): m/z 455.079 ([M+H]+, calc. 455.082); ESI-TOF (negative mode, 5 mM ammonium acetate-ammonium hydroxide, pH 9.9): m/z: 453.055 ([M-H]-, calc. 453.066). Concentration of SAICAR solution was calculated based on UV absorbance (ε_{269}: 13,800 $M^{-1}cm^{-1}$; (25)). Purity was assessed by analyzing it using anion-exchange chromatography in a smaller scale as described above. [$^{13}C_4$]-SAICAR was prepared as above in a smaller scale using [$^{13}C_4$]-fumaric acid (Cambridge Isotope Laboratory) as a substrate.

Cell culture and transfection

Cells were maintained in high glucose Dulbecco's Modified Eagle Media (DMEM) with 4.5 g/L (25 mM) glucose and L-glutamine, supplemented with 10% fetal bovine serum (FBS). Cells were grown at 37°C, 5% CO_2, and 85% humidity. Cells were passaged using 0.05% Trypsin-EDTA. Dialyzed FBS (Invitrogen) was in all experiments to avoid the effect of glucose in FBS. Cells were transfected with desired plasmids using Neon Nucleotransfector (Invitrogen) as in the vendor's instruction. Transfected cells were recovered in antibiotic-free media for 24 hours and then in selection media for 1–2 weeks. Transfection

efficiency was measured by monitoring GFP expression, when it is available, after 24 hours. Typical transfection efficiency was higher than 90%. Cell numbers were counted using Moxi-Z cell counter (Orflo). To measure cell numbers, cells were detached with trypsin-EDTA and diluted with isotonic buffer (Beckman Coulter). In the case of *adsl-kd* and *paics-kd* cells, decrease of target proteins were measured using Western analysis (>60 % and > 80 % reduction of PAICS and ADSL protein levels, respectively).

Metabolite extraction and analysis

For the analysis of metabolites in medium and in cells, cells (5×10^6 cells per dish) were seeded in 150 cm^2 dishes. After 1 – 2 days, cell numbers were counted, and the medium (25 mL from each dish) was transferred to 50 mL tubes. These tubes were stored at – 80 °C or analyzed immediately. Adherent cells (1×10^7 – 2×10^7 cells per dish) were quenched with ice cold DI water and liquid nitrogen was poured onto plates (23). Metabolites were extracted adding 2.0 mL 50% MeOH, 50% 25 mM ammonium acetate and cells were scraped off the dish at 4oC. The solution was incubated on ice while rocking for 15 minutes. The cell debris was removed by centrifugation. The solution was transferred to a chilled Amicon Ultra-15 centrifugal filter device (MWCO 3 kDa). The dish was washed again with fresh 2.0 mL ice-cold extraction buffer. Combined solution was filtered through the centrifugal filter device. When desired, the filtrate was freeze-dried and reconstituted in 0.150 mL of 15 mM ammonium acetate

aqueous solution or in 0.150 mL buffered methanol (95% methanol, 5% water, 5 mM ammonium acetate), and insoluble materials were removed by centrifugation (15,000 g for 15 min at 4°C). This cellular metabolite sample was stored at –80°C or analyzed immediately. Amounts of selected metabolites were analyzed using enzymatic analysis methods (26) and using LC-MS as described below. When desired, [$^{13}C_4$]-SAICAR of known concentration was added to the extraction buffer.

Pulldown of metabolite-protein complexes

HeLa cells transfected with p31-N-HtS-PKM1 or p31-N-HtS-PKM2, which code His_6-TEV cleavage site-StrepII-tagged PKM1 or PKM2, were grown in 10-cm dishes in media until they became ~80% confluent. When desired cells were washed three times with glucose-free media and then incubated in glucose-free media for 30 min. The dish was placed on ice, and cells were washed once with phosphate buffered saline (PBS). Cells were lysed with 2 mL ice-cold modified RIPA buffer, and debris was removed by centrifugation (16,000g 5 min 4°C). Subsequent steps were carried out at 4°C or on ice unless specifically noted otherwise. Cleared lysate was then applied to Strep-tactin magnetic beads (Qiagen) and incubated for 1 hour with agitation. Beads were separated with a magnet, and washed three times (5 min each) with 20 mM ammonium acetate in water. Metabolites bound were recovered with methanol, and the solution was

subjected to LC-MS analysis. Proteins were eluted with buffer containing 2 mM d-biotin and then subjected to SDS-PAGE and Western analysis.

Reverse-phase LC-MS

A 5-μL portion of sample (typically in aqueous 0.01-0.1 % formic acid) was injected to a reverse-phase column (Phenomenex Luna C18 (2) 3 μm bead, 20 mm column) connected to an Agilent 1200 LC – 6210 AccurateMass ESI-TOF mass spectrometer. Chromatography solvent system used was: 0-4 min: 100 % solvent A (0.01 % formic acid in water, flow rate: 0.50 mL/min at ambient temperature), 4 -14 min: linear gradient to 100 % solvent B (0.01 % formic acid in acetonitrile), 14 – 16 min: 100 % B, 16 – 18 min: back to A, 18 – 22 min: solvent A. Mass range from 50 to 1000 was monitored (positive ion mode, 1 Hz).

Hydrophilic interaction chromatography LC-MS

A 50-μL portion of sample in methanol was injected to a Luna-NH_2 column (Phenomenex; 3um beads, 150x 2 mm) equilibrated in solvent C (acetonitrile) with a flow rate of 1 mL/min. Bound metabolites were eluted with solvent D (water, 5 mM ammonium bicarbonate – ammonium hydroxide, pH 9.9) as in literature (23). All LC-MS data were analyzed using Agilent MassHunter software package. For the determination of absolute SAICAR amount in sample, a sample was mixed with [$^{13}C_4$]-labeled SAICAR standard solution (10 nM-100 μM) during the metabolite extraction step, and the amount of SAICAR in cell extract was

determined by comparing LC-MS peak areas of [^{12}C]-SAICAR with that of [$^{13}C_4$]-labeled SAICAR.

Western blotting

Anti-ADSL (mouse monoclonal) and anti-PKM2 (rabbit monoclonal) antibodies were from Signalway. Anti-PAICS (mouse monoclonal) and anti-GAPDH (rabbit monoclonal) antibodies were from Sigma-Aldrich. Horseradish-peroxidase conjugated anti-mouse and anti-rabbit immunoglobulin antibodies were from Cell Signaling and Thermo Scientific, respectively. Cells were lysed in ice-cold RIPA buffer, and cellular proteins were separated by SDS-PAGE. Proteins in gels were then transferred to nitrocellulose membranes using an iBLOT gel transfer device (Invitrogen), and probed with primary antibodies. Antibodies were then detected using horseradish-peroxidase conjugated secondary antibodies.

Cell survival test

Cells (10^3 cells) were seeded in a well of a 96 well plate coated with fibronectin. Cells were allowed to adhere and grow for 24 hours in high glucose DMEM supplemented with FBS. Cells were washed with target media (high or no glucose DMEM with 10% dialyzed FBS) several times. Cells were incubated with target media for 0- 48 hours. Media were aspirated, and cells were stained with 0.4 mM Trypan Blue solution for less than five minutes. Excess trypan blue was

washed away with PBS. Images of cells (bright field) were obtained using a Zeiss Axiovert 40 CFL with a 10× objective. More than 50 cells were counted in each well, and three wells were counted per experiment.

Identification of SAICAR-insensitive PKM2 mutant

Because PKM1, which is only 23 amino acids different from PKM2, is insensitive to SAICAR, we speculated that mutating one or two of these PKM2-specific residues may yield a PKM2 mutant insensitive to SAICAR but still retains the basal activity and the FBP-sensitivity. We have screened PKM2 mutants by mutating each of residues noted below (red type in the sequence alignment shown below) to corresponding ones in PKM1 Among mutants tested (K433E, Q393K, L392R, R399V), only the Q393K mutant was insensitive to SAICAR and sensitive to FBP.

```
HsPKM1      LSGETAKGDYPLEAVRMQHLIAREAEAAMFHRKLFEELVRASSHSTDLMEAMAMGSVEAS 420
HsPKM2      LSGETAKGDYPLEAVRMQHLIAREAEAAIYHLQLFEELRRLAPITSDPTEATAVGAVEAS 420
            ****************************:.:* .***** * :. .:*  ** *.:.:****

HsPKM1      YKCLAAALIVLTESGRSAHQVARYRPRAPIIAVTRNPQTARQAHLYRGIFPVLCKDPVQE 480
HsPKM2      FKCCSGAIIVLTKSGRSAHQVARYRPRAPIIAVTRNPQTARQAHLYRGIFPVLCKDPVQE 480
            :** :.*.****:**************************************************
```

REFERENCES

1. D. Hanahan, R. A. Weinberg. (2011). Hallmarks of cancer: the next generation. *Cell* 144(5), 646.

2. P. P. Hsu, D. M. Sabatini. (2008). Cancer cell metabolism: Warburg and beyond. *Cell* 134(5), 703.

3. W. H. Koppenol, P. L. Bounds, C. V. Dang. (2011). Otto Warburg's contributions to current concepts of cancer metabolism. *Nat Rev Cancer* 11(5), 325.

4. H. R. Christofk *et al.* (2008). The M2 splice isoform of pyruvate kinase is important for cancer metabolism and tumour growth. *Nature* 452(7184), 230.

5. A. Le *et al.* (2010). Inhibition of lactate dehydrogenase A induces oxidative stress and inhibits tumor progression. *Proc Natl Acad Sci U S A* 107(5), 2037. [2836706].

6. A. Wolf *et al.* (2011). Hexokinase 2 is a key mediator of aerobic glycolysis and promotes tumor growth in human glioblastoma multiforme. *J Exp Med* 208(2), 313. [3039857].

7. S. Mazurek. (2011). Pyruvate kinase type M2: a key regulator of the metabolic budget system in tumor cells. *Int J Biochem Cell Biol* 43(7), 969.

8. G. A. Spoden *et al.* (2009). Pyruvate kinase isoenzyme M2 is a glycolytic sensor differentially regulating cell proliferation, cell size and apoptotic cell death dependent on glucose supply. *Exp Cell Res* 315(16), 2765.

9. M. G. Vander Heiden, L. C. Cantley, C. B. Thompson. (2009). Understanding the Warburg effect: the metabolic requirements of cell proliferation. *Science* 324(5930), 1029. [2849637].

10. A. N. Macintyre, J. C. Rathmell. (2011). PKM2 and the Tricky Balance of Growth and Energy in Cancer. *Mol Cell* 42(6), 713.

11. P. Lee, R. F. Colman. (2007). Expression, purification, and characterization of stable, recombinant human adenylosuccinate lyase. *Protein Expr Purif* 51(2), 227.

12. M. E. Sant, S. D. Lyons, L. Phillips, R. I. Christopherson. (1992). Antifolates induce inhibition of amido phosphoribosyltransferase in leukemia cells. *J Biol Chem* 267(16), 11038.
13. Standards of medical care in diabetes--2006. *Diabetes Care* 29 Suppl 1, S4.

14. X. Li, T. A. Gianoulis, K. Y. Yip, M. Gerstein, M. Snyder. (2010). Extensive in vivo metabolite-protein interactions revealed by large-scale systematic analyses. *Cell* 143(4), 639. [3005334].

15. H. R. Christofk, M. G. Vander Heiden, N. Wu, J. M. Asara, L. C. Cantley. (2008). Pyruvate kinase M2 is a phosphotyrosine-binding protein. *Nature* 452(7184), 181.

16. X. Tong, F. Zhao, C. B. Thompson. (2009). The molecular determinants of de novo nucleotide biosynthesis in cancer cells. *Curr Opin Genet Dev* 19(1), 32. [2707261].

17. C. V. Dang. (2010). Glutaminolysis: supplying carbon or nitrogen or both for cancer cells? *Cell Cycle* 9(19), 3884.

18. N. Raimundo, B. E. Baysal, G. S. Shadel. (2011). Revisiting the TCA cycle: signaling to tumor formation. *Trends Mol Med* 17(11), 641. [3205302].

19. R. J. Giannone *et al.* (2007). Dual-tagging system for the affinity purification of mammalian protein complexes. *Biotechniques* 43(3), 296.

20. H. Edelhoch. (1967). Spectroscopic determination of tryptophan and tyrosine in proteins. *Biochemistry* 6(7), 1948.

21. M. A. Lorenz, C. F. Burant, R. T. Kennedy. (2011). Reducing time and increasing sensitivity in sample preparation for adherent mammalian cell metabolomics. *Anal Chem* 83(9), 3406. [3094105].

22. J. G. Flaks, M. J. Erwin, J. M. Buchanan. (1957). Biosynthesis of the purines. XVI. The synthesis of adenosine 5'-phosphate and 5-amino-4-imidazolecarboxamide ribotide by a nucleotide pyrophosphorylase. *J Biol Chem* 228(1), 201.

23. L. N. Lukens, J. M. Buchanan. (1959). Biosynthesis of the purines. XXIII. The enzymatic synthesis of N-(5-amino-1-ribosyl-4-imidazolylcarbonyl)-L-aspartic acid 5'-phosphate. *J Biol Chem* 234(7), 1791.

24. O. H. L. Janet V. Passonneau, *Enzymatic analysis: A practical guide*. (Humana Press, 1993).

CHAPTER 3

SAICAR Induces Protein Kinase Activity of PKM2 that is Necessary for Sustained Proliferative Signaling of Cancer Cells

*This chapter was previously published in *Molecular Cell* (Keller et al, 2014). Figure 3-6 and 3-9 were generated with help from Zainab Doctor and Figure 3-10 was generated with help from Zach Dwyer. All other results presented in this chapter represent original work. For the purposes of this dissertation, modifications to the text and figures were made.

ABSTRACT

Abnormal metabolism and sustained proliferation are hallmarks of cancer. Pyruvate kinase M2 (PKM2) is a metabolic enzyme that plays important roles in both processes. Recently, PKM2 was shown to have protein kinase activity phosphorylating histone H3 and promoting cancer cell proliferation. However, the mechanism and extent of this novel protein kinase in cancer cells remain unclear. Here, we report that binding of SAICAR, a metabolite abundant in proliferating cells, induces PKM2's protein kinase activity *in vitro* and in cells. Protein microarray experiments revealed that more than 100 human proteins– mostly protein kinases– are phosphorylated by PKM2-SAICAR. In particular, PKM2-SAICAR phosphorylates and activates Erk1/2, which in turn sensitizes PKM2 for SAICAR-binding through phosphorylation. Additionally, PKM2-SAICAR was necessary to induce sustained Erk1/2 activation and mitogen-induced cell proliferation. Thus, the ligand-induced protein kinase activity from PKM2 is a mechanism that directly couples cell proliferation with intracellular metabolic status.

INTRODUCTION

Highly proliferative cells, such as cancer cells, display metabolic properties distinct from their neighboring normal cells (Vander Heiden, Cantley, Thompson, 2009). For example, cancer cells uptake more glucose than their neighboring normal cells and ferment lactate even when sufficient oxygen is supplied (Vander Heiden, Cantley, Thompson, 2009). The observed altered metabolism is regarded as a hallmark of cancer (Hanahan and Weinberg, 2011). However, the molecular basis connecting altered metabolic status to cell proliferation is still not completely understood.

Pyruvate kinase isoform M2 (PKM2) is a metabolic enzyme enriched in highly proliferating cells and most types of cancer cells (Mazurek et al., 2002; Christofk et al., 2008). PKM2 was recently identified as a major contributor for altered cellular metabolism and the growth of tumors, as replacing PKM2 with other isoforms of pyruvate kinases in cancer cells alleviates abnormal cellular metabolism, renders cells susceptible to stress *in vitro*, and limits the growth of tumor in xenografts (Christofk et al 2008). In addition, various pharmacological reagents targeting PKM2 in an isozyme-specific manner influence cell growth and proliferation (Chen et al., 2011; Anastasiou et al., 2012), suggesting that PKM2 may be a potential target of clinical applications (Vander Heiden, 2013).

Since the identification of PKM2 as a major contributor to cancer cell growth (Christofk et al 2008), research has focused on identifying the underlying mechanism of this isozyme-specific action to develop therapeutics and/or

diagnostic tools (for review, see Gupta and Bamezai, 2010; Luo and Semenza, 2012; Mazurek, 2011). Recent results revealed that PKM2 in cancer cells has previously unrecognized properties distinct from other pyruvate kinase isoforms. First, PKM2 translocates from the cytoplasm to the nucleus of cancer cells upon stimulus, suggesting that PKM2 may have functions beyond glycolysis (Yang, et al., 2011). Indeed, PKM2 interacts with transcription factors and activates their functions (Luo et al., 2011).

Furthermore, PKM2 extracted from cancer cells shows protein kinase activity (Gao et al, 2012; Yang, et al., 2012a). Normally, pyruvate kinases catalyze the phosphotransfer reaction between phosphoenolpyruvate (PEP) and ADP, producing pyruvate and ATP. Surprisingly, PKM2 purified from cancer cells is capable of phosphorylating histone H3 threonine 11 (H3 T11) *in vitro* using PEP as a phospho-donor (Yang et al., 2012a). As expected, ADP inhibits the reaction *in vitro* (Yang et al., 2012a), suggesting that the same active site is used for both pyruvate kinase and protein kinase activity. Additionally, the phosphorylation of H3 by PKM2 was found in cells, and leads to increased cell proliferation by inducing expression of several genes including *MYC* and *CCND1* (Yang et al., 2012a).

Although this reaction occurs in cancer cells, the results observed by *in vitro* phosphorylation of H3 T11 by PKM2 purified from cancer cells imply that the reaction may not be robust enough to be significant in a biologically relevant context (Yang et al., 2012a). Additionally, recombinant PKM2 expressed and

purified from *E. coli* did not display H3 T11 kinase activity (Yang et al., 2012a). Thus, protein kinase activity of PKM2 is dependent on alternative modifications or ligand-binding, while pyruvate kinase activity is not. Indeed, phosphorylation of PKM2 by Erk1/2 appears to promote its protein kinase activity in cells (Yang et al., 2012b). However, the Erk1/2-mediated phosphorylation of PKM2 has not been shown to fully induce protein kinase activity *in vitro*.

To determine the mechanism defining how PKM2 contributes to cancer growth in an isozyme-specific manner, we previously searched for cellular metabolites that bind to PKM2 in an isozyme-selective manner (Keller et al., 2012). From our study, we found that SAICAR (succinyl-5-aminoimidazole-4-carboxamide-1-ribose-5'-phosphate), an intermediate of the *de novo* purine nucleotide biosynthesis process, accumulates in glucose-starved cancer cells and isozyme-selectively and directly activates pyruvate kinase activity of PKM2 *in vitro* and in cultured cancer cells, promoting survival in glucose-deprived conditions (Keller et al, 2012).

Here we report that the PKM2-SAICAR interaction is necessary and sufficient to induce robust protein kinase activity from PKM2 *in vitro* and in cancer cells. We also report that the PKM2-SAICAR complex phosphorylates over 100 human proteins – mostly protein kinases – that were previously unrecognized substrates. In particular, PKM2-SAICAR directly activates Erk1 *in vitro* and within cells. As has been previously shown (Yang et al, 2012b), activated Erk1/2 phosphorylates PKM2. We found that the phosphorylation of PKM2 by Erk1/2

sensitizes PKM2 for SAICAR-binding, leading to a positive feedback loop. Additionally, upon EGFR activation, cellular SAICAR concentration is elevated, which is necessary to induce sustained activation of Erk1/2 and proliferative signaling via PKM2. These results provide a detailed molecular mechanism describing how two hallmarks – altered metabolism and sustained proliferative signaling – are interrelated in highly proliferating cells.

RESULTS

SAICAR-binding induces protein kinase activity of recombinant PKM2

Unlike purified recombinant PKM2, PKM2 extracted from cancer cells is capable of phosphorylating histone H3 threonine 11 (H3 T11) using PEP as a phosphate donor (Yang et al., 2012a). We attempted to reconstitute the activity *in vitro* using purified recombinant PKM2 (rPKM2) and PEP as the sole phosphate donor. First, we tested whether allosteric activators of PKM2, such as FBP (Mazurek et al., 2002) or SAICAR, can induce protein kinase activity from rPKM2 (**Fig. 3-1A**). When the phosphorylation of recombinant histone H3 T11 by rPKM2 was probed *in vitro*, rPKM2 alone was not sufficient to efficiently phosphorylate H3 T11, as noted by Lu and coworkers (Yang, et al. 2012a; **Fig. 3-1B**). The addition of FBP (Mazurek et al., 2002), slightly improved PKM2 protein kinase activity, while the addition of SAICAR drastically stimulated PKM2's H3 T11 kinase activity (**Fig. 3-1B**). In typical reactions, less than 10 nanomolar PKM2 was sufficient to completely phosphorylate excess (1- 2 μM) recombinant H3 T11 within 10 - 15 min, in the presence of SAICAR (k_{cat} 6 s^{-1}), suggesting that the PKM2-SAICAR complex is capable of carrying out a multiple turnover reaction. The Michaelis-Menten constant (K_m) of the complex was measured to be approximately 1-2 uM for monomeric histone H3.1 (**Fig. 3-1C**) and 5 uM for PEP (**Fig. 3-1D**). The low uM K_m for PEP of the PKM2-SAICAR complex indicates that it is likely a relaxed form of PKM2 that is responsible for the phosphorylation of H3 T11. We would like to note that this reaction does not include any nucleotides.

Figure 3-1. SAICAR induces protein kinase activity from recombinant PKM2. (A) A schematic representation of the experiment. (B) Phosphorylation of recombinant histone H3.1 monomer (2 uM) by recombinant PKM2 (rPKM2, 10 nM) in the presence of PEP (0.10 mM) and ligands (FBP or SAICAR, 0.5 mM). The reaction mixture was incubated at 37°C for 5 min, quenched by the addition of SDS PAGE gel loading buffer, and subjected to SDS-PAGE. Phosphorylation of H3.1 T11 was monitored using anti-phospho-T11 H3 antibody as described in the Experimental Procedures. (C) Effect of H3.1 concentration on PKM2's protein kinase activity. In the presence of SAICAR (0.5 mM), the reaction follows a typical Michaelis-Menten kinetics. FBP (0.5 mM) only marginally activates the kinase activity of PKM2. (D) Effect of PEP concentration on the phosphorylation of H3.1 T11 by the PKM2-SAICAR complex. (E and F) The inhibition of the PKM2-SAICAR mediated H3.1 T11 phosphorylation (E) by ADP and (F) by FBP. (G) Phosphorylation of purified and dephosphorylated *Xenopus laevis* nucleosome by PKM2-ligand complexes. (H) Effect of glucose and SAICAR concentration on cellular H3 T11 phosphorylation and the level of Myc.

**Figure is presented on the following page.*

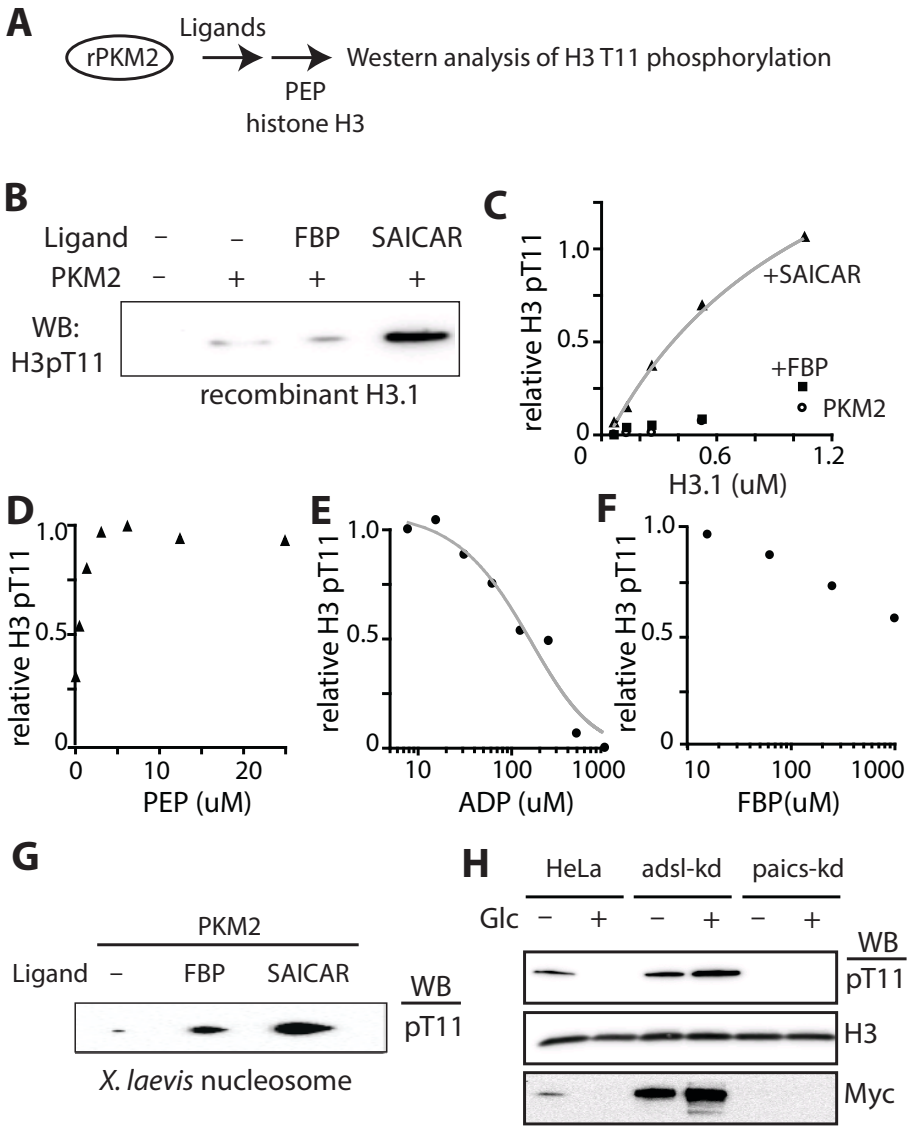

Figure 3-1. SAICAR induces protein kinase activity from recombinant PKM2. (*Continued from previous page)

Thus, we have shown that PEP is likely the direct source of phosphate. To further ensure that PEP is the phosphate donor, we measured the production of pyruvate using lactate dehydrogenase varying protein substrate concentrations (**Fig. 3-2A**). We found that pyruvate is indeed formed upon the addition of histone H3.1. The rate of pyruvate formation was dependent on the concentration of H3.1 and SAICAR. The k_{cat} (~ 5 s^{-1}) and the K_m (~ 1μM H3.1) values measured using this method (**Fig. 3-2A**) were similar with values obtained by monitoring H3.1 phosphorylation (**Fig. 3-1C**). The H3.1-dependent pyruvate production rate was stimulated by SAICAR (EC_{50} ~ 250 μM). The activation of protein kinase activity by SAICAR was barely observable when the SAICAR-insensitive mutant PKM2 Q393K was utilized (Keller et al., 2012; **Fig. 3-2C**). Together these results indicate that PEP is indeed a phosphate donor for the histone H3.1 mediated by the PKM2-SAICAR complex.

The protein kinase activity of the PKM2-SAICAR complex was inhibited by ADP (**Fig. 3-1E**) in a manner similar to PKM2 purified from cancer cell nucleoplasm (Yang et al., 2012a) suggesting that the PKM2-SAICAR complex uses an identical active site for both protein and pyruvate kinase activities. The protein kinase activity of the SAICAR-PKM2 complex was inhibited by FBP, a glycolysis intermediate that activates PKM2's pyruvate kinase activity (**Fig. 3-1F**). Suppression of protein kinase activity of PKM2-SAICAR by FBP indicates that these PKM2-activating metabolites regulate PKM2 in two distinct mechanisms:

Figure 3-2. PKM2-SAICAR complex phosphorylates histone H3.1. (A) Protein kinase activity was measured by monitoring the production of pyruvate using a lactate dehydrogenase coupled assay while varying PEP and recombinant histone H3.1 concentrations. PKM2 pre-incubated with 500 uM SAICAR or without any ligand were used (avg. ± s.e.m.) (**B**) Protein kinase activity was carried out as in (A) varying SAICAR concentrations with histone H3.1 (1 mM) as the substrate (EC_{50}: ~250 mM SAICAR). (**C**) Phosphorylation of recombinant histone H3.1 (1 mM) by PKM2 Q393K (10 nM) in the presence of varying SAICAR concentrations and 0.5 mM PEP (10 minutes reaction time at ambient temperature). Wild type PKM2 (WT) phosphorylation of H3.1 in the absence or presence of 125 mM SAICAR was included for comparison. (**D**) Phosphorylation of different subtype of recombinant histone H3 monomers (1 uM) by PKM2 (10 nM)-SAICAR (0.5 mM). '3.1/H4' denotes H3.1/H4 heterotetramer. (**E**) Phosphorylation of HA-tagged H3.1 and H3.3 in HeLa cells. H3.3 was not robustly phosphorylated in any of the conditions tested. In the right panel, HeLa cells were transfected with HA-H3.3. HA or total H3 was immunoprecipitated and pT11 H3 was monitored. As expected, when total H3 is IP'ed, pT11 is detected. However, when only H3.3 is pulled down, no phosphorylation is detected. In the left panel, minor phosphorylation is seen in the *adsl-kd* cells, however, this is not seen in the subsequent right blot. It is possible that the brightness of the signal of pT11 H3 in wild-type HeLa cells (IP: H3) washed out the signal of bands of very low signal. **Figure is presented on the following page.*

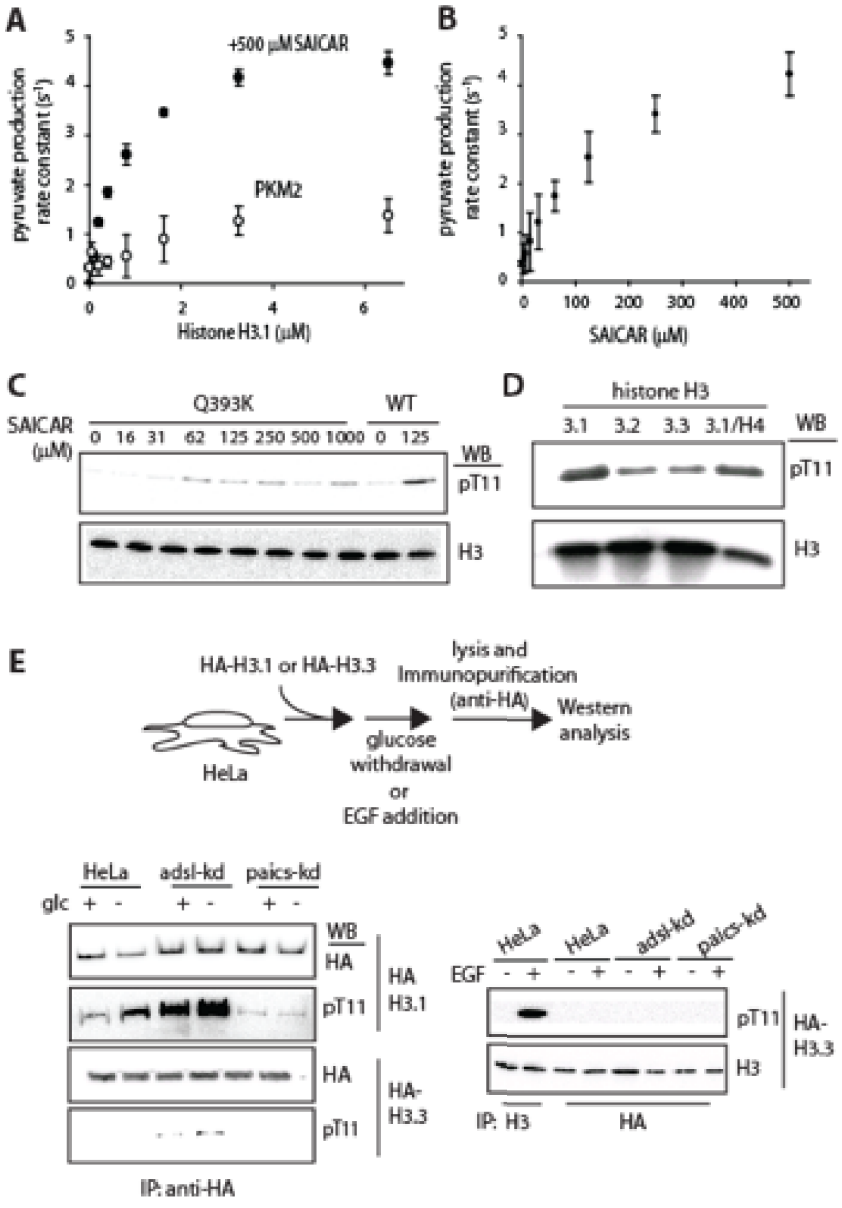

Figure 3-2. PKM2-SAICAR complex phosphorylates histone H3.1 (*continued from previous page)

FBP primarily induces PKM2's pyruvate kinase activity while SAICAR activates both pyruvate (Keller et al., 2012) and protein kinase activities of PKM2.

Because there are three different subtypes of H3 and each plays distinct roles in mammals (Hake and Allis, 2006), we asked whether the PKM2-SAICAR complex displays H3 subtype specificity (**Fig. 3-2D** and **3-2E**). Among H3 subtypes, only H3.1 was robustly phosphorylated by the PKM2-SAICAR complex, while phosphorylation of other H3 subtypes (H3.2 and H3.3) was not as efficient *in vitro* (**Fig. 3-2D**). These findings suggest that PKM2-SAICAR may distinguish between H3 subtypes.

Histone H3.1 is incorporated into nucleosomes in a replication-dependent manner and mostly found as a component of nucleosomes (Hake and Allis, 2006). Thus, we tested whether PKM2-SAICAR phosphorylates H3 in a nucleosome. When dephosphorylated nucleosomes purified from *Xenopus laevis* were used as a substrate, H3.1 T11 in the nucleosomes was phosphorylated by PKM2-SAICAR as efficiently as the H3.1 monomer (**Fig. 3-1G**).

Next, we asked if SAICAR induces the phosphorylation of histone H3 T11 in cancer cells. Using HeLa cells with altered SAICAR metabolism (Keller et al., 2012) we monitored the phosphorylation of H3 T11 and subsequent accumulation of c-Myc (**Fig. 3-1H**). Previously, we reported that the cellular concentration of SAICAR is elevated when HeLa and other cancer cells were deprived of glucose (Keller et al, 2012). In addition, we also reported that

knocking down the expression of the SAICAR cleavage enzyme adenylosuccinate lyase (*adsl-kd*) constitutively elevates the cellular concentration of SAICAR while knocking down SAICAR synthase (*paics-kd*) prevents the accumulation of SAICAR (Keller et al, 2012). When HeLa cells were subjected to a SAICAR-accumulating condition (30 min in glucose-free medium), the phosphorylation of H3 T11 and the level of Myc protein were both elevated (**Fig. 3-1H**). In cells constitutively accumulating SAICAR (*adsl-kd* cells), H3 T11 phosphorylation and Myc expression were both constitutively elevated (**Fig. 3-1H**). Meanwhile, cells in which the SAICAR synthase was knocked down (*paics-kd*) did not show any evidence of H3 T11 phosphorylation nor Myc expression regardless of glucose conditions (**Fig. 3-1H**). These results indicate that the elevation of SAICAR concentration is necessary to induce H3 T11 phosphorylation and Myc expression in HeLa cells.

In accordance with our previous *in vitro* result describing the H3-subtype specificity of the PKM2-SAICAR complex (**Fig. 3-2D**), the SAICAR-dependent phosphorylation of H3 T11 in HeLa cells was also H3-subtype specific (**Fig. 3-2E**). When HeLa, *adsl-kd*, and *paics-kd* cells were transfected with plasmids encoding hemagglutinin (HA)-tagged H3.1 or H3.3 (Kim et al., 2011), we observed subtype specific phosphorylation of H3 T11, which also correlates with cellular level of SAICAR. In HeLa cells, HA-tagged H3.1 T11 was phosphorylated in conditions accumulating SAICAR while phosphorylation of HA-tagged H3.3 T11 was never observed. In *adsl-kd* cells, H3.1 T11 was constitutively

phosphorylated while the phosphorylation could not be induced in *paics-kd* cells. Phosphorylation of H3.3 T11 was not detectable in either HeLa or *paics-kd* cells. Marginal H3.3 phosphorylation was detectable in *adsl-kd* cells, albeit at far lower levels than H3.1. The level of Myc correlated with the phosphorylation of H3.1 T11 in all conditions tested. These results indicate that SAICAR accumulation is necessary to induce H3.1 T11 phosphorylation and Myc expression in HeLa cells.

SAICAR accumulation induces nuclear localization of PKM2

Most pyruvate kinases are localized in the cellular cytoplasm where glycolysis occurs. In normal conditions, PKM2 is also localized in cytoplasm and is excluded from the nucleus (Yang et al., 2011). However, stimulation of cells with epidermal growth factor (EGF) induces partial nuclear localization of PKM2 in glioblastoma cells (Yang et al., 2011).

As we found that SAICAR stimulates PKM2-mediated phosphorylation of a nuclear protein (histone H3.1) both *in vitro* and in cells (**Fig. 3-1**), we speculated that SAICAR accumulation might be connected with the nuclear localization of PKM2. To test this possibility, cellular localization of endogenous PKM1/2 was probed in various conditions (**Fig. 3-3**). In HeLa cells maintained in glucose-rich medium in the absence of EGF, PKM2 was excluded from nucleus as expected (**Fig. 3-3A**). However, upon glucose depletion, PKM2 localized partially to the cell nucleus (**Fig. 3-3A**) in a manner similar to PKM2 in EGF-treated glioblastoma cells (Yang et al., 2011). Similar to glucose-deprivation, EGF-treatment also

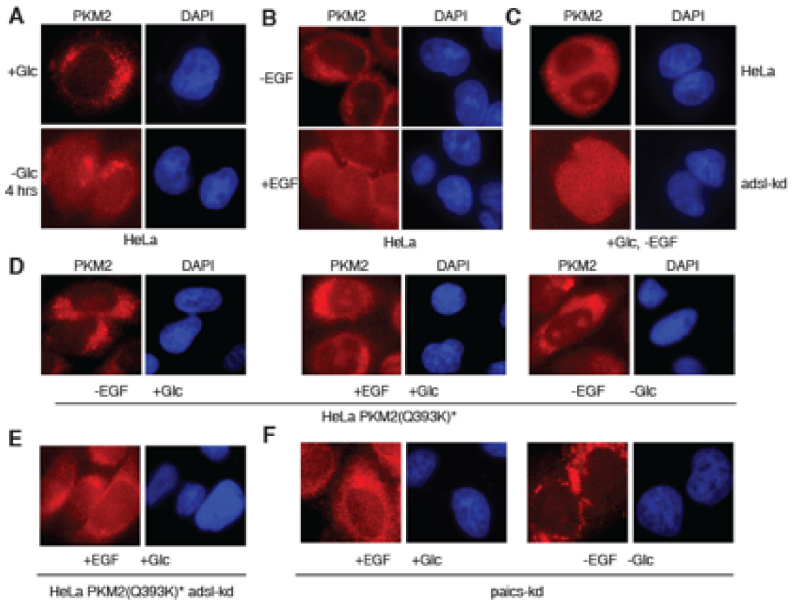

Figure 3-3. Effect of SAICAR on the subcellular localization of endogenous PKM2. (A) Effect of glucose withdrawal on the subcellular localization of PKM2 ('+Glc' and '-Glc' denote DMEM with 25 mM glucose and in glucose-free DMEM for 4 hours, respectively). (**B**) Effect of EGF on the subcellular localization of PKM2 ('-EGF' and '+EGF' denotes medium without EGF and in medium containing 10 ng/mL human EGF for 3 hours, respectively). (**C**) Effect of constitutive SAICAR accumulation on PKM2 subcellular localization. (**D**) Effect of SAICAR-insensitive PKM2 mutant (PKM2 Q393K). (**E**) Effect of constitutive SAICAR accumulation on the localization of the SAICAR-insensitive PKM2 mutant. (**F**) Subcellular localization of PKM2 in cells whose SAICAR synthase expression was knocked down.

produced a similar localization pattern of endogenous PKM2 in HeLa cells (**Fig. 3-3B**). Cells constitutively accumulating SAICAR (*adsl-kd* cells) showed nuclear localization of PKM2 regardless of condition (**Fig. 3-3C**). When endogenous

PKM2 was replaced with a SAICAR-insensitive PKM2 Q393K mutant (Keller et al., 2012) in HeLa cells, the subcellular localization change was not inducible by EGF, glucose withdrawal, or *adsl-kd* (**Fig. 3-3D-E**). These results indicate that the interaction between PKM2 and SAICAR is necessary for the nuclear localization of PKM2.

Due to the observed role of SAICAR in the nuclear localization of PKM2, we decided to examine the effect of SAICAR on the constitutively nuclear mutant PKM2 R399E (Gao et al. 2012; **Fig. 3-4**). Recombinant PKM2 R399E was purified from *E. coli* and the kinetic parameters measured. PKM2 R399E had a significantly lower K_m for PEP than wild type PKM2 (20 mM), indicating that this mutant exists in the relaxed form (**Fig. 3-4A**). PKM2 R399E is hypersensitive to SAICAR both in pyruvate kinase activity (**Fig. 3-4B**; R399E EC_{50} SAICAR: 12 mM, PKM2 wild-type EC_{50} SAICAR: 300 mM) and in protein kinase activity using H3.1 as a substrate (**Fig. 3-4C**; R399E EC_{50} SAICAR: ~30 mM, PKM2 EC_{50} SAICAR: ~200-300 mM).

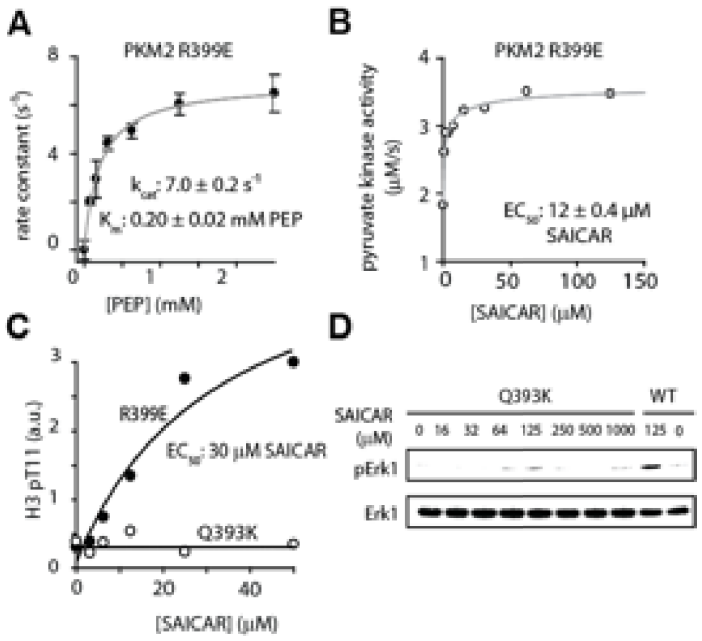

Figure 3-4. Constitutively nuclear PKM2 mutant is hypersensitive to SAICAR. (**A**) Pyruvate kinase activity assay with varying amount of PEP indicates that a constitutively nuclear PKM2 mutant (R399E; Gao et al., 2012) is in its relaxed form (K_m for PEP in low μM) instead of the tense form typically found in the wild-type PKM2. (**B** and **C**) PKM2 R399E mutant is also hypersensitive to SAICAR (EC_{50} 12 μM SAICAR, in comparison with EC_{50} value of 0.3 mM SAICAR for the wild-type PKM2) when its pyruvate kinase activity (**B**) and histone H3.1 T11 kinase activity (**C**) were measured in the presence of varying amount of SAICAR. (**D**) Protein kinase activity of PKM2 Q393K was measured using Erk1 (1 μM) as a substrate (0.5 mM PEP, 30 min at ambient temperature). Phosphorylation of Erk1 by Wild-type PKM2 (WT, 10 nM) in the presence or absence of 125 mM SAICAR is also included.

PKM2-SAICAR phosphorylates many proteins involved in cell proliferation

Our results show that SAICAR induces protein kinase activity of PKM2 *in vitro,* and that this activity is necessary for histone H3.1 T11 phosphorylation in HeLa cells. Next, to better understand the extent of this novel protein kinase activity, we searched for additional human proteins phosphorylated by PKM2-SAICAR. For this purpose, a human proteome microarray representing 9,479 recombinant human proteins was incubated in a solution containing PEP and PKM2 in the presence or absence of SAICAR (**Fig. 3-5**). Phosphorylated proteins were then visualized using ProQ Diamond stain. Because PEP is the only phosphate donor in this experiment, it is unlikely that the results will be influenced by the presence of immobilized protein kinases, which use ATP.

Using this approach, more than 150 proteins were identified as potential substrates for PKM2-SAICAR (**Table 3-1**). To our surprise, the vast majority of these proteins were protein kinases (more than 80 human protein kinases; **Table 3-1**; Gene ontology (GO) term enrichment: $p < 1e\text{-}77$; 12.6-fold enrichment of GO:0004672, "protein kinase activity"). These potential PKM2-SAICAR substrates include both receptor kinases such as EGFR and non-receptor protein kinases. In particular, many protein kinases involved in the mitogen-activated protein kinase (MAPK) pathway (MAPK1, MAPK3, MAP2K1, MAP2K2, MAP3K11, MAP3K2, MAP3K3) (Chang and Karin, 2001) were identified as potential substrates of PKM2-SAICAR. Among the proteins phosphorylated by the PKM2-SAICAR complex, at least 23 (ABL1, ABL2, ALK, CCDC6, CHEK2,

EGFR, ERBB2, FGFR1, FGFR2, FGFR3, JAK2, JAK3, KDR, KIT, MAP2K1, MAP2K2, MET, NTRK3, PCM1, PDGFRA, RET, ROS1, and SYK) have been implicated in cancer at the genetic level, according to the Cancer Gene Atlas database (http://cancergenome.nih.gov/). Several additional proteins (e.g. Cdc25A, Cdk2, Cdk4) involved in cell cycle progression (Nilsson and Hoffmann, 2000; Bartek et al., 2004) were also identified as potential substrates for PKM2-SAICAR. Interestingly, recent work has identified Bub3, a spindle assembly checkpoint point, as a substrate for PKM2 (Jiang et al., 2013). It is not yet clear what features of these proteins are recognized by PKM2-SAICAR. However, these results clearly indicate that preferred substrates for PKM2-SAICAR are protein kinases and other proteins involved in cell proliferation.

Next, we individually tested phosphorylation of several selected potential substrates (**Fig. 3-6**). Because proteins involved in the MAPK pathway (Pearson et al., 2001; Chang and Karin, 2001) were enriched in our protein microarray results, we focused on validating these proteins as substrates of PKM2-SAICAR. As Erk1/2 (also known as MAPK3 and MAPK1, respectively; Roskoski, 2012) has been reported to be involved in the regulation of PKM2 (Yang et al., 2012b), we first tested whether PKM2-SAICAR phosphorylates Erk1 using PEP as a phosphate donor (**Fig. 3-6A**). Indeed, PKM2-SAICAR phosphorylates recombinant Erk1 expressed and purified from *E. coli*, when the reaction product was analyzed using ProQ Diamond phosphoprotein staining. The phosphorylation was inhibited by ADP and, to a lesser degree, by FBP, in a

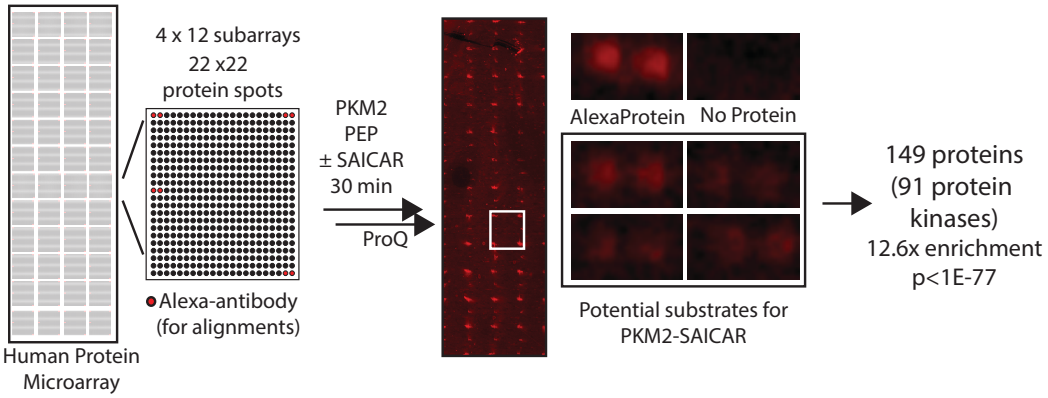

Figure 3-5. Protein microarray analysis revealed proteins phosphorylated by the PKM2-SAICAR complex. Schematic overview of the protein microarray used is shown. The array contains 48 (4x12) sub-arrays. In each sub-array, there are 484 (22x22) spots, including Alexa-labeled antibody spots used to align the array images. Proteins or controls were spotted in doublets. Most proteins were also immobilized in another subarray (total 4 spots). The protein array was incubated with 5 mL solution containing rPKM2 with or without SAICAR for 30 min followed by the addition of PEP. After a 30 min reaction, phosphorylated proteins were detected with ProQ Diamond. A representative protein microarray result is shown along with zoomed images.

Serine/Threonine Kinase	Receptor Tyrosine Kinase	Non-Receptor Tyrosine Kinase	Transcription Factor	Other Proteins
AKT3	ALK	ABL1	ALS2CR8	ADD1
BRSK1	CSF1R	ABL2	CARF	ALDOC
CAM2KB	EGFR	BLK	CASZ1	BEAN1
CAMKK2	EPHA1	BMX	HMBOX1	BIN1
CHEK1	EPHA2	DYRK1B	HSF1	BMI1
CHEK2	EPHA5	DYRK3	MEF2A	C10orf47
CHUK	EPHA8	FER	MEF2D	C19orf26
DCAMKL2	EPHB3	JAK2	MEF2D	C20orf67
DCLK2	EPHB4	JAK3	NFIC	CASS4
DYRK1B	ERBB2	PTK2	NFYA	CCDC6
DYRK3	FGFR1	SYK	NR1D1	CDC25A
GSK3A	FGFR2	TTN	NR4A1	CYPF12
HIPK1	FGFR3		RP5-860F19.3	DIXDC1
IKBKB	FGFR4		RXRA	EIF4G3
IKBKE	FLT1		RXRA	EP400NL
MAP2K1	FLT4		SOX5	EPB49
MAP2K2	KDR		TOX2	FAM122A
MAP3K11	KIT		TSC22D4	FSD1
MAP3K2	LTK		WDR62	GRB7
MAP3K3	MERTK		ZXDC	PM_2148
MAP4K2	MET			IL1B
MAPK12	MST1R			KANK4
MAPK13	NTRK2			KBTBD7
MAPKAPK2	NTRK3			KIAA1509
MAPKAPK3	PDGFRA			KIF26A
MAPKAPK5	PDGFRA alpha			NUP35
MARK2	RET			PAPOLA
NEK1	ROS1			PCM1
NEK6	TEK			PEPD
NLK	TYRO3			PHACTR4
PAK2				PSCD1
PAK6				R3HDM2
PAK7				RAG1AP1
PBK				SC4MOL
PDPK1				SDCCAG3
PRKAA2				SNAP91
PRKCE				SOCS3
PRKCQ				TFF2
PRKD1				WAC
PRKD3				ZFAND5
PRKG2				
RPS6KA2				
RPS6KA3				
RPS6KA5				
STK25				
STK33				
STK4				
TAOK2				
TBK1				
TSSK2				
TTN				
WNK2				

Table 3-1. List of proteins identified as potential PKM2-SAICAR substrates from the protein microarray experiment.

manner similar to the phosphorylation of H3.1 T11 by PKM2-SAICAR. When the reaction product was probed with an antibody specific to Erk1/2 phosphorylated at its activation loop threonine (T202 in human Erk1) and/or tyrosine (Y204 in human Erk1) residues, the antibody effectively recognized Erk1 phosphorylated by PKM2-SAICAR. This suggests that PKM2-SAICAR may phosphorylate either T202 or Y204 of Erk1. As discussed later, we indeed found that T202 is the likely site of phosphorylation. Similar to histone H3.1, the activation of protein kinase activity by SAICAR was abolished when the SAICAR-insensitive PKM2 Q393K mutant was utilized (**Fig. 3-4D**).

As PKM2-SAICAR phosphorylates the activation loop of Erk1 *in vitro*, we tested the effect of this phosphorylation on its enzymatic activity. Erk1, like other canonical MAPKs, is an inefficient catalyst without activation. Full activation of Erk1 requires two phosphorylation reactions of the activation loop T202 and Y204 (Roskoski, 2012). The phosphorylation by PKM2-SAICAR activated Erk1 more than 150-fold (**Fig. 3-6B**). In comparison, dually phosphorylated Erk2 (denoted with an 'A' in **Fig. 3-6B**) was even more active than Erk1 phosphorylated with PKM2-SAICAR. This result is consistent with the reported k_{cat} value of Erk1/2 phosphorylated at T202 alone (reported k_{cat} values for non-phosphorylated, pT, pY, and pT-pY Erk2 are 1, 227, 620, and 8940 s^{-1}, respectively; Sugden et al., 2011). SAICAR-insensitive PKM2 Q393K mutant did not phosphorylate Erk1 even in the presence of SAICAR (**Fig. 3-4D**). Thus, Erk1 was indeed phosphorylated and partially activated by PKM2-SAICAR, at least *in vitro*.

Typically, in MEK-mediated phosphorylation of Erk1/2, the phosphorylation of the activation loop tyrosine precedes the phosphorylation of the activation loop threonine (Haystead et al., 1992). However, threonine mono-phosphorylated Erk1/2 was also has been detected in cells (Sugden et al., 2011). To further locate the phosphorylation site, we used recombinant Erk1 mutants whose activation loop residues were mutated (T202A and Y204F). PKM2-SAICAR was unable to phosphorylate Erk1 T202A, but was still able to phosphorylate the Y204F mutant (**Fig. 3-6C**). These data show that the T202 is the likely site of phosphorylation, and the phosphorylation of Erk1 by PKM2-SAICAR appears distinct from the MEK-mediated Erk1/2 activation.

In addition to Erk1, we also tested the phosphorylation by PKM2-SAICAR of several additional selected recombinant proteins found to be phosphorylated by PKM2-SAICAR in the protein microarray experiment (**Fig. 3-5** and **3-6D**). When commercial recombinant epidermal growth factor receptor (EGFR; Carpenter, 1987) expressed and purified from insect cells was tested as a substrate, it was phosphorylated in a manner dependent on PKM2, SAICAR, and PEP. Similar results were observed with other recombinant proteins (MEK1 and PAK2) identified as potential PKM2 substrates from the microarray experiment. MAPK pathway proteins (B-Raf and Grb2) not phosphorylated by PKM2-SAICAR in the microarray experiment were subjected to individual tests; none were phosphorylated by PKM2-SAICAR.

Figure 3-6. Phosphorylation of EGFR/MAPK signaling proteins by PKM2-SAICAR complex. (A) Phosphorylation of recombinant Erk1 by the PKM2-SAICAR complex. Recombinant Erk1 was subjected to phosphorylation by PKM2 in the presence or absence of various ligands (0.5 mM each) and probed with ProQ Diamond phosphoprotein staining, Western blotting with anti-active Erk1/2 antibody, with anti-Erk1/2 antibody, and with anti-PKM2 antibody. (B) Effect of PKM2-SAICAR on the activity of Erk1. Protein kinase activity of Erk1, after treatment with PKM2 in the absence or in the presence of 0.50 mM SAICAR, was monitored using a fluorogenic Erk1/2 activity assay kit. 'A' denotes the use of commercial active Erk2 instead of Erk1. Means +/- SEM are noted (n = 3). (C) Identification of the residue(s) phosphorylated by PKM2-SAICAR. Recombinant Erk1, Erk1 T202A, and Erk1 T204F were subjected to phosphorylation in the presence or absence of 0.5 mM SAICAR and probed with anti-active Erk1/2 antibody. (D) Phosphorylation of other proteins by the PKM2-SAICAR complex. A few positive hits (EGFR, MEK1, PAK2) and negative hits (B-Raf and Grb2) were individually tested for the phosphorylation by PKM2 in the presence of various ligands.

*Figure presented of the following page.

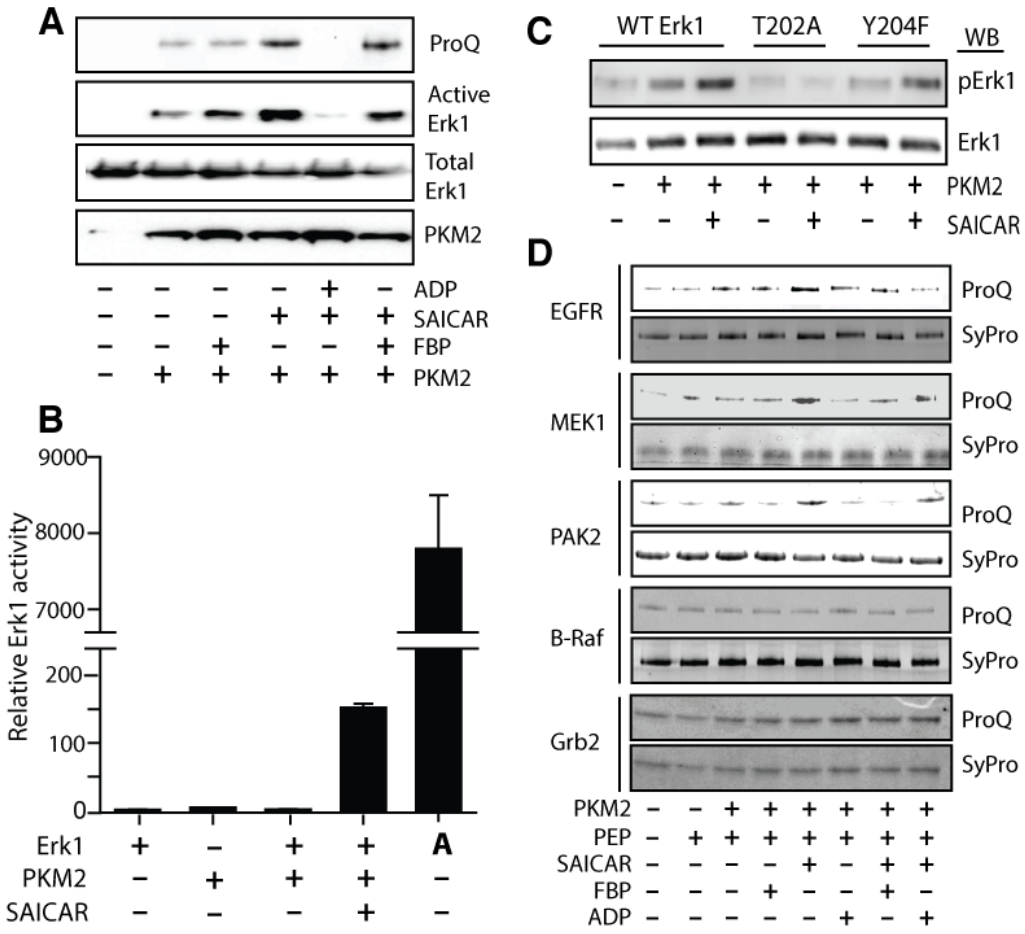

Figure 3-6. Phosphorylation of EGFR/MAPK signaling proteins by PKM2-SAICAR complex. (*Continued from previous page)

PKM2-SAICAR complex phosphorylates protein substrates in cells

Our results indicate that there is an intimate relationship between PKM2-SAICAR and EGF/MAPK signaling. Next, we asked if SAICAR is functionally involved in EGF/MAPK signaling in cancer cells. We first measured cellular levels of SAICAR in HeLa and in H1299 cells before and after EGF addition (**Fig. 3-7A**). Cellular SAICAR levels were elevated rapidly in these cells upon EGF addition (**Fig. 3-7A** and **3-8**) to a level sufficient to activate PKM2 (EC_{50} 300 mM; Keller et al. 2012). Thus, SAICAR may be a relevant ligand for PKM2 upon EGFR activation, in addition to glucose deprivation as previously reported.

Next, we asked if the interaction between PKM2 and SAICAR is involved in EGF-induced protein phosphorylation in cells. We first tested the phosphorylation of total H3 T11 in cells, as the antibody does not distinguish subtypes (**Fig. 3-7B** and **C**). H3 pT11 and Myc levels were both elevated upon EGFR activation in HeLa cells as previously reported (Yang et al., 2012a). In cells constitutively accumulating SAICAR (*adsl-kd*; Keller et al, 2012), both H3 pT11 and Myc levels were constitutively elevated (**Fig. 3-7B** and **C**). When endogenous PKM2 was replaced with SAICAR-insensitive PKM1 (**Fig. 3-7B**) or PKM2 mutant (Q393K; Keller et al., 2012; **Fig. 3-7C**), EGF addition was not able to induce H3 T11 phosphorylation or Myc expression (**Fig. 3-7B** and **C**) regardless of cellular SAICAR level. Our data suggest that PKM2-SAICAR is necessary for EGF-induced phosphorylation of H3 T11 and the subsequent

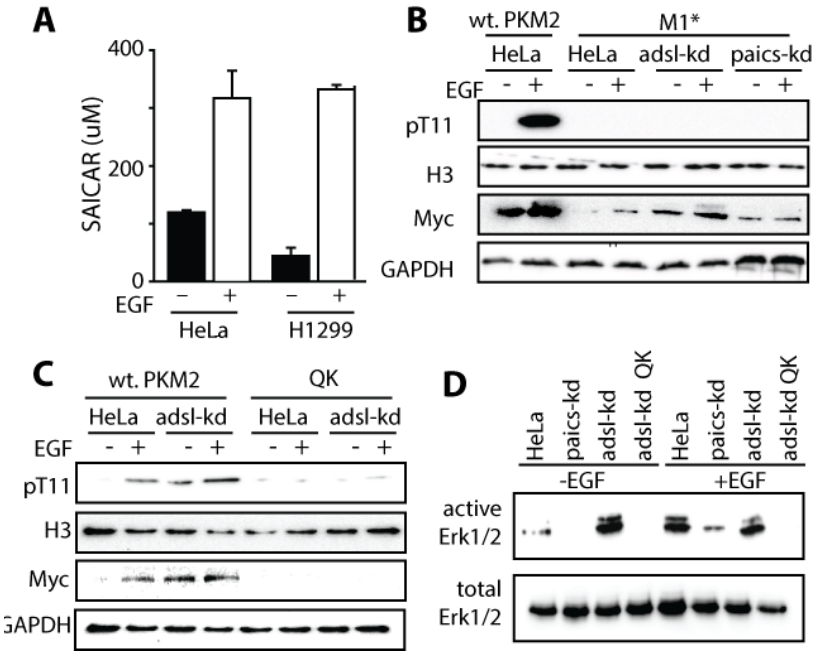

Figure 3-7. SAICAR-PKM2 interaction is necessary and sufficient to induce H3 T11 and Erk1/2 phosphorylation. (A) Addition of EGF (10 ng/mL; 2 hrs) is sufficient to induce cellular concentration of SAICAR in HeLa and in H1299 cells. Mean +/- SEM are noted (n = 3). (B and C) Effect of PKM2-SAICAR interaction on EGF-dependent phosphorylation of H3 T11 and *MYC* expression. Cells were incubated in EGF-free DMEM (DMEM, 25 g/L glucose, 10% dialyzed FBS) or for 3 hrs in medium supplemented with 10 ng/mL EGF. 'M1*' and 'QK' denote cells in which endogenous PKM1 and PKM2 were knocked down, and knockdown resistant PKM1 or SAICAR-insensitive PKM2 Q393K mutant from plasmids were expressed, respectively. (D) Effect of PKM2-SAICAR interaction on Erk1/2 activation.

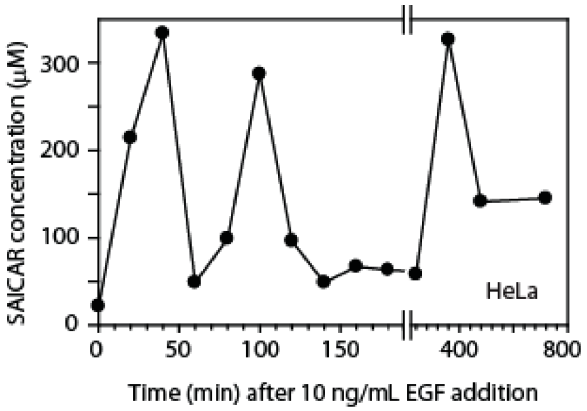

Figure 3-8. Effect of EGF addition on the cellular concentration of SAICAR in HeLa cells. HeLa cells were incubated in DMEM supplemented with dialyzed FBS (10%) for 24 hrs. The medium was replaced with medium supplemented with dialyzed FBS and 10 ng/mL recombinant human EGF. Cells were harvested at each time point and cellular concentration of SAICAR was analyzed using LC-MS as previously described (Keller et al., 2012).

accumulation of Myc. The phosphorylation of H3 T11 by PKM2-SAICAR in EGF-treated cells was also specific to H3.1 subtype (**Fig. 3-2**).

In a similar manner, we probed the activation of Erk1/2 in HeLa cells (**Figure 3-7D**). In HeLa cells, addition of EGF induces activation of Erk1/2 as expected. Cells with constitutively elevated levels of SAICAR (*adsl-kd*) showed constitutive activation of Erk1/2, while *paics-kd* cells were unable to activate Erk1/2 in response to EGF (**Fig. 3-7D**). Additionally, the PKM2-SAICAR interaction was required for Erk1/2 activation in cells, as replacing endogenous PKM2 with the SAICAR-insensitive PKM2 Q393K mutant (QK in **Fig. 3-7D**) was sufficient to prevent Erk1/2 activation in *adsl-kd* cells. Overall, our results show that PKM2-SAICAR phosphorylates protein substrates (histone H3 and Erk1/2) in cancer cells.

Positive feedback regulation between PKM2-SAICAR and Erk1/2

Recently, Erk2 was reported to phosphorylate PKM2, which is required for PKM2's nuclear translocation and subsequent protein kinase activity (Yang et al., 2012b). Along with our data, these results indicate that PKM2-SAICAR and Erk1/2 may form a positive feedback regulation loop, where the activation of one protein renders the other more likely to be activated. To test this possibility, we phosphorylated recombinant PKM2 with constitutively active Erk2. After phosphorylation, recombinant PKM2 was re-purified and subjected to pyruvate kinase (**Fig. 3-9A**) and histone H3 T11 kinase (**Fig. 3-9B**) activity assays. Upon

Erk2-mediated phosphorylation, PKM2 became far more sensitive to SAICAR (EC_{50} shifts from 0.3 mM to 10 μM SAICAR). Considering that the cellular concentration of SAICAR in non-stimulated cancer cells ranges between 10-100 μM (Keller et al, 2012), our results indicate that Erk-mediated phosphorylation sensitizes PKM2 to SAICAR, even when the cellular concentration of SAICAR is restored to the original level. Thus, our results support the previous finding that the phosphorylation of PKM2 alone induces nuclear localization and cell proliferation in cells (Yang et al, 2012b). Together, these results indicate that PKM2-SAICAR and Erk1/2 are mutually sensitizing each other to promote MAPK protein kinase signaling (**Fig. 3-9C**).

PKM2-SAICAR is necessary and sufficient for proliferation signaling

A common consequence of a positive feedback loop is a switch-like behavior (Mitrophanov and Groisman, 2008). Because PKM2-SAICAR and Erk1/2 form a positive feedback loop *in vitro*, PKM2-SAICAR may contribute to sustained proliferative signaling, a hallmark of cancer cells (Hanahan and Weinberg, 2012). To test this possibility, HeLa cells and their derivatives were briefly (30 min) incubated with medium containing EGF. The medium was then replaced with medium lacking EGF, and the activation of Erk1/2 over time was monitored (**Fig. 3-9D**). In comparison with non-transfected HeLa cells, *adsl-kd* cells showed a more rapid activation of Erk1/2, which supports our view that PKM2-SAICAR primes Erk1/2 activation (**Fig. 3-7A-B**). In addition, the activation

Figure 3-9. SAICAR-PKM2 interaction is necessary and sufficient for sustained proliferative signaling. (A and B) Phosphorylation of PKM2 by active Erk1 sensitizes PKM2 for SAICAR binding. Recombinant PKM2 was phosphorylated by active GST-tagged Erk1. The effect of the phosphorylation on PKM2's sensitivity was measured (A) by monitoring pyruvate kinase activity (mean +/- SEM. are noted; n =3) and (B) by monitoring H3.1 T11 kinase activity. Upon phosphorylation by Erk1/2, PKM2 becomes more sensitive (EC_{50} 0.30 mM and 12 μM SAICAR before and after phosphorylation by Erk1/2, respectively). (C) A schematic summary. (D) Effect of SAICAR-PKM2 on the activation of Erk1/2. HeLa, *adsl-kd*, QK, and *adsl-kd* QK, SA, and *adsl-kd* SA cells were grown in DMEM supplemented with dialyzed FBS, briefly incubated in medium containing 10 ng/mL recombinant EGF, and then incubated in EGF-free medium. Cells were harvested, and Erk1/2 activation was monitored by Western blot, probing with antibody activated Erk1/2. (E) Effect of SAICAR-PKM2 on cell proliferation. Cells with increased SAICAR had an increased proliferation rate, regardless of the addition of EGF. Those cells without inducible SAICAR levels or those where the PKM2-SAICAR interaction was disrupted showed less sensitivity to growth factor addition.

*Figure presented on following page

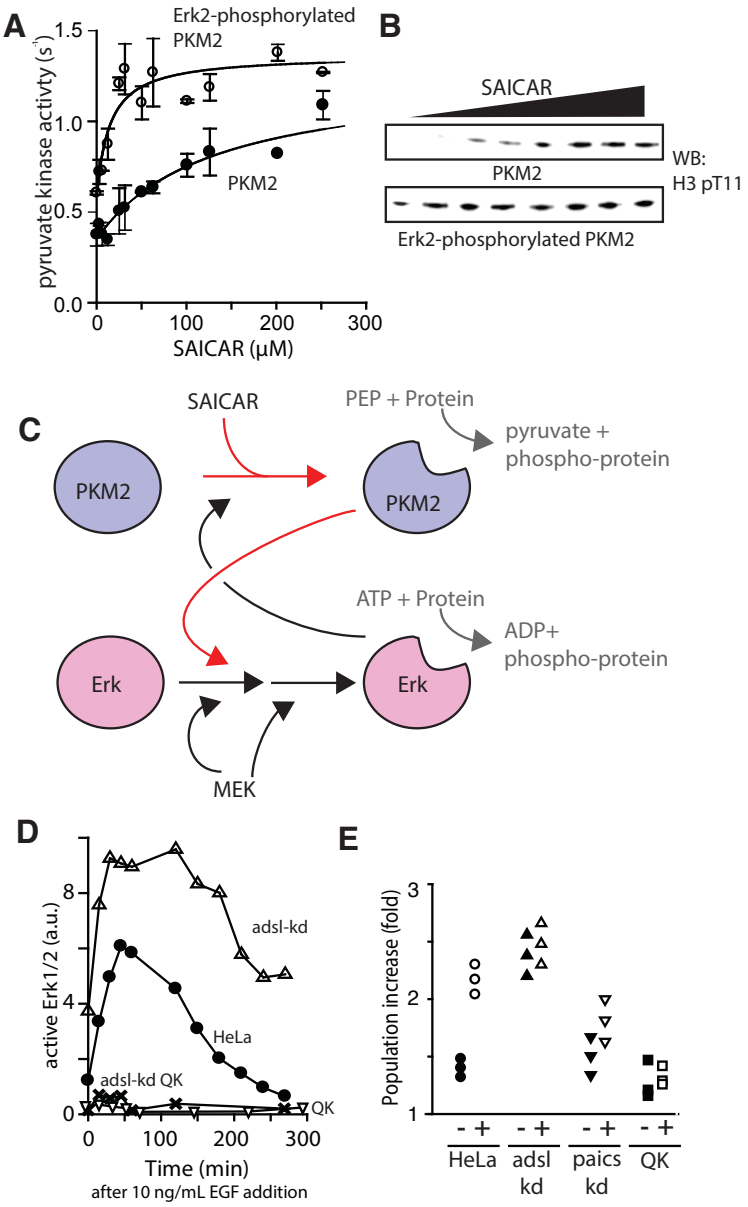

.

Figure 3-9. SAICAR-PKM2 interaction is necessary and sufficient for sustained proliferative signaling

of Erk1/2 in *adsl-kd* cells was sustained for a longer period of time (**Fig. 3-9D**). Replacing PKM2 with the SAICAR-insensitive PKM2 Q393K (or QK) mutant in wild-type or *adsl-kd* cells showed only marginal activation of Erk1/2 in comparison to HeLa cells, indicating that PKM2-SAICAR is a core component required to sustain Erk1/2 activation (**Fig. 3-9D**).

To further examine our proposed positive feedback loop, we next replaced PKM2 with the PKM2 S37A mutant that is insensitive to Erk1/2 (Yang et al. 2012b). First, we purified recombinant PKM2 S37A and determined the kinetic parameters. In our hands, the activity of PKM2 S37A is slightly lower than wild type PKM2 (**Fig. 3-10A**, k_{cat}: 0.5 s^{-1}, wild type k_{cat}: 2-4 s^{-1}). PKM2 S37A is still sensitive to SAICAR in both pyruvate kinase activity (**Fig. 3-10B**, $EC_{50} \sim 250$ μM SAICAR) and protein kinase activity (**Fig. 3-10C**) assays. We then replaced wild type PKM2 with PKM2 S37A mutant in HeLa and *adsl-kd* cells ('SA' and 'SA adsl-kd' in **Fig. 3-10D**). When Erk1/2 signaling in these cells was monitored, the activation of Erk1/2 in PKM2 S37A cells was more rapidly diminished (**Fig. 3-9D**). This result is consistent with the mutual sensitization model (**Fig. 3-9C**).

We next sought to determine whether the PKM2-SAICAR interaction is necessary for mitogen-induced cell proliferation (**Fig. 3-9E**). HeLa cells and their derivatives were incubated for one day in the presence or absence of EGF, and the population size increase was monitored. As expected, EGF stimulated the proliferation of HeLa cells, while *adsl-kd* cells showed constitutive hyper-proliferation. Conversely, EGF only marginally stimulated the proliferation of

paics-kd cells. Additionally, cells where endogenous PKM2 was replaced with the PKM2 Q393K mutant were also nearly insensitive to EGF. Thus, our results support that SAICAR and its interaction with PKM2 are necessary for the mitogen-induced proliferation of cancer cells. Finally, we replaced endogenous PKM2 is replaced with the non-phosphorylatable S37A mutant, which is reported to be excluded from the nucleus (Yang et al. 2012b). EGF did not significantly stimulate proliferation in HeLa cells with PKM2 S37A mutant (**Fig. 3-9 and 3-10E**). Cells over-accumulating SAICAR (adsl-kd) were also affected by the replacement of PKM2 with PKM2 S37A mutant, and were not stimulated by EGF or SAICAR. These results show that the sustained Erk signaling mediated by the mutual sensitization of PKM2-SAICAR and Erk is a necessary component for the mitogen-induced proliferation.

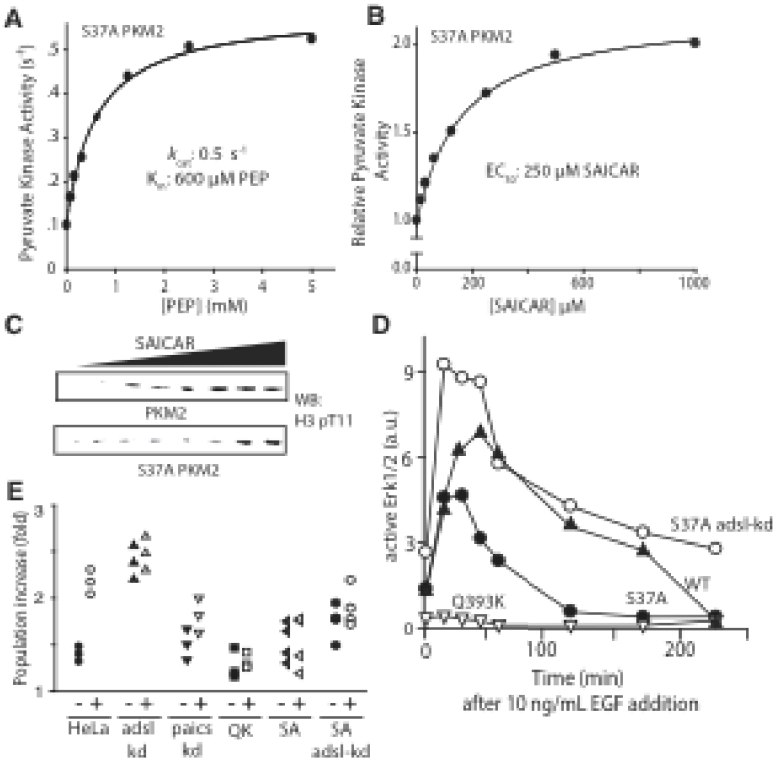

Figure 3-10. Characterization of PKM2 S37A mutant's enzyme activities (**A**) Pyruvate kinase activity assay (rate constants) with varying amount of PEP indicates that PKM2 S37A mutant has pyruvate kinase activity similar to the wild-type PKM2 although kinetic parameters are slightly different (k: 0.5 s^{-1}; K_m: 600 mM PEP). (**B** and **C**) PKM2 S37A mutant is as sensitive to SAICAR as wild type PKM2 in both pyruvate kinase activity (**B**) and histone H3.1 T11 kinase activity (**C**). **(D)** Effect of phosphorylation of PKM2 on Erk1/2 signaling. Disruption of phosphorylation of PKM2 by S37A mutant lead to decreased Erk1/2 signaling in both wild type and *adsl-kd* cells. **(E)** Effect of SAICAR-PKM2 on cell proliferation. Non-phosphorylatable PKM2 mutant containing cells showed less sensitivity to growth factor addition.

DISCUSSION

Protein kinases are known to play important regulatory roles in many biological processes. In eukaryotic cells, well-defined families of protein kinases catalyze protein phosphorylation. These typical protein kinases use ATP as a phosphate donor, and share common structural and sequence features. In addition to these classical protein kinases, there has been speculation that other energetic molecules, like PEP, may play a role in protein phosphorylation in mammalian cells, but an enzyme catalyzing this reaction was not identified (Jeyasingham and Carlson, 1998; Khandelwal et al., 1983). In bacteria, PEP can be used for protein phosphorylation, as shown in the PEP-dependent sugar phosphotransferase system of *Bacillus* (Postma et al., 1993). PKM2 is the first identified mammalian protein, to our knowledge, that phosphorylates protein substrates using PEP as a phosphate donor. However, because recombinant PKM2 alone was unable to reproduce the results obtained with PKM2 purified from cancer cells, investigating the molecular basis of this novel protein kinase activity was difficult. In this paper, we showed that metabolite binding is sufficient to induce the protein kinase activity of PKM2. Our results can expand our understanding of protein kinases by identifying a new dimension of regulation.

In addition to the previously known substrate histone H3 (Yang et al., 2012a), we also identified many human proteins as potential substrates for PKM2-SAICAR, with the vast majority of proteins involved in the regulation of cell proliferation. Further investigation on how PKM2-SAICAR recognizes its

substrates may reveal a previously unrecognized feature common to these proteins involved in cell cycle regulation.

Previous work on PKM2 has revealed an interaction between MAPK activity and PKM2, showing that Erk1/2 phosphorylates PKM2 (Yang et al., 2012b). In our work, the reciprocal reaction – phosphorylation of MAPK protein kinases by PKM2 – also occurs *in vitro* and in cells upon the binding of SAICAR to PKM2. Our result challenges the view that PKM2 is a passive recipient of MAPK protein kinase signaling and suggests that PKM2 is a more active component that is necessary for the MAPK protein kinase signaling.

Intricately related to MAPK activity is cell cycle control and proliferation. As has been well documented, malignant tumor cells frequently display sustained proliferation. Many different mechanisms such as mutations in genes encoding MAPK signaling contribute to the sustained proliferation of cancer cells. However, many types of cancer cells show sustained proliferation without showing any mutations in these genes. The altered metabolism associated with most cancer cells, including upregulation of PKM2, may thus be a mechanism to sustain cell proliferation in those cells.

MATERIALS AND METHODS

Materials

The preparation of SAICAR, analysis of cellular SAICAR concentration, recombinant PKM2, and pyruvate kinase assays were performed as previously described (Keller et al., 2012). Plasmids for bacterial expression of human Erk1 (Addgene plasmid 29578) and active Mek2 (Addgene plasmid 29580), which were originally constructed by D. Maly (U. Washington), were obtained from Addgene. Expression plasmid for GST-PAK2 (Addgene plasmid 31671) was originally constructed by A. Brunet lab (Banko et al, 2011). Plasmids encoding mutant Erk1 and PKM2 were constructed using QuikChange Lightening site directed mutagenesis kit (Agilent). Plasmids constructed in our lab were sequenced from both ends of inserts or mutation sites.

Proteins

Recombinant Erk1 (and its mutants), constitutively active MEK2, MAPK11, and GST-PAK2 were expressed in *E. coli* BL21 Codonplus RIL (DE3) cells harboring appropriate plasmids. Cells were grown in 0.50 liter Terrific Broth supplemented with chloramphenicol (25 μg/mL) and ampicillin (50 μg/mL) or kanamycin (50 μg/mL) at 37°C until optical density at 600 nm (OD_{600}) reached 0.6-0.8. Protein expression was induced by the addition of isopropylthio-β-d-galactopyranoside to 0.5 mM followed by incubation at 22°C for 12-18 hours. All subsequent steps were carried out at 4°C or on ice unless specifically noted

otherwise. Cells were collected by centrifugation (5,000 g 20 min), and the cell pellet was resuspended in lysis buffer (20 mM HEPES, 500 mM NaCl, 5% glycerol, 1 mM DTT, 10 mM imidazole, pH 7.4 for His-tag proteins; 50 mM Tris-HCl, pH 8.0, 150 mM NaCl, 1 mM DTT for GST-tagged proteins) supplemented with phenylmethylsulfonyl fluoride (0.3 mM). Cells were lysed by sonication, and cell debris was removed by centrifugation (15,000g for 20 min). Cleared lysate was applied to 5 mL HiTrap Chelating column (for His-tagged proteins; charged with zinc chloride) or 5 mL GST Capture Column (for GST-tagged proteins). After washing with lysis buffer until A_{280} reached baseline, bound proteins were eluted with linear gradient of the lysis buffer supplemented with 500 mM imidazole (for His-tagged proteins) or 10 mM reduced glutathione (for GST-tagged proteins). SDS-PAGE and Commassie Blue staining determined the fractions containing protein. Desired fractions were combined and dialyzed against 10 mM sodium phosphate, 1.8 mM potassium phosphate, pH 7.4, 137 mM NaCl, 2.7 mM KCl, 5% glycerol, 0.5 mM EDTA, 2 mM DTT buffer. Proteins were concentrated, if desired, using Amicon Ultracel centrifugal filters. Protein concentrations were determined by measuring absorbance at 280 nm in denaturing conditions as in literature (Edelhoch, 1969), and stored at -80°C or at 4°C. Recombinant Erk1 was stable only for about a week after its purification in our hands, and was thus used within a week of lysis. Recombinant histone H3, H3/H4 tetramer, and H2A/H2B tetramer were purchased from New England Biolabs. Purified nucleosomes were gifts from G. Bowman's lab (Johns Hopkins University). The

purified nucleosomes were found to contain H3 pT11, according to our Western analysis. Thus, the nucleosome was treated with biotinylated alkaline phosphatase (NEB). The alkaline phosphatase was removed from the reaction using 25 uL magnetic avidin beads (Pierce) and then the remaining dephosphorylated nucleosome was used for **Figure 1**. Recombinant human EGF was purchased from Sigma-Aldrich. Recombinant Grb2, Mek2, B-Raf, and EGFR expressed and purified from insect cells were purchased from Invitrogen.

Cell culture

Mammalian cells were maintained and propagated in Dulbecco's Modified Eagle Medium (DMEM; 4 g/L glucose, 4 mM glutamine, without pyruvate) supplemented with 10% undialyzed fetal bovine serum (FBS), penicillin, and streptomycin at 37°C, 5% carbon dioxide, and humid conditions unless specifically noted otherwise. For glucose depletion or controlled EGF experiments, dialyzed FBS (Invitrogen) was used instead of normal FBS. For glucose depletion experiments, glucose-free DMEM (Invitrogen) was used. For controlled EGF experiments, recombinant EGF (10 ng/mL; Sigma-Aldrich) was added to medium containing dialyzed FBS. Cells were transfected with plasmids using the Neon Nucleotransfector (Invitrogen) using cell-type specific parameters provided by the vendor. Cell viability was determined using tryphan blue cell staining. To count cell numbers, cells were resuspended in trypsin/EDTA

solution, diluted immediately with isotonic buffer, and then counted using a Moxi-Z cell counter.

Subcellular localization of PKM2

HeLa cells grown on coverslips were washed with PBS, fixed with 4% paraformaldehyde in phosphate buffered saline (PBS) for 5 min at room temperature, permeabilized with 0.01% Triton-X-100 in PBS for 5 min at room temperature, incubated in 5% goat serum in PBS for 1 hour, and stained with rabbit anti-PKM2 antibody (Sigma) for 45 min. Following incubation with solution containing DAPI and TRITC-conjugated secondary antibody (Sigma), microscopic images were obtained using a Zeiss AxioVert 200 fluorescence microscope (Integrated Imaging Center, Johns Hopkins University, 63x optical zoom).

Protein Microarray

Human Protein Microarray ProtoArray v5.0 slide (Invitrogen) was blocked in 5% protease-free BSA (Roche) diluted in HPLC grade water (Fisher) for 30 minutes at room temperature without rocking and subsequently washed three times with HPLC grade water. The slide was then immersed into a 5-mL solution containing 10 nM rPKM2, 5% glycerol, 6.2 mM $MgCl_2$, 150 mM KCl, 10 mM HEPES, pH 7.4, and 0 or 0.5 mM SAICAR at 37°C for 30 minutes, followed by the addition of 0.5 mM PEP and incubated at 37°C for another 30 minutes. The

slide was washed three times with HPLC grade water. A Pro-Q Diamond Phosphoprotein Stain Kit (Invitrogen) was used to stain phosphorylated proteins using the protocol provided by the vendor for staining of nitrocellulose blots. Fluorescence signals were detected using a Typhoon 9410 Variable Mode Imager (excitation 550 nm, excitation 580 nm, 600 PMT, 10 um particle size; Integrated Imaging Center, Johns Hopkins University). Images were analyzed using ImageJ software with a microarray plugin. Sub-arrays were aligned using AlexaFluor-conjugated protein spots in each subarray.

Spectroscopic analysis of PKM2's protein kinase activity

Assay performed under similar condition to typical pyruvate kinase assays. The experiment was carried out in the absence of ADP or other nucleotides. In short, PKM2 (10 nM) was incubated for 30 minutes at 37°C with varying recombinant histone H3.1 concentrations in buffer (10 mM HEPES pH 7.4, 100 mM KCl, 6.2 mM $MgSO_4$) in the presence or absence of 500 uM SAICAR. After incubation, NADH (0.2 mM) and LDH (50 U/mL) were added, and immediately before detection, PEP (200 uM) was added. Change in fluorescence was measured for 30 minutes (excitation: 540 nm/emission: 590 nm), using the Tecan Infinite Series 200 Pro.

Protein kinase assays

The reaction solution [0.1-10 nM PKM2, 0-4 μM histone (NEB, typically 1 uM H3 monomer concentration), 150 μM PEP, 50 mM HEPES, pH 7.4, 100 mM potassium chloride, 6.2 mM magnesium acetate, and 5% glycerol] was incubated at 25°C for 1-120 minutes (typically 5 min). After the reaction, the solution was mixed with an equal volume of SDS-gel loading buffer (375 mM Tris-HCl, pH 8, 10% SDS, 50% glycerol, 1 mM DTT, 0.1% bromophenol blue) and incubated at 95^{o}C for 10 minutes. All other protein kinase assays were performed as described, with a fixed concentration of PKM2 (10 nM), for 30 minutes, unless specifically noted otherwise. Solutions were subjected to SDS-PAGE, staining with ProQ Diamond (Invitrogen), or Western blot analysis. For the determination of catalytic efficiency (k_{cat}), a reaction was carried out with higher concentration of PKM2 (10 nM) for 1 hour, and the resulting signal was assumed to represent the completed reaction.

Western Blot

Western blots were performed as described by AbCam. In brief, cells were lysed in ice-cold RIPA buffer (20 mM Tris-HCl, pH 7.5, 150 mM NaCl, 1 mM EDTA, 1 mM EGTA, 1% NP-40, 1% sodium deoxycholate) supplemented with 1 mM phenylmethylsulfonyl fluoride and 1 mM sodium fluoride, and total protein amount was measured using a Pierce 660 reagent (Thermo Scientific) with bovine serum albumin as a standard. Proteins were separated by SDS-PAGE, and transferred to nitrocellulose membranes. The membrane was blocked with

phosphate-buffered saline (PBS) supplemented with 5% bovine serum albumin, and probed with the appropriate primary antibody (rabbit anti-phospho-p42/p44, rabbit anti-p42/p44, rabbit anti-pT11-Histone H3, and rabbit anti-Histone H3 from Cell Signaling; rabbit anti-GAPDH and mouse-anti-Myc from Sigma-Aldrich) overnight at 4°C. After primary antibody incubation, membranes were probed with horseradish peroxidase (HRP) conjugated goat anti-rabbit IgG or goat anti-mouse IgG secondary antibodies (Bio-Rad). HRP-conjugated secondary antibodies were then detected using commercial chemiluminescence substrates (Pierce). Chemiluminescence images were acquired using a FluorChem M FM0455 imager.

Protein microarray experiments

Protein microarray experiments were carried out using Invitrogen Human protein microarrays, recombinant PKM2, and PEP in the presence and in the absence of SAICAR. Phosphorylated proteins were detected using ProQ Diamond stain (Invitrogen). An extensive description of this experiment is provided in the Supplementary Information.

Phosphorylation of PKM2

Recombinant PKM2 (1 μM) and recombinant GST-Erk1 (10 nM) were incubated together in a buffer containing 1 mM ATP, 50 mM Tris-HCl, pH 7.0, 150 mM NaCl, 1 mM DTT, 1 mM $MgCl_2$ for 30 minutes at 25°C. The reaction

solution was passed through glutathione-agarose resin (Sigma-Aldrich) to deplete GST-Erk1. Unbound proteins were eluted with 50 mM Tris, pH 8.0, 150 mM NaCl, 1 mM DTT, 1 mM MgCl2 buffer. Fractions were then subjected to SDS-PAGE and either Coomassie or Pro-Q diamond staining (Invitrogen). Fractions containing phosphorylated PKM2 were identified using Pro-Q diamond staining. Concentration of phosphorylated PKM2 was determined by measuring A280 in denaturing conditions (Edelhoch, 1969) using a calculated extinction coefficient (28,910 M^{-1} cm^{-1}).

Erk1/2 activity assay

A 10 μL reaction (25 nM rPKM2, 1 μM rErk1, 150 μM PEP, 50 mM HEPES pH 7.4, 100 mM potassium chloride, 10% glycerol, 6.2 mM magnesium chloride, and 1 mM DTT) was incubated for 30 minutes at room temperature. The Erk1 reaction was serially diluted using water, and 8 μL of diluted solution was added to 32 μL Omnia Kinase Assay solution (10 μM Omnia Peptide 17, 1 mM ATP, 0.2 mM DTT, and proprietary buffer components from the vendor; Invitrogen) in a black transparent bottom 96-well plate. The emission at 485 nm (excitation at 360 nm) was recorded every minute for 60 minutes at 30°C using a Tecan Infinity M2 fluorescence microplate reader.

REFERENCES

Anastasiou, D., Yu, Y., Israelsen, W.J., Jiang, J.K., et al. (2012) Pyruvate kinase M2 activators promote tetramer formation and suppress tumorigenesis. Nat. Chem. Biol. *8*, 839-847.

Bartek, J., Lukas, C., and Lukas, J. (2004) Checking on DNA damage in S phase. Nat. Rev. Mol. Cell Biol. *5*, 792-804.

Carpenter, G. (1987) Receptors for epidermal growth-factor and other polypeptide mitogens. Annu. Rev. Biochem. *56*, 881-914.

Chang, L.F., and Karin, M. (2001) Mammalian MAP kinase signaling cascades. Nature *410*, 37-40.

Chen, J., Xie, J., Jiang, Z., Wang, B., Wang, Y., Hu, X. (2011) Shikonin and its analogs inhibit cancer cell glycolysis by targeting tumor pyruvate kinase-M2. Oncogene *30*, 4297-4306.

Christofk, H.R., Vander Heiden, M.G., Harris, M.H., Ramanathan, A., Gerszten, R.E., Wei, R., Fleming, M.D., Schreiber, S.L., and Cantley, L.C. (2008) The M2 splice isoform of pyruvate kinase is important for cancer metabolism and tumor growth. Nature *452*, 230-233.

Chung, S., Arrell, D.K., Faustino, R.S., Terzic, A., Dzeja, P.P. (2010) Glycolytic network restructuring integral to energetics of embryonic stem cell cardiac differentiation. J. Mol. Cell Cardiol. *48*, 725-734.

Crews, C.M., Erickson, R.L. (1993) Extracellular signals and reversible protein phosphorylation – What to MEK of it all. Cell *74*, 215-217.

Edelhoch, H. (1969) Spectroscopic determination of tryptophan and tyrosine in proteins. Biochemistry *6*, 1948-1954.

Gao, X., Wang, H., Yang, J.J, Liu, X, and Liu, Z.R. (2012) Pyruvate kinase M2 regulates gene transcription by acting as a protein kinase. Mol. Cell *45*, 598-609.

Gupta, V., and Bamezai, R.N. (2013) Human pyruvate kinase M2: a multifunctional protein. Protein Sci. *19*, 2031-2044.

Hake, S.B., and Allis, C.D. (2006) Histone H3 variants and their potential role in indexing mammalian genomes: the “H3 barcode hypothesis”. Proc. Natl. Acad. Sci. U.S.A. *103*, 6428-6435.

Hanahan, D., and Weinberg, R.A. (2011) Hallmarks of cancer: the next generation. Cell *144*, 646-674.

Hanks, S.K., Quinn, A.M., and Hunter, T. (1988) The protein kinase family: conserved features and deduced phylogeny of the catalytic domains. Science *241*, 42-52.

Haystead, T.A.J., Dent, P., Wu, J., Haystead, C.M.M., and Sturgill, T.W. (1992) Ordered phosphorylation of p42MAPK by MAP kinase kinase. FEBS Lett. *306*, 17-22.

Jeyasingham, M.D., and Carlson, G.M. (1998) Evaluation of phosphoenolpyruvate as a phosphoryl group donor for phosphoproteins in skeletal muscle. Arch. Biochem. Biophys. *357*, 285-292.

Jiang, Y., Li, X., Yang, W., Hawke D.H., Xia, Y., Aldape, K., Wei, C., Guo, F., Chen, Y., and Lu, Z. (2014) PKM2 regulates chromosome segregation and mitosis progression of tumor cells. Molecular Cell*. pii: S1097-2765(13)00826-5. doi: 10.1016/j.molcel.2013.11.001*

Khandelwal, R.L., Mattoo, R.L., Waygood, E.B. (1983) Phosphoenolpyruvate-dependent protein kinase activity in rat skeletal muscle. FEBS Lett. *162*, 127-132.

Keller, K.E., Tan, I.S., and Lee, Y.S. (2012) SAICAR stimulates pyruvate kinase isoform M2 and promotes cancer cell survival in glucose-limited conditions. Science *338*, 1069-1072.

Kim, H., Heo, K., Choi, J., Kim, K., An, W. (2011) Histone variant H3.3 stimulates HSP70 transcription through cooperation with HP1 γ. Nucleic Acids Res. *39*, 8329-8341.

Koppenol, W.H., Bounds, P.L., and Dang, C.V. (2011) Otto Warburg's contributions to current concepts of cancer metabolism. Nature Rev. Cancer *11*, 325-337.

Lee, J., Kim, H.K., Han, Y.M., Kim, J. (2008) Pyruvate kinase isozyme type M2 (PKM2) interacts and cooperates with Oct-4 in regulating transcription. Int. J. Biochem. Cell Biol. *40*, 1043-1054.

Luo, W., Hu, H., Chang, R., Zhong, J., Knabel, M., O'Meally, R., Cole, R.N., Pandey, A., and Semenza, G.L. (2011) Pyruvate kinase M2 is a PHD3-stimulated coactivator for hypoxia-inducible factor 1. Cell *145*, 732-744.

Luo, W., and Semenza, G.L. (2012) Emerging roles of PKM2 in cell metabolism and cancer progression. Trends Endocrinol. Metab. *23*, 560-566.

Mazurek, S., Grimm, H., Boschek, C.B., Vaupel, P., and Eigenbrodt, E. (2002) Pyruvate kinase type M2: a crossroad in the tumor metabolome. Br. J. Nutr. *S1*, S23-S29.

Mazurek, S. (2011) Pyurvate kinase type M2: a key regulator of the metabolic budget system in tumor cells. Int. J. Biochem. Cell Biol. *43*, 969-980.

Mitrophanov, A.Y., and Groisman, E.A. (2008) Positive feedback in cellular control systems. Bioessays. *30*, 542-555.

Nilsson, I., and Hoffmann, I. (2000) Cell cycle regulation by the Cdc25 phosphatase family. Prog. Cell Cycle Res. *4*, 107-114.

Pearson, G., Robinson, F., Gibson, T.B., Xu, B.E., Karandikar, M., Berman, K., Cobb, M.H. (2001) Mitogen-activated protein (MAP) kinase pathways: regulation and physiological functions. Endocrine Rev. *22*, 153-183.

Postma, P.W., Lengeler, J.W., Jacobson, G.R. (1993) Phosphoenolpyruvate:carbohydrate phosphotransferase systems of bacteria. Microbiol. Mol. Biol. Rev. *57*, 543-594.

Roskoski, R. Jr. (2012) Erk1/2 MAP kinases: structure, function, and regulation. Pharmacol. Res. *66*, 105-143.

Sugden, P.H., Markou, T., Fuller, S.J., Tham, E.L., Molkentin, J.D., Paterson, H.F., Clerk, A. (2011) Monophosphothreonyl extracellular signal-regulated kinases 1 and 2 (ERK1/2) are formed endogenously in intact cardiac myocytes and are enzymically active. Cell Signal. *23*, 468-477.

Vander Heiden, M.G., Cantley, L.C., Thompson, C.B. (2009) Understanding the Warburg effect: the metabolic requirements of cell proliferation. Science *324*, 1029-1033.

Vander Heiden, M.G. (2013) Exploiting tumor metabolism: challenges for clinical translation. J. Clin. Invest. *123*, 3648-3651.

Yang, W., Xia, Y, Ji, H., Zheng, Y., Liang, J., Huang, W., Gao, X., Aldape, K., and Lu, Z. (2011) Nuclear PKM2 regulates beta-catenin transactivation upon EGFR activation. Nature *480*, 118-122.

Yang, W., Xia, Y., Hawke, D., Li, X, Liang, J., Xing, D., Aldape, K., Hunter, T., Alfred Yung, W.K., and Lu, Z. (2012a) PKM2 phosphorylates histone H3 and promotes gene transcription and tumorigenesis. Cell *150*, 685-696.

Yang, W., Zheng, Y., Xia, Y., Ji, H., Chen, X., Guo, F., Lyssiotis, C.A., Aldape, K., Cantley, L.C., Lu, Z., (2012b) Erk1/2-dependent phosphorylation and nuclear translocalization of PKM2 promotes the Warburg effect. Nat. Cell. Biol. *14*, 1295-1304.

CHAPTER 4

Investigating the elements and mechanism of

SAICAR accumulation in cancer cells

ABSTRACT

The cellular metabolite SAICAR has been shown to be important for cancer cell proliferation and survival by activating the pyruvate kinase and protein kinase activities of PKM2. As a response to both glucose starvation and EGF addition, SAICAR levels accumulate in cells, but the mechanism leading to this accumulation were not understood. Here, we report that SAICAR accumulation is not limited to glucose-depletion or EGF addition, but is more likely a common phenomenon upon growth stimulating conditions. Compounds promoting cell differentiation, apoptosis, or those without their cognate receptor did not lead to cellular SAICAR accumulation. Additionally, the protein level of the SAICAR synthetase, PAICS, was elevated in conditions that lead to SAICAR accumulation, but not in those in which SAICAR levels remained unchanged. Downstream elements, including Erk1/2 activation, histone H3 phosphorylation, and PKM2 nuclear localization occurred in a manner consistent with cellular SAICAR levels. PAICS protein level was stabilized by the addition of growth factor, independent of transcription or translation. Furthermore, metabolic flux in SAICAR accumulating conditions is consistent with activation of PAICS protein, rather than inhibition of SAICAR cleavage through ADSL. Finally, we found that PAICS protein level is elevated by at least two-fold in 95% of human cancers. Taken together, these data suggest that cancer cells rely upon a common mechanism to couple cell proliferation and metabolic flux in a variety of conditions. Additionally, PAICS protein appears to be a previously unrecognized

target of the MAPK cascade, adding a layer of complexity to cell coordination upon external stimuli.

INTRODUCTION

Cancer cells must coordinate their cellular response with external stimuli to thrive in the tumor microenvironment (1). However, it has been well documented that tumor cells have reduced dependence on external growth factor signaling (2). In some cases, cancer cells produce growth factors themselves or express constitutively active mutants of proteins involved in signaling cascades (2).

To accomplish this, cancer cells express distinct proteins that differ from their normal cell counterparts. Among these expressed proteins is the glycolytic enzyme pyruvate kinase M2 (PKM2). PKM2 is one of four isoforms of pyruvate kinase in humans, which all catalyze the final step of glycolysis, generating pyruvate and ATP from phosphoenol pyruvate (PEP) and ADP (3). Unlike the other isoforms, PKM2 is highly expressed in highly proliferating cells, including both fetal and cancer cells. (3,4). Although PKM2 is less active biochemically than its counterpart PKM1, PKM2 is known to play important roles in both cancer cell growth and proliferation in stress conditions (3,4).

Recently, PKM2 was shown to be activated by the cellular metabolite succinyl-aminoimidazole-carboaximide ribosyl-5'-phosphate (SAICAR) in both pyruvate and protein kinase activity (5,6). Cellular SAICAR accumulates upon glucose starvation and epidermal growth factor (EGF) addition and binds to PKM2 (6). The interaction between PKM2-SAICAR prolongs the MAPK signaling cascade by activating Erk1/2 and participating in a positive feedback loop (6).

Additionally, SAICAR promotes nuclear localization of PKM2 and the phosphorylation of histone H3, enhancing expression of target genes such as c-Myc (6). Furthermore, the PKM2-SAICAR complex was shown to phosphorylate over 100 cellular proteins, many with roles in cell proliferation and growth (6).

While the role of the PKM2-SAICAR interaction is now more defined, the mechanism by which SAICAR accumulates and conditions in which accumulation occurs are both unexplored. The biosynthetic pathway in which SAICAR is generated and degraded is well defined, although little research has investigated the regulation of these specific enzymatic steps. SAICAR generation is step seven of the *de novo* purine nucleotide synthesis pathway and is produced by the enzyme phosphoribosylaminoimidazole carboxylase (PAICS, also known as SAICAR synthetase, (7)). PAICS catalyzes two sequential steps in the purine biosynthesis pathway (7):

(1) AIR[1] + CO_2 → = CAIR[2]

(2) CAIR + L-aspartate + ATP → SAICAR + ADP + P_i

Cancer cells often utilize *de novo* nucleotide synthesis instead of the salvage pathways most normal cells use. Thus, many cancers exhibit increased sensitivity to perturbations in *de novo* nucleotide synthesis pathways, and have become targets for anti-cancer drugs (8, 9). As of yet, PAICS regulators have not been studied. However, the enzymatic activity of PAICS has been targeted. L-alanosine, an analog of L-aspartate, can be metabolized by PAICS into a

[1] 5'-phosphoribosyl-5-aminoimidazole = AIR
[2] 5'-phosphoribosyl-4-carboxy-5-aminoimidazole = CAIR

potent inhibitor of adenylosuccinate synthetase, which performs the first committed step of *de novo* AMP biosynthesis, and is currently on the market as an anti-cancer drug (8). However, the sensitivity to this drug is limited to cancers with a deficiency in methylthioadenosine phosphorylase.

SAICAR is cleaved by ADSL in step eight of *de novo* purine biosynthesis. Interestingly, ADSL also performs two enzymatic reactions, but the reactions are non-sequential (11):

(3) SAICAR → AICAR[3] + fumarate

(4) Adenylosuccinate[4] → AMP + fumarate

Beyond its role in generating purines needed for DNA replication, ADSL is thought to regulate cellular processes by controlling both AMP and fumarate levels in cells (12). Again, little research has been conducted on the regulation of ADSL protein activity or its expression.

Here, we report that SAICAR accumulates upon addition of growth factors, but not in conditions leading to cell death, differentiation, or in conditions in which the cognate receptor is not present in the cell. SAICAR accumulation correlates with phosphorylation of Erk1/2, PKM2 nuclear localization, and phosphorylation of histone H3. We also found that PAICS protein level correlates with SAICAR accumulation, and is likely responsible for the observed SAICAR increase. PAICS appears to be stabilized by the addition of growth factor, most likely through a phosphorylation event, and appears independent of transcription and

[3] 5-aminoimidazole-4-carboxamide ribotide = AICAR

[4] Adenylosuccinate is also denoted succinyladenosine monophosphate or SAMP

translation. Additionally, we found that PAICS protein is overexpressed in over 95% of human cancers. Furthermore, metabolic flux in SAICAR accumulating conditions is consistent with activation of PAICS protein, rather than inhibition of ADSL. From these data, we show that the PAICS protein is a key factor in cancer cell response to growth factors and other external stimuli, leading to increased cellular SAICAR and downstream activation of PKM2 as a protein kinase. Our findings highlight that PAICS is a peripheral, but important, member of the MAPK cascade, which may potentially be regulated in other cellular contexts beyond cancer biology.

RESULTS

Cellular SAICAR levels increase upon both glucose deprivation and EGF addition (6). However, it remains unclear whether SAICAR accumulation was limited to these two conditions or if it represented a broader response to a variety of conditions. To establish the breadth of SAICAR accumulation in response to external stimuli, we incubated HeLa cells with eleven different signaling factors (BNDF, EGF, GDNF, FGF, IGF, HGF, NGF, Ret A, TGF, TNF, VEGF) or a phosphate-buffered saline control, and subsequently measured cellular SAICAR concentration using liquid-chromatography mass spectrometry (LC-MS) after one hour of stimulation (5, Table 4-1, Figure 4-1A). As expected, EGF addition led to increased cellular SAICAR. We also found that a number of growth factors lead to SAICAR accumulation, including BDNF, GDNF, FGF, IGF, HGF, TGF, and VEGF (Figure 4-1). Interestingly, each compound stimulated SAICAR production to a different degree, and the overall result represented a gradient of cellular concentrations (Figure 4-1). The conditions that did not lead promote SAICAR accumulation either led to apoptosis (TNF), cell differentiation (Retinoic Acid), or the cognate receptor was not present (NGF) (Figure 4-1A). Of note, the presence of the GDNF receptor in HeLa cells is not yet defined. However, GDNF is known to be capable of binding other receptor tyrosine kinases (RTKs), albeit at a lower affinity, potentially explaining the observed phenomenon.

Next, we sought to ensure that effectors of SAICAR accumulation were also activated in these conditions. When cells were incubated with growth factor,

Table 4-1. List of the factors utilized in this study and amounts of each added to cell culture media. Factors were reconstituted in phosphate buffered saline with 0.5% BSA.

Growth Factor	Amount (ng/mL)
EGF	10
BDNF	1000
FGF	500
GDNF	10
HGF	10
IGF	2
NGF	1
Ret. A	300
TGF	0.2
TNF	0.1
VEGF	1

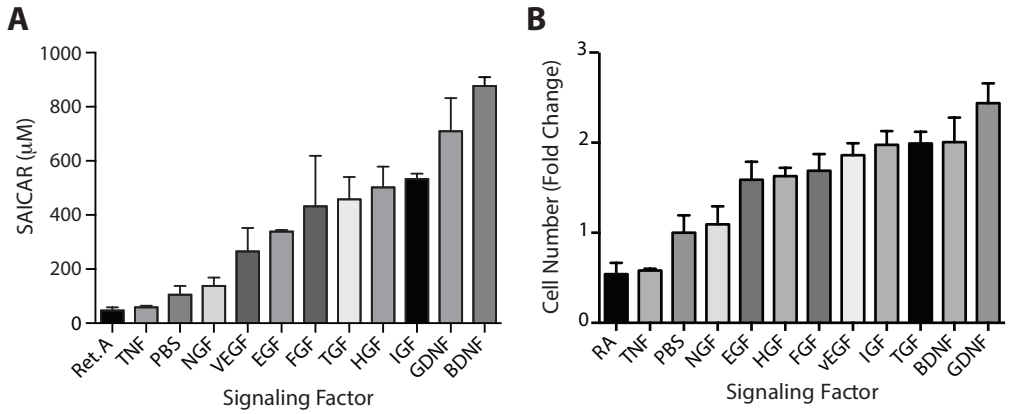

Figure 4-1. Signaling factors lead to an increase in cellular SAICAR. A) Amount of cellular SAICAR measured by LC-MS. HeLa cells were incubated with the various signaling factors (amounts listed in Table 4-1) for one hour, metabolites extracted, and cellular SAICAR measured. SAICAR was quantified using a ^{13}C-SAICAR standard of a known amount and normalized to total metabolite absorbance at A_{260} nm. B) Cell number increases with the addition of some signaling factors. HeLa cells were incubated with various signaling factors for twenty-four hours and the cell number was measured.

Erk1/2 phosphorylation was increased in all conditions that lead to SAICAR accumulation, with the exception of VEGF (Figure 4-2). Additionally, after a six-hour incubation, SAICAR accumulating conditions promoted PKM2 nuclear localization and subsequent phosphorylation of histone H3 threonine 11 (Figure 4-3). Conditions in which SAICAR was not elevated did not show activation of Erk1/2, phosphorylation of H3 (data not shown), nor relocalization of PKM2 (Figure 4-2 and 4-3). Finally, cell proliferation correlated to cellular SAICAR level (Figure 4-1B). Thus, all conditions in which there is an accumulation of SAICAR lead to a common output: activation of proliferative signaling.

Accumulation of SAICAR can be the result of several different scenarios, including activation of SAICAR synthesis, inhibition of SAICAR cleavage, and/or increased flux through the *de novo* purine nucleotide biosynthetic pathway. To begin to differentiate between the possibilities, the concentrations of up- and downstream metabolites were examined by LC-MS. The expectation is that if elevated SAICAR levels are due to increased flux, the upstream metabolite AICOR, SAICAR, and the downstream metabolite AICAR will increase together. If SAICAR synthesis is upregulated, AICOR will be depleted while SAICAR and AICOR levels will increase, while if SAICAR cleavage is inhibited, AICOR and SAICAR will increase. If AICOR levels decrease (Figure 4-4A,B). Upon growth factor addition, we found that the upstream metabolite AICOR is depleted in phase with SAICAR accumulation, while AICAR accumulates with SAICAR (Figure 4-4A, B).

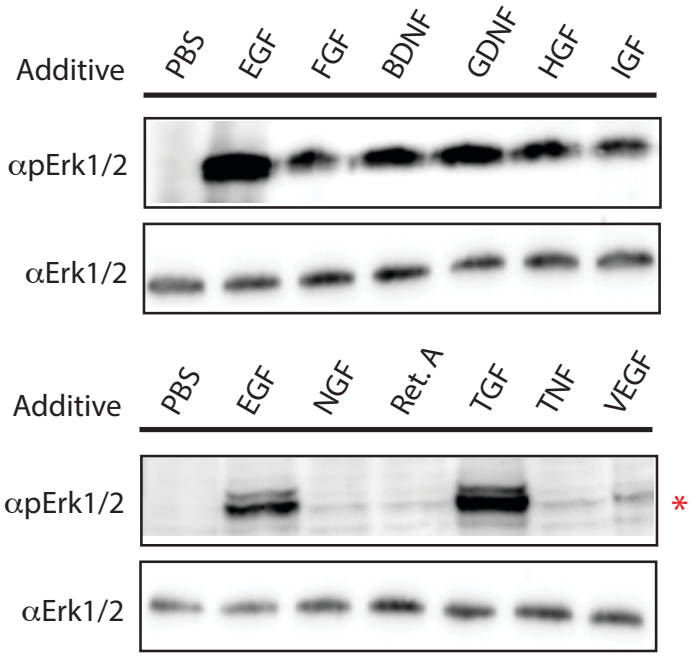

Figure 4-2. Signaling factors lead to an increase in phosphorylated Erk1/2 in HeLa. HeLa cells were incubated with the various signaling factors (amounts listed in Table 4-1) for one hour and then lysed. Phosphorylated and total Erk1/2 levels were visualized by Western blot. Phosphorylated Erk1/2 was found in nearly all conditions with elevated SAICAR levels, with the exception of VEGF.

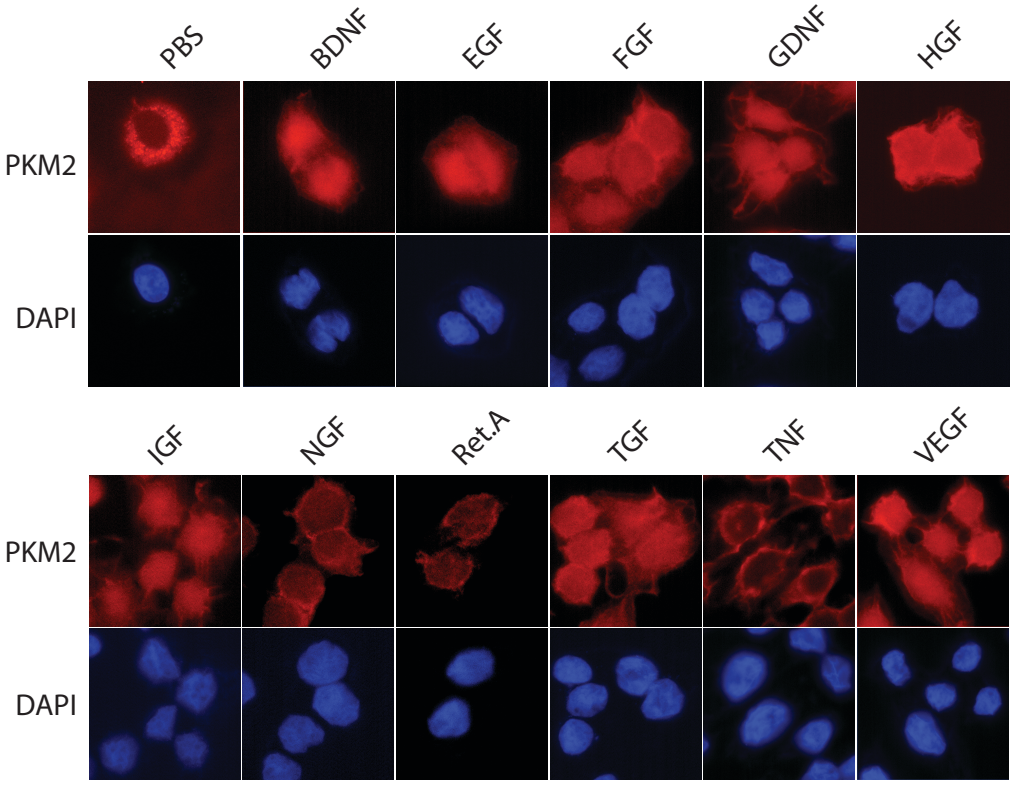

Figure 4-3. Signaling factors lead to PKM2 nuclear localization. HeLa cells were incubated with the various signaling factors (amounts listed in Table 4-1) for six hours and PKM2 localization was visualized by immunofluorescence. Growth factors leading to SAICAR accumulation also lead to PKM2 nuclear localization; in all other conditions, PKM2 was excluded from the nucleus.

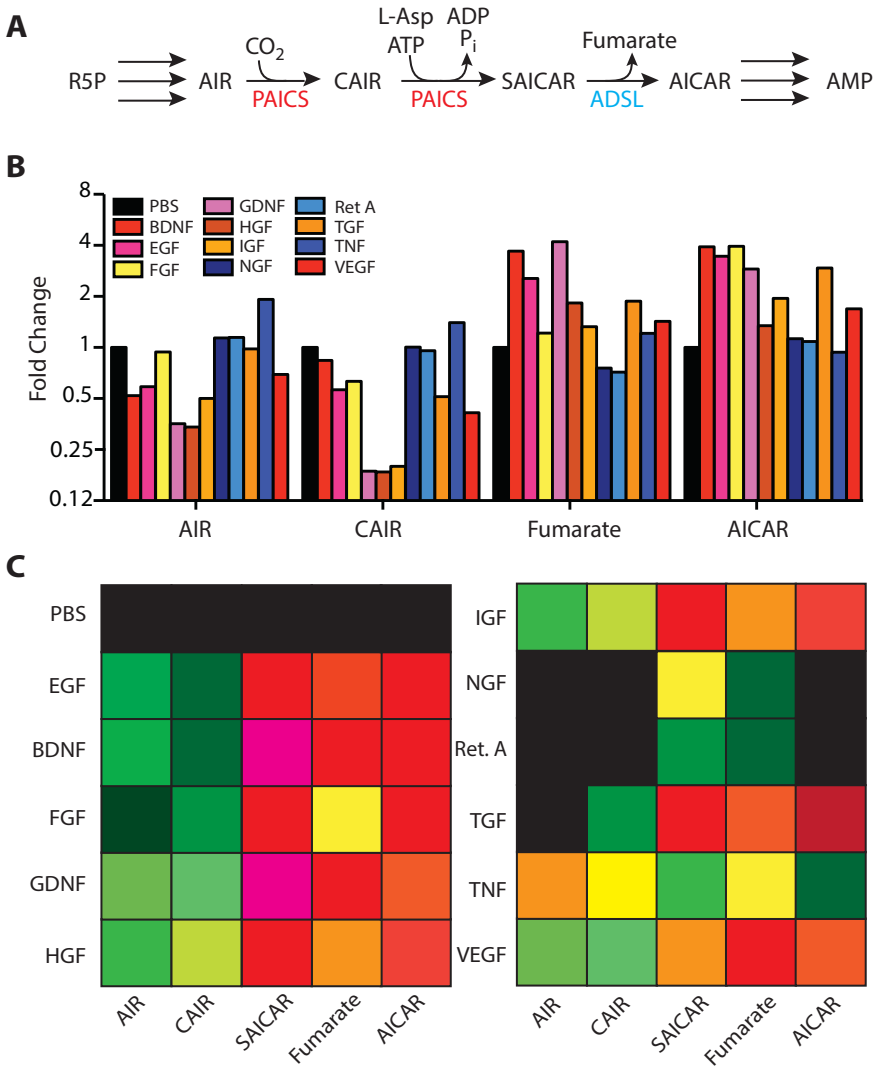

Figure 4-4. SAICAR and downstream metabolites accumulate upon signaling factor addition. A) Schematic representation of SAICAR metabolism. PAICS (red) generates SAICAR, while ADSL (blue) cleaves SAICAR. HeLa cells were incubated with signaling factors for one hour and metabolites were analyzed by LC-MS. B) Fold change relative to PBS control in upstream and downstream metabolites. C) Heat map showing relative metabolite level change (red refers to upregulation; green refers to down regulation).

This was true in all SAICAR accumulating conditions (including glucose depletion). Additionally, our previously published data support that upstream activation is likely. In *adsl-kd* cells, which over-accumulate SAICAR in normal conditions, produce additional SAICAR upon glucose starvation (5). Further SAICAR accumulation would not be expected if downstream proteins were inhibited, as ADSL is knocked down by over 90% in this cell line. These findings support the hypothesis that activation of upstream elements leads to SAICAR accumulation.

To probe the question more directly, we next examined PAICS protein levels upon addition of signaling factors. PAICS protein was elevated in all conditions leading to SAICAR accumulation, but not in conditions in which SAICAR levels remained the same (Figure 4-5A and B). We also found that the amount of PAICS protein correlate linearly with cellular SAICAR concentration (Figure 4-5C). In contrast, ADSL, the SAICAR cleavage enzyme, seems slightly decreased upon adding signaling factors, although this result is not limited to SAICAR accumulating conditions (Figure 4-5A). Furthermore, the PAICS protein level in glucose-depleted cells was elevated in an oscillatory manner in phase with SAICAR accumulation (data not shown). To determine if the increase of PAICS was due to stabilization of the protein or from increased translation of the mRNA, the translation elongation inhibitor cycloheximide was added to cells pre-incubated with the SAICAR stimulating growth factor EGF.

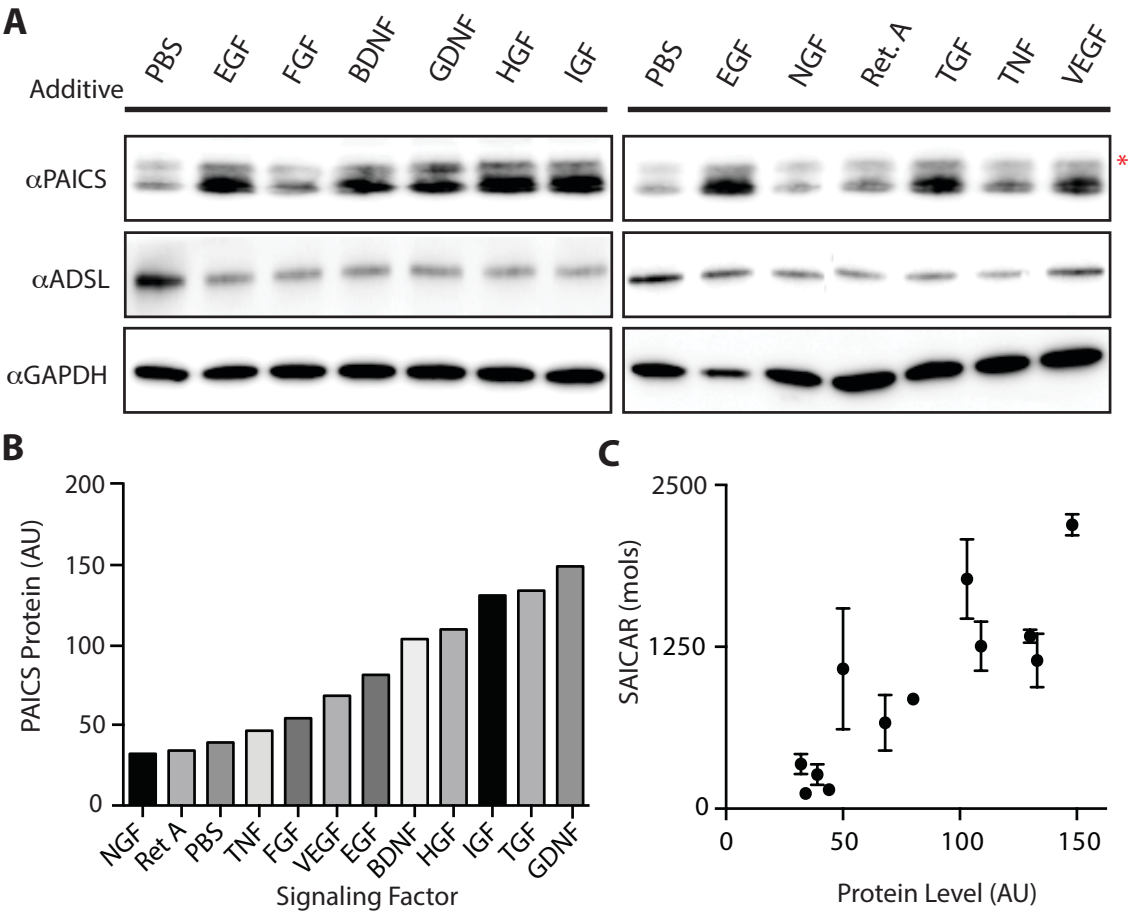

Figure 4-5. PAICS protein is elevated upon signaling factor addition. A) HeLa cells were incubated with signaling factors for one hour. PAICS and ADSL protein levels were monitored by Western blot. PAICS protein was elevated in conditions where SAICAR accumulates, while ADSL levels appeared to decrease regardless of condition, as compared to PBS. B) PAICS protein was quantified from Western blots and normalized to GAPDH loading control. Conditions that did not lead to SAICAR accumulation also had lower levels of PAICS protein overall. C) PAICS protein level is plotted against cellular SAICAR levels. PAICS protein and SAICAR levels are positively correlated.

PAICS protein was elevated for up to 4 hours with EGF addition; after 6 hours protein level reached baseline levels (Figure 4-6). Cycloheximide increased PAICS protein levels after thirty min and maintained elevated levels for six hours (Figure 4-6). Furthermore, cycloheximide alone elevates PAICS levels, indicating that PAICS and SAICAR may potentially act as general stress response elements (Figure 4-6). These pieces of data together suggest SAICAR synthesis is stimulated upon signaling factor addition, potentially through the stabilization of the PAICS protein.

As these results suggest that PAICS protein level should be important for cancer cell signaling and proliferation, we next searched available databases for PAICS expression level in various cancer types and tissues. Our search revealed that PAICS is expressed in 100% of cancer tissues, as visualized by immunohistochemistry (Figure 4-7A). Over 75% of samples were deemed to have high PAICS expression, while only 1.5% had low expression (Figure 4-7B). In contrast, high expression of the SAICAR cleavage enzyme ADSL does not appear correlated with cancer (Figure 4-7A). Less than 10% of samples have high ADSL protein expression, while over 30% have little or no detectable ADSL (Figure 4-7B). Additionally, in a published microarray study examining cancers with overexpressed c-Myc, the authors found that PAICS is overexpressed in 95% of cancers tested by approximately two-fold or more, while ADSL expression is either unaltered or diminished.

.

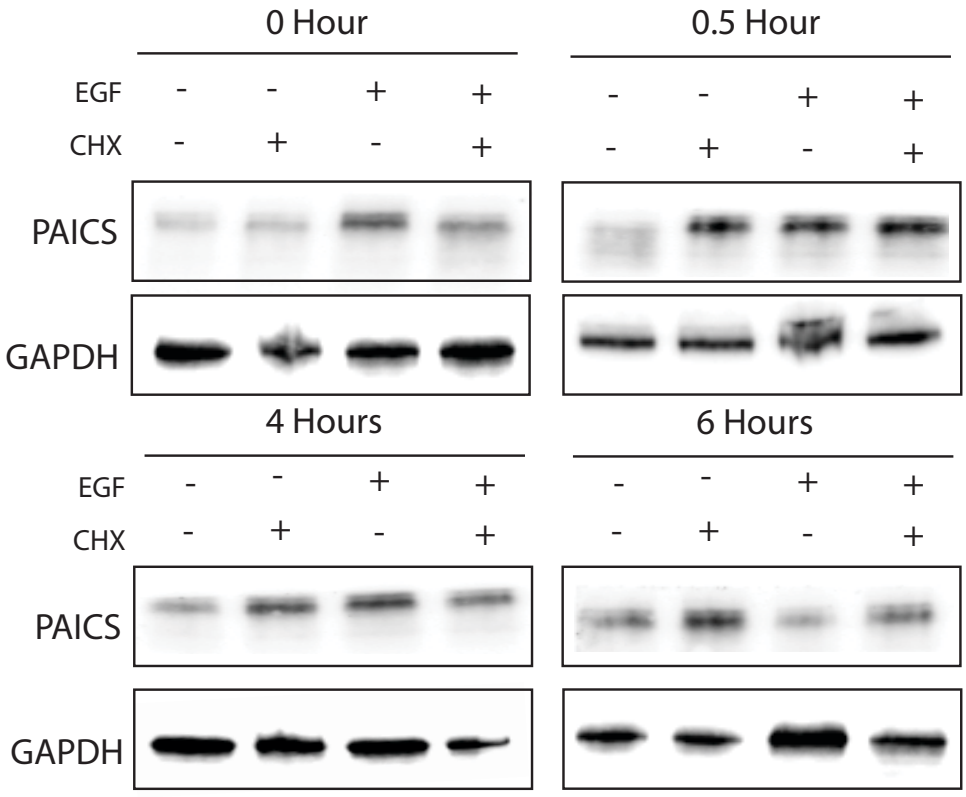

Figure 4-6. PAICS protein is stabilized by the addition of cycloheximide (CHX) and EGF. HeLa cells were incubated with 10 ng/mL EGF for one hour. CHX was added to the media for the noted amount of time, then cells were lysed, and PAICS protein level and GAPDH protein were measured by Western blot. EGF stabilized PAICS protein for up to 4 hours, while CHX stabilized PAICS protein after thirty minutes and for as long as 6 hours.

Figure 4-7. PAICS protein is elevated in many cancer tissue types, while ADSL protein level is more variable. The data in this figure were compiled from the Protein Atlas Database from immunohistochemistry staining of cancer tissue samples from a tissue database. A) PAICS protein level (top panel) and ADLS (bottom panel) in various cancer tissue types denoted in the figure. Data represented as a percentage of all tissue samples analyzed for protein presence. B) Percent of samples of all cancer cell tissues that have high, medium, low, or not detectable levels of either PAICS or ADSL protein.

*Figure is on the next page.

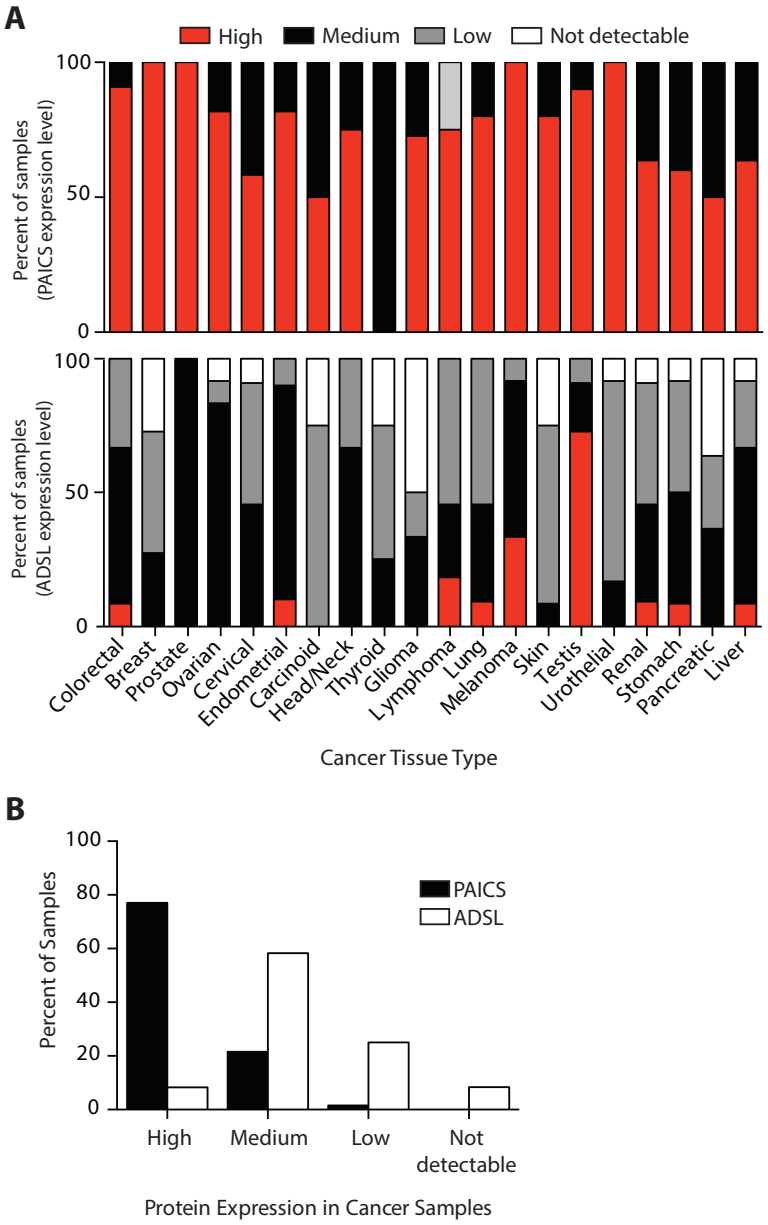

Figure 4-7. PAICS protein is elevated in many cancer tissue types, while ADSL protein level is more variable. *Figure legend is located on the previous page.

DISCUSSION

Cells must respond to their environment in order to regulate their growth and proliferation. To do so, different external signals must be integrated to yield similar outcomes, as are those observed by growth factor addition. Here, we show that many growth factors lead to an increase in the protein PAICS and the metabolite this protein generates, SAICAR. The increase in cellular SAICAR promotes MAPK signaling, PKM2 protein kinase activity, and transcription of genes responsible for growth and proliferation. The data suggest that SAICAR acts as a more general signal to promote cancer cell growth and proliferation. Cancer cells are less reliant on external growth factors for signaling, potentially due to SAICAR accumulation. However, glucose-deprivation and cyclohexamide addition also lead to an increase in PAICS protein and SAICAR accumulation, indicating that SAICAR elevation may also reflect a response to stress conditions, not just growth factors. As SAICAR activates PKM2 pyruvate kinase activity to promote energy generation in stress conditions, increased PAICS expression and thus increased cellular SAICAR would prove beneficial to cancer cells. Indeed, PAICS protein is expressed highly in many cancer types and tissues. Further entangling the roles for SAICAR, the apoptosis factor TNF and the differentiation factor retinoic acid, which can be considered stress conditions, did not lead to an increase in either cellular SAICAR or PAICS protein, indicating that cells can discriminate between various signals and this response is only a suited for a subset of these signals.

The increase of cellular SAICAR and PAICS protein in stress conditions (glucose-deprivation and CHX treatment) may represent a cancer specific regulatory pathway that has not yet been identified. Low glucose conditions are commonly found in tumor microenvironments, as well as hypoxia, but cancer cells are able to proliferate regardless (1, 2). Interestingly, hypoxia has been shown to inhibit mRNA translation, similar to the CHX treatment (14). To counteract the inhibitory signals upon both hypoxia and glucose deprivation, and to thrive in these environments, cancer cells may integrate these signals differently and promote growth and proliferation through SAICAR and PKM2.

As of yet, the mechanism underlying PAICS stabilization and SAICAR accumulation is not clear, although this study represents a step forward in identifying conditions that lead to this outcome. Interestingly, large proteomic studies have shown that PAICS protein is phosphorylated in a number of cancer cell lines at tyrosine 22 (16-19). This site shows some homology to an Src-kinase consensus sequence, providing some insight into a possible mechanism for protein stabilization (20). Furthermore, a protein of a higher mass (or slower mobility) was observable when probing for PAICS, either due to non-specific interactions or indicating that a post-translational modification was present. In either case, it remains clear that PAICS and cellular SAICAR concentration are important to cancer cell metabolism and proliferative signaling.

The importance of the PAICS protein and SAICAR accumulation may not be limited to cancer cell biology, but could represent a more general response to

external stimuli in undifferentiated tissues. Fetal and stem cells express the PKM2 isoform and readily utilize growth factors to trigger growth and proliferation. Stimulation of *de novo* nucleotide biosynthesis through PAICS and the subsequent oscillation of SAICAR levels can promote both generation of important anabolic precursors and energy production through the allosteric activation of PKM2, to allow the cell to grow and divide when signaled to do so. The link between cellular metabolism and growth signaling would provide a developmental advantage, as cells would only proceed if the appropriate conditions were met.

A full-scale study of both conditions that lead to SAICAR accumulation and cell types that have inducible SAICAR concentration must be explored to determine the overall role for both PAICS and SAICAR in cell biology. Furthermore, the PAICS protein may prove to be a viable therapeutic target, which could provide a blockade to the proliferative signaling due to SAICAR-PKM2, while specifically targeting cancer cells while sparing adult differentiated cell types.

Materials and Methods

Materials

Analysis of cellular SAICAR levels and other metabolite levels were performed as previously described (6, 7). In brief, the data was analyzed using Agilent MassHunter and all treatments were repeated in triplicate. For the determination of SAICAR concentration, [$^{13}C_4$]-labeled SAICAR standard solution was mixed with the extracted metabolites, and the amount of SAICAR in cell extract was determined by comparing LC-MS peak areas of [^{12}C]-SAICAR with that of [$^{13}C_4$]-labeled SAICAR. Additionally, AICAR, AIR, CAIR, and fumarate peaks were integrated and normalized to the A_{260} of the corresponding sample. Each result is presented as a fold change of each metabolite in comparison to the control (PBS alone). All data represents the average and the standard deviation.

Cell culture

HeLa cells were maintained and grown in Dulbecco's Modified Eagle Medium containing 4g/L glucose and 4 mM glutamine (DMEM) and supplemented with 10% fetal bovine serum (FBS), penicillin, and streptomycin. Cells were kept at 37°C, 5% carbon dioxide, and humid conditions. For all experimental conditions, dialyzed FBS (Invitrogen) was added to DMEM in place of normal FBS. Prior to the start of the experiment, cells were seeded to 25%

confluency and grown to 80% confluency. Cells were incubated in dialyzed FBS containing DMEM for at least 24 hours.

Signaling Factor Addition

Signaling factors were resuspended as suggested by the vendor, typically in phosphate buffered saline (PBS) supplemented with 0.5% BSA or in PBS alone. HeLa cells were incubated in DMEM with dialyzed FBS for 24 hours before the experiment start. Growth factors [EGF (10 ng/mL Sigma-Adlrich), BDNF (1000 ng/mL, Sigma-Aldrich), FGF (500 ng/mL, Invitrogen), GDNF (10 ng/mL, Gibco), HGF (10 ng/mL Sigma-Aldrich), IGF (2 ng/mL, Gibco), NGF (1 ng/mL), retinoic acid (300 ng/mL), TGF (0.2 ng/mL, Gibco), TNF (0.1 ng/mL, Cell Signaling Technology), or VEGF (1 ng/mL, Sigma-Aldrich)] were added to the media. The amount of signaling factor added was the experimentally determined EC_{50} for cell proliferation, differentiation, or cell death (dependent on factor added) as provided by the literature of the vendor. For cellular SAICAR concentration measurement, via LC-MS, PAICS protein level, ADSL protein level, or the phosphorylation of Erk1/2 proteins, cells were incubated with the growth factor for one hour in dialyzed FBS containing DMEM. For phosphorylation of histones or PKM2 localization studies, HeLa cells were incubated with the signaling factors for six hours, and for cell proliferation measurement, incubation time with the various signaling factors was twenty-four hours. Cell number was

counted using a Moxi-Z cell counter (n=3-5) after cells were trypsinized and diluted in PBS.

Subcellular localization of PKM2

Prior to the experiment, HeLa cells were grown on coverslips in a six-well dish in DMEM supplemented with dialyzed FBS. Signaling factors or PBS were added to cells and incubated for six hours. The coverslips were then washed thoroughly with PBS, fixed with 4% paraformaldehyde and permealized with 0.01% Triton X-100. Cells were blocked in 5% goat serum diluted in PBS for 1 hour and stained with rabbit anti-PKM2 antibody (Sigma-Aldrich) in 5% goat serum (1:200 dilution) for forty-five minutes. Coverslips were then washed with PBS and incubated with DAPI, briefly. After washing with PBS, TRITC-labeled goat ant-rabbit antibody (Sigma Aldrich) in PBS (1:400) was added to coverslips for two hours. Coverslips were mounted on slides and microscopic images were obtained using a Zeiss AxioVert 200 fluorescence microscope (Integrated Imaging Center, Johns Hopkins University, 40X optical zoom).

Western Blot

Cells were first washed in PBS and then lysed in ice-cold non-denaturing buffer (20 mM Tris HCl, pH 8, 137 mM NaCl, 1% NP-40, 2 mM EDTA) supplemented with 1 mM phenylmethylsulfonyl fluoride and 5 mM sodium fluoride. Total protein concentration using the Pierce 660 kit (Thermo Scientific),

using bovine serum albumin as a standard (Cell Signaling Technology). Membranes were probed with primary antibody (rabbit anti-phospho-p42/p44, rabbit anti-p42/p44, rabbit anti-pT11-Histone H3, and rabbit anti-Histone H3 from Cell Signaling; rabbit anti-GAPDH, mouse anti-PAICS, mouse anti-ADSL, and mouse-anti-Myc from Sigma-Aldrich) overnight at 4°C. Membranes were then probed with horseradish peroxidase (HRP) conjugated goat anti-rabbit IgG or goat anti-mouse IgG secondary antibodies (Bio-Rad). HRP-conjugated secondary antibodies were then detected using a commercial chemiluminescence substrate kit (Pierce). Chemiluminescence images were acquired using a FluorChem M FM0455 imager.

Cyclohexamide Addition

HeLa cells were grown in high glucose DMEM supplemented with 10% dialyzed FBS and PS for 24 hours prior to experiment. EGF (10 ng/mL) was added to each plate for one hour. Cyclohexamide (0.1 mg/mL) was added to each plate for 0, 0.5, 1, 2, 4, or 6 hours. Cells were then lysed with non-denaturing lysis buffer and blotted for GAPDH and PAICS.

Protein Atlas Data Analysis

The Protein Atlas Database (proteinatlas.org) was utilized to analyze the expression of both PAICS and ADSL protein. Data was compiled from *in situ* hybridization in cancer tissue samples was quantified and plotted by cancer type

or by expression pattern. Cancer tissue data is represented as a percentage of the total number of samples denoted high, medium, low, or not detectable expression. Overall expression data is represented as the number of samples with high, medium, low, or not detectable levels. Denoted levels of protein expression represent those determined by the Protein Atlas.

References:

(1) Hanahan D, Weinberg, RA. (2011). Hallmarks of cancer: the next generation. *Cell* 144(5), 646.

(2) Cooper GM. The Cell: A Molecular Approach. 2nd edition. Sunderland (MA): Sinauer Associates; 2000. The Development and Causes of Cancer.

(3) Mazurek S. (2011). Pyruvate kinase type M2: a key regulator of the metabolic budget system in tumor cells. *Int J Biochem Cell Biol* 43(7), 969.

(4) Christofk H, Vander Heiden M, Harris M, Ramanathan A, Gerszten R, Wei R, Fleming M, Schreiber S, and Cantley L. (2008) The M2 splice isoform of pyruvate kinase is important for cancer metabolism and tumor growth. Nature *452*, 230-233.

(5) Keller K, Tan I, and Lee YS. (2012) SAICAR stimulates pyruvate kinase isoform M2 and promotes cancer cell survival in glucose-limited conditions. *Science 338*, 1069-1072

(6) Keller K, Doctor Z, Dwyer Z, and Lee YS. (2014) SAICAR Induces Protein Kinase Activity of PKM2 that is Necessary for Sustained Proliferative Signaling of Cancer Cells. *Mol. Cell* 53, 700-709

(7) Batova A, Diccianni MB, Omura-Minamisawa M, Yu J, Carrera C, Bridgeman L, Kung F, Pullen J, Amylon, M, and Yu, A. (1999) *Cancer Res 59*, 1492-7.

(8) Casey, P. J., and Lowenstein, J. M. (1987) *Biochem Pharmacol 36*, 705-9.

(9) Tyagi A, and Cooney DA. (1980) *Cancer Res 40*, 4390-7.

(11) Spiegel EK, Colman RF, Patterson D (2006). "Adenylosuccinate lyase deficiency". *Mol. Genet. Metab.* **89** (1–2): 19–31

(12) Lee P, Colman RF (2007). "Expression, purification, and characterization of stable, recombinant human adenylosuccinate lyase". *Protein Expr. Purif.* **51** (2): 227–34.

(13) Uhlen M, Oksvold P, Fagerberg L, Lundberg E, Jonasson K, Forsberg M, Zwahlen M, Kampf C, Wester K, Hober S, Wernerus H, Björling L, Ponten F. Towards a knowledge-based Human Protein Atlas. *Nat Biotechnol.* 2010 28(12):1248-50.

(14) Lui L, Cast T, Jones R, Keith B, Thompson C, Simon C (2006). Hypoxia-Induced Energy Stress Regulates mRNA Translation and Cell Growth. *Mol Cell* 21;4 521-531.

(15) Uhlén M, Björling E, Agaton C, Szigyarto CA, Amini B, Andersen E, Andersson AC, Angelidou P, Asplund A, Asplund C, Berglund L, Bergström K, Brumer H, Cerjan D, Ekström M, Elobeid A, Eriksson C, Fagerberg L, Falk R, Fall J, Forsberg M, Björklund MG, Gumbel K, Halimi A, Hallin I, Hamsten C, Hansson M, Hedhammar M, Hercules G, Kampf C, Larsson K, Lindskog M, Lodewyckx W, Lund J, Lundeberg J, Magnusson K, Malm E, Nilsson P, Odling J, Oksvold P, Olsson I, Oster E, Ottosson J, Paavilainen L, Persson A, Rimini R, Rockberg J, Runeson M, Sivertsson A, Sköllermo A, Steen J, Stenvall M, Sterky F, Strömberg S, Sundberg M, Tegel H, Tourle S, Wahlund E, Waldén A, Wan J, Wernérus H, Westberg J, Wester K, Wrethagen U, Xu LL, Hober S, Pontén F.
A human protein atlas for normal and cancer tissues based on antibody proteomics**.** *Mol Cell Proteomics.* 2005 4(12):1920-32.

(16) Li J, Ning Y, Hedley W, Saunders B, Chen Y, Tindill N, Hannay T, Subramaniam S. (2002). The Molecule Pages database. Nature. 420 ,716-7.

(17) Obenauer,J.C., Cantley,L.C., and Yaffe,M.B. (2003). Scansite 2.0: Proteome-wide prediction of cell signaling interactions using short sequence motifs. Nucleic Acids Res. 31,3635.

(18) Protein Kinase Resource (PKR) http://pkr.sdsc.edu/html/index.shtml

(19) Bateman A, Birney E, Cerruti L, Durbin R, Etwiller L, Eddy SR, Griffiths-Jones S, Howe KL, Marshall M, Sonnhammer EL. (2002) The Pfam protein families database. Nucleic Acids Res. 30:276.

(20) Songyang Z, Carraway K, Eck M, Harrison S, Feldman R, Mohammadi M, Schlessinger J, Hubbard S, Smith D, Eng C, Lorenzo M, Ponder B, Mayer B, and Cantley L. (1995) Catalytic specificity of protein-tyrosine kinases is critical for selective signaling. Nature. 373; 536-539

CHAPTER 5

Concluding Remarks

For decades, it has been understood that cancer cells have an altered metabolism and also express a unique subset of proteins as compared to healthy, normal cells. The metabolic hallmark of cancer cells is that these cells uptake more glucose, produce more lactate, are less reliant on oxygen, and often use alternative carbon sources to produce energy, such as glutamine. Additionally, a barrage of oncogenes and tumor suppressors have been identified, such as c-Myc, p53, and HIF1a, that contribute to the uncontrolled growth and proliferation observed in cancer cells. However, there has been little focus on the interaction between metabolites and proteins in cancer types and tissues. Furthermore, little research has focused on the implications of variable metabolism and a unique protein profile in other systems, such as the alteration made in cells during development and in the maintenance of the stem cell niche.

In this dissertation, we identify and explore the interaction between a cellular metabolite SAICAR, which is elevated in cancer cells in stress conditions, and pyruvate kinase M2 (PKM2) that is highly expressed in a number of cancers. First, the discovery of the PKM2-SAICAR interaction indicates that there is an intimate relationship, at least for some scenarios, between cancer cell metabolism and the protein expression profile. Additionally, we have found that the binding of SAICAR to PKM2 renders PKM2 an active protein kinase. This is one of the first demonstrations that a simple allosteric interaction can lead to a change in protein function, rather than just protein activity. The findings of this thesis are important both in the field of PKM2 regulation and cancer cell

metabolism, but also bring about important basic biological questions: are protein-metabolite interactions more ubiquitous than previously thought and if so, what are there functions? Our research has brought forth the notion that there may be several hereto-unknown regulatory systems that further interconnect the pathways that have been well studied for so long.

Summary of my contribution to the field

Earlier in this dissertation, I have provided in depth discussions on the conclusions and relevance of our work. In this section, I will briefly summarize the findings of the preceding chapters and discuss the impact on both the field of cancer metabolism and general biology.

SAICAR binds to PKM2 and promotes cancer cell survival in glucose limited conditions

Pyruvate kinase M2 is expressed in cancer cells, and like other pyruvate kinases, catalyzes the final step of glycolysis from phosphoenol pyruvate to pyruvate. Surprisingly, PKM2 has a low intrinsic catalytic activity, as compared to other isoforms. To explain this phenomenon, a model was generated that PKM2 acts as a glycolytic bottleneck in cancer cells, thus promoting anabolic processes and ultimately cell growth and proliferation. Although this model was enticing, there were loopholes in the argument. For instance, lactate production is drastically increased in cancer cells. As lactate is generated from pyruvate, an

inactive pyruvate kinase would lead to a depletion of lactate, not an accumulation. Additionally, without an active pyruvate kinase, energy would be rapidly depleted in low glucose conditions, which are commonly observed in a tumor microenvironment. Thus, the bottleneck model is insufficient to describe the role of PKM2 in cancer cells.

PKM2 has other unique biochemical properties, including its ability to be regulated by cellular metabolites. In the second chapter of this thesis, we sough to identify cellular metabolites that regulate PKM2 in a context-dependent manner. We developed a technique to monitor protein-metabolite interactions by using low-temperature gel filtration and subsequent analysis by liquid chromatography-mass spectrometry. Using this technique, we found that SAICAR, a *de novo* purine biosynthesis intermediate, binds to PKM2 in glucose-limited conditions. Subsequently, we showed that SAICAR levels increase in glucose-starved cancer cells to near millimolar levels. SAICAR binds and activates PKM2, both *in vitro* and *in vivo*. In cells lines with artificially altered SAICAR levels, we found that maintaining an inducible SAICAR concentration is necessary for the Warburg effect. Finally, we found that increased cellular SAICAR protects cells from death in nutrient-limited conditions in a PKM2-dependent manner.

The interaction between PKM2 and SAICAR shows evidence of cross talk between an energy generating pathway (glycolysis) and an energy-utilizing pathway (nucleotide biosynthesis). During conditions of nutrient-limitation, cells

must tightly regulate energy production and cell division. Our data suggests that PKM2 reflects the bridge point between these two competing pathways. First, PKM2 serves as a bottleneck for the glycolytic pathway and allows for generation of glycolytic intermediates. These metabolites can then be rerouted towards other anabolic pathways, including the pentose phosphate pathway, to generate more precursor molecules for growth and cell division. As intermediates are funneled into anabolic pathways and energy is depleted, SAICAR levels increase. SAICAR then can bind to PKM2, activating it, and lead to a metabolic flux shift towards energy generation. This oscillatory mechanism can provide a cell fine tuned control when the external environment is changing, giving it an advantage. Our data challenges the model that PKM2 is a stagnant protein and poses a more general model that PKM2 serves as a biological sensor for cancer cells.

However, the data we presented left several unanswered questions, some of which are touched upon in other parts of this dissertation. First, the mechanisms by which a transient interaction between PKM2 and SAICAR leads to long-term cell survival remained unclear. Furthermore, the mechanism leading to SAICAR accumulation was completely unexplored in this section. This paper is not the only demonstration of SAICAR accumulation in cells, but it is the first to show that it is context specific and not due to a mutation in the nucleotide biosynthesis pathway. Finally, although we tested a few cancer cell lines, the breadth of SAICAR accumulation among cancer cell types and tissues was not

tested, nor among different cellular conditions. This was addressed to a moderate degree in chapter four of this thesis.

Beyond the elucidation of PKM2's role in cancer metabolism, the technique generated in this work provides a large step forward in the identification of protein-metabolite interactions. As a consequence of our work, we have noted that there are likely hundreds of unknown interactions between proteins and metabolites. This technique can be adapted to any protein that can be recombinantly expressed and purified in reasonable quantities. As an example of the versatility of the technique, an unpublished screen was attempted in our lab on over 80 related proteins across all three domains. Metabolite binding analysis revealed many previously unknown interactions, as well as confirmation of known interactions. The utilization of this technique can open the door for new fields to emerge in general biology and protein biochemistry.

SAICAR renders PKM2 an active protein kinase

During the time that we identified SAICAR as an allosteric activator of PKM2, new research emerged that PKM2 had an additional role as a protein kinase. At this time, the known substrates for PKM2 were limited to histone H3 and stat3. Additionally, several research groups reported that recombinantly expressed PKM2 was unable to phosphorylate these protein substrates *in vitro*; only protein purified from the nucleus of cancer cells was able to act as a protein kinase. At this time, the work was controversial, due to the slow catalysis and

the lack of robustness in the system. It was possible that the result was an artifact of nuclear purification or that the reaction was in fact not enzyme catalyzed. Furthermore, all published reactions were performed in enzyme excess conditions, so it was unclear whether PKM2 could perform multiple-turnovers.

Due to our discovery of the PKM2-SAICAR interaction, and other data hinting that PKM2 quaternary structure was important to its function (pyruvate vs. protein kinase activity), we speculated that a metabolite binding event may alter PKM2 intrinsic function. In chapter three of this dissertation, we identify SAICAR as an inducer of PKM2 protein kinase activity. Additionally, we identified EGF as another inducer of SAICAR accumulation, indicating that SAICAR may act as a more general messenger than we previously envisioned. Using a proteomic approach, we expanded the number of PKM2 substrates from two (histone H3 and stat3) to over 100 cellular proteins. We confirmed several hits from the screen, and also rigorously tested the interaction between PKM2-SAICAR and the MAPK cascade component Erk1. We found that PKM2 appears to be an integral member of MAPK signaling, at least in the context of cancer cells. Finally, we found that Erk1/2 and PKM2-SAICAR participate in a positive feedback loop, sensitizing each other through phosphorylation for prolonged signaling, even in the absence of stimuli.

The MAPK cascade has been extensively studied for decades and most of the components are well defined, thus it remains surprising that PKM2 was not

identified as a target of this cascade until recently. Despite the surprise, this data suggests the exciting possibility that potentially there are a number of members within this and other well described pathways that have not yet been discovered. Furthermore, the vast number of PKM2-SAICAR substrates indicates that PKM2 is a promiscuous protein kinase, and supports our previous assertion that PKM2 may act as a central regulator of cell state. Of these substrates, we found that a number are protein kinases themselves. Thus, in cancer cells, PKM2 may serve to trigger or expand signaling cascades upon external stimuli and ultimately promote cell proliferation and survival. One enticing theory is that the expression of PKM2 allows cancer cells to become less dependent on growth factors, a commonly observed phenomenon in cancer. If PKM2 becomes activated as a protein kinase, it can then go on to turn on many proteins in other pathways that are not part of the typical response for that particular stimulus. For instance, we found that c-Myc expression is induced upon glucose starvation. It is unlikely that normal cells would express a proliferation factor when starved of glucose; it may be that the activation of PKM2 in this circumstance activates expression of such factors inappropriately, allowing for uncontrolled growth while other cells remain quiescent.

From a biochemical standpoint, the findings of this chapter are exciting. The identification of a ligand inducing a new function in a protein is unique and novel, and we are unaware of another scenario in which this occurs. Current views of ligand-protein interactions typically focus on the ability of a ligand to

initiate a gross or minor structural change in a protein that makes the protein more or less likely to perform its enzymatic task. However, our work demonstrates that a ligand-binding event can initiate an entirely new function for a protein. For clarification, we are not claiming that PKM2 can miraculously perform another type of reaction (i.e. phosphorylation induced to acetylation), but we are showing a mechanism by which PKM2 is now able to recognize an entirely new set of substrates that are not similar to the original substrate (ADP).

Although the data in this chapter describes how the transient PKM2-SAICAR interaction leads to long-term survival of cancer cells, it brings up an important and seemingly contradictory element: SAICAR accumulation occurs both in glucose starvation and EGF addition. This is an intriguing path to study; two external stimuli that are not usually linked lead to the same output. The mechanism leading to SAICAR accumulation is thus critical to our understanding of the general role of SAICAR in cancer cells and potentially other cell systems. Furthermore, the identification of over 100 substrates leaves 100 potential projects for future scientists. Each substrate may have a unique story with a distinct set of inputs or activation of PKM2 may lead to phosphorylation of all 100 proteins in a mesh of signaling cascades. In either case, there is much to be explored and discovered.

PAICS protein level may be a readout for and also responsible for SAICAR accumulation

In chapter four of this dissertation, the mechanism of SAICAR accumulation is explored. Due to several pieces of data, we focused on the SAICAR synthetase, PAICS, as a likely candidate for regulation. We noticed that PAICS protein level was elevated in phase with SAICAR accumulation in glucose starved cancer cells. Additionally, we found that addition of EGF, another SAICAR accumulating condition, lead to an increase in PAICS protein. We then tested the breadth of SAICAR accumulation in response to external stimuli and found that many growth factors lead to an increase in SAICAR and also an increase in PAICS protein. Thus, we believe that PAICS protein level may be a reasonable read out for SAICAR accumulation in cancer cells.

In nearly every case where an elevated PAICS protein level (and SAICAR accumulation) was detected, all the downstream elements of PKM2 activation were observed, including Erk1/2 phosphorylation, histone H3 phosphorylation, c-Myc expression, and PKM2 nuclear localization. Furthermore, the SAICAR cleavage enzyme ADSL did not show the same dependence on condition, indicating that inhibition of ADSL is most likely not the mechanism of action. Interestingly, PAICS protein was also stabilized by the addition of cycloheximide, a translation inhibitor. As of yet, this data is not yet explained, although it points to SAICAR accumulation as a cellular sensor of stress conditions. Finally, we found that PAICS protein appears to be highly expressed in nearly all cancer cell types and tissues, while ADSL appears more variable. This indicates that PAICS protein is likely important to cancer cell biology, and that likely this is due to

SAICAR, rather than activation of nucleotide biosynthesis (as both ADSL and PAICS protein would be expected to be upregulated).

Although this data offers a start in the analysis of SAICAR accumulation, it is far from complete. A more thorough analysis of both the conditions leading to SAICAR accumulation and cancer cell types and tissues must be investigated. Additionally, there is basically no literature on the regulation of PAICS, beyond some very basic kinetics studies. It is likely that PAICS is also a cellular sensor for external stimuli, in particular, in stress conditions. PAICS contains a Src homology domain and also appears to be stabilized upon certain conditions. It is not unreasonable to speculate that potentially PAICS is regulated through Src phosphorylation, which stabilizes the protein. However, much is still unknown and there is a vast array of experiments that can be done to identify the PAICS regulatory mechanism.

Overall

From the data in this thesis, a more general biological question arises. PKM2 is not just a cancer specific protein; it is also expressed in fetal and stem cells. Fetal and stem cells often rely heavily on *de novo* nucleotide biosynthesis, in which SAICAR is a key component. Thus, is the PKM2-SAICAR interaction specific to cancer or is it a phenomenon derived from development? This question remains to be answered, but the idea brings about exciting possibilities.

SAICAR could be a metabolite important in development, or even more broadly in stem cell maintenance.

Regardless of the outcome, the results of this thesis provide solid groundwork for those interested in perusing basic biological and biochemical questions about proteins and the ligands that modulate their activity.

APPENDIX 1.

COMPREHENSIVE SCREEN OF ADSL ACTIVATORS AND INHIBITORS

INTRODUCTION

Cancer cells often alter their metabolic properties to proliferate and survive in stress conditions, commonly found in a tumor microenvironment. Often, they utilize *de novo* synthesis in lieu of salvage pathways to generate nucleotides, making the involved enzymes and metabolites viable therapeutic targets (Tyagi et al. 1980, Casey et al. 1987). Our lab identified SAICAR, a *de novo* purine nucleotide biosynthesis intermediate, as a metabolite that accumulates in nutrient-limited conditions and activates pyruvate kinase M2 (PKM2, Keller et al. 2012). SAICAR is necessary for cancer cell growth and survival in glucose deprived cancer cells and additionally is necessary for proliferative signaling upon epidermal growth factor (EGF) addition (Keller et al. 2014).

SAICAR is generated by the enzyme PAICS (also known as SAICAR synthetase) and is cleaved by ADSL. PAICS catalyzes two sequential steps in the purine biosynthesis pathway (Batava et al. 1999):

(1) AIR[5] + CO_2 → = CAIR[6]

(2) CAIR + L-aspartate + ATP → SAICAR + ADP + P_i

ADSL also catalyzes two reactions, however these are nonsequential (Lee et al. 2007):

(3) SAICAR → AICAR[7] + fumarate

(4) Adenylosuccinate[8] → AMP + fumarate

---

[5] 5'-phosphoribosyl-5-aminoimidazole = AIR
[6] 5'-phosphoribosyl-4-carboxy-5-aminoimidazole = CAIR
[7] 5-aminoimidazole-4-carboxamide ribotide = AICAR

Currently, not much is known about the regulation of either enzyme.

Beyond acting as the SAICAR cleavage enzyme, ADSL is also thought to control levels of AMP and fumarate in cells (Lee et al. 2007). Additionally, deficiency of ADSL, which is a rare autosomal disease, leads to psychomotor defects such as mental retardation, and in extreme cases, can lead to early mortality (Spiegel et al. 2006). Due to the importance of ADSL as a regulatory enzyme in normal cells, cancer cells, and in developmental disorders, we sought to identify compounds that both inhibit and activate ADSL. We identified several compounds and sought to confirm a candidate. However, of the candidates screened, inhibition appeared to be the result of non-specific interactions. Thus, the findings of this study are inconclusive.

[8] Adenylosuccinate is also denoted succinyladenosine monophosphate or SAMP

RESULTS AND DISCUSSION

To identify compounds that regulate ADSL activity, we performed a screen using the library of pharmacological active compounds (LOPAC), which contains 1280 different drugs. We monitored the degradation of adenylosuccinate to AMP spectroscopically. Through this screen, we identified several compounds that either activate or inhibit ADSL activity (Figure A1-1). We chose one subgroup of compounds and individually tested their effect on ADSL activity. For ease, compounds are named numerically and the structures are noted (Figure A1-2). Compound 1 was an initial hit from the LOPAC screen and when tested, it inhibited ADSL activity significantly with an IC_{50} = 0.75 ± 2 mM (Figure A1-3A). Further testing revealed that compound 1 competitively inhibited ADSL activity (Figure A1-3B). Additionally, we tested the effect of compound 1 on cell proliferation, as ADSL inhibition leads to an increase in cellular SAICAR. We found that compound 1 increased cell proliferation in a concentration dependent manner (Figure A1-4).

We also tested compounds that were structurally related to compound 1. We found that all compounds tested inhibited ADSL activity, regardless of alteration made to the base molecule (Figure A1-5). Analine, compound 1, compound 2, compound 3, and compound 4 inhibited ADSL with an IC_{50} of 1 mM, 0.75 mM, 2.5 mM, 1.25 mM, and 2.5 mM (Figure A1-5). These data suggest that the observed inhibition of ADSL, at least in this class of molecules, is likely non-specific.

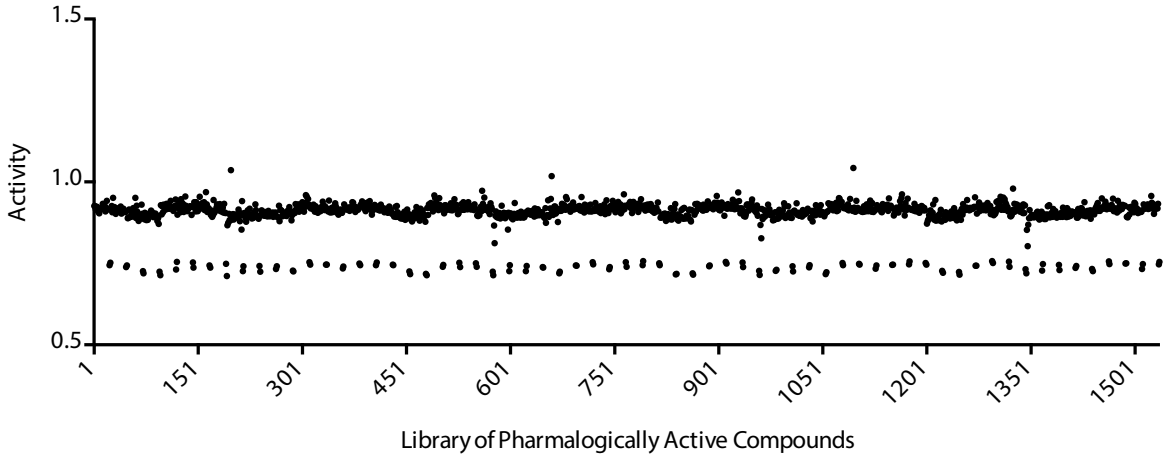

Figure A1-1. Screen of compounds that regulate ADSL activity. ADSL was mixed with each compound from the Library of Pharmalogically Active Compounds (LOPAC). Activity was determined by monitoring the change in the absorbance at 280 nm over one hour.

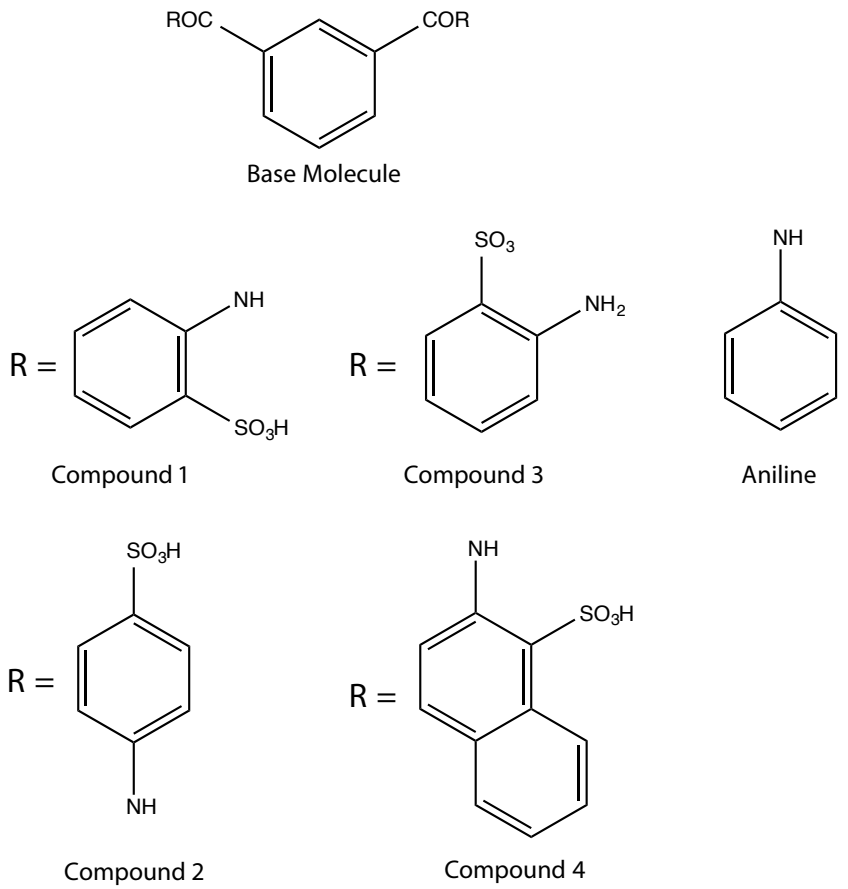

Figure A1-2. Compounds tested for regulation of ADSL activity based on hits from the LOPAC screen. The base molecule is located in the top of the figure. Each compound tested has a different "R" group, which is represented in the bottom four panels. Aniline was also tested as a potential regulator of ADSL activity.

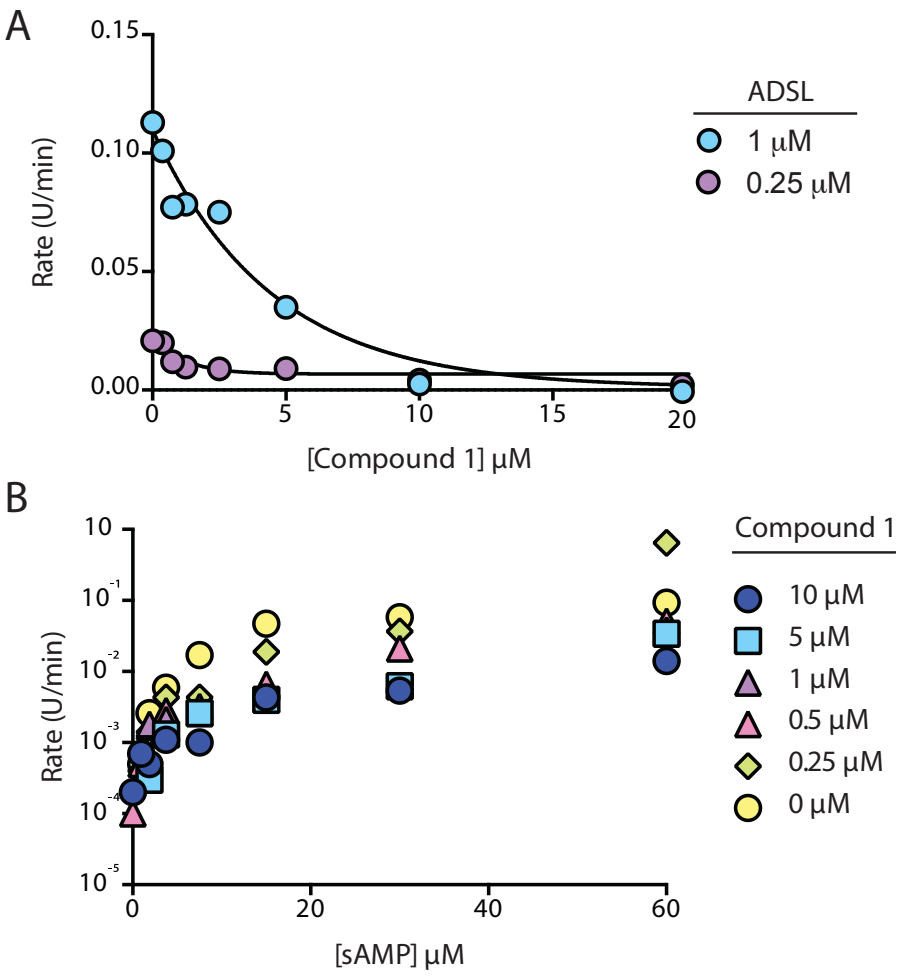

Figure A1-3. Compound 1 is a competitive inhibitor of ADSL activity. A) ADSL activity was monitored at two concentrations in the presence of compound 1. Compound 1 inhibits ADSL with an IC_{50} of ~1 mM. B) The substrate adenylosuccinate (sAMP) concentration was titrated and the activity of ADSL was monitored in the presence of 0, 0.25, 0.5, 1, 5, or 10 mM compound 1.

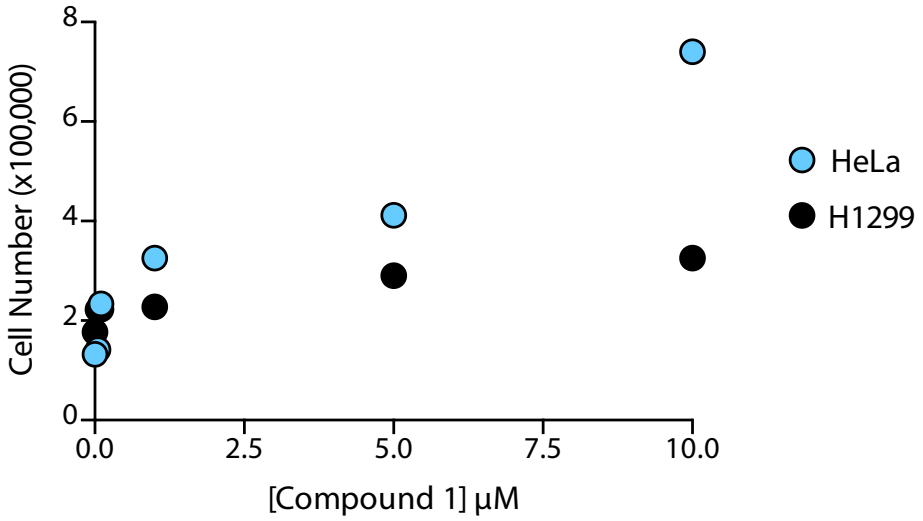

Figure A1-4. Compound 1 promotes cell proliferation of cancer cells.

When compound 1 was added to HeLa or H1299 cells, cell number increased in a concentration dependent matter.

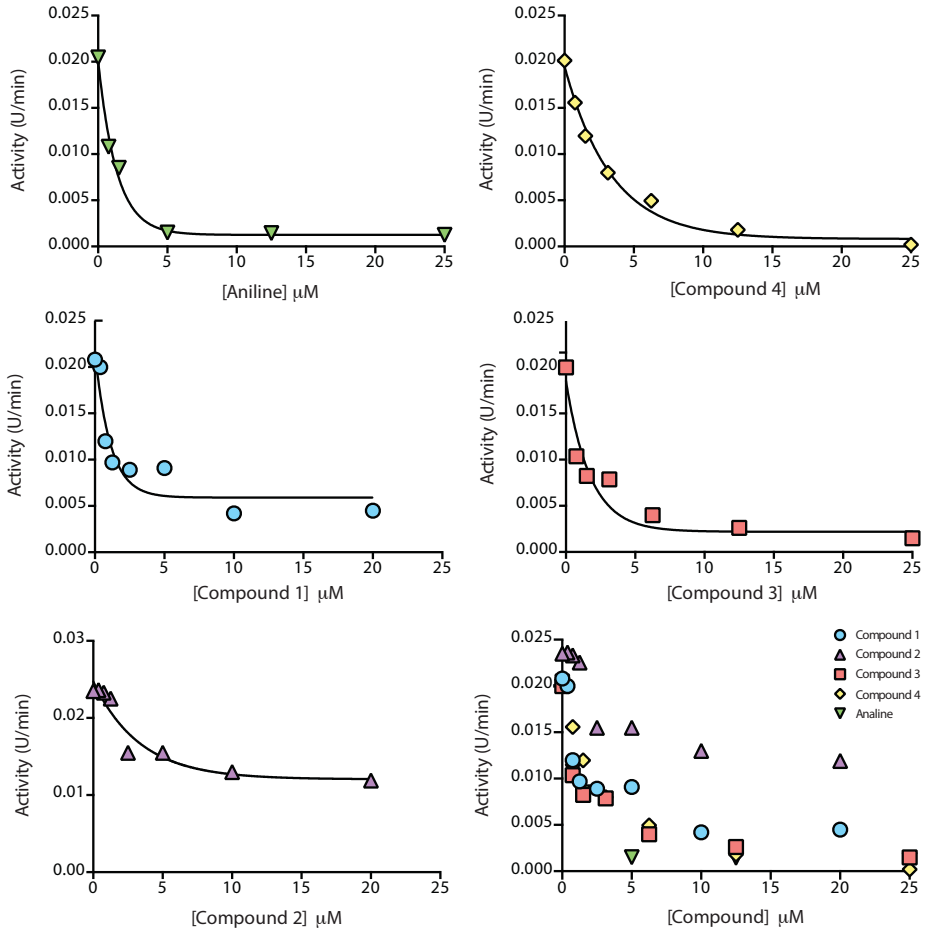

Figure A1-5. The effect of various compounds on ADSL activity. The structures of the compounds tested are listed in figure A1-2. Activity was measured by monitoring the absorbance at 280 nm due to the transition of adenylosuccinate to AMP. All compounds tested inhibit ADSL activity, with different potencies. Each compound tested is shown on individual plots and for comparative purposes, plotted together.

MATERIALS AND METHODS

Compounds

Young-Sam Lee generated compounds 1-4 synthetically. Anline was purchased from Sigma-Aldrich.

ADSL Purification

Cell harboring the ADSL plasmid (Addgene) were grown in 1L LB supplemented with kanamycin and chloroamphenicol until the OD_{600} reached between 1-2. Cells were induced with 0.5 mM IPTG for 18 hours at 25°C. After induction, cells were centrifuged at room temperature at 6000xg for 15 minutes. The cell pellet was resuspended in 20 mM HEPES pH 7.4, 500 mM NaCl, 10% glycerol, 5 mM imidazole, and 2 mM DTT, sonicated, and centrifuged at 15000 RPM at room temperature. ADSL was purified with an IMAC resin and a linear gradient of imidazole. Fractions containing ADSL protein were pooled and assessed with Coomassie for purity. ADSL was dialyzed into 20 mM HEPES pH 7.4, 150 mM NaCl, 10% glycerol, and 2 mM DTT. Of note, ADSL is temperature sensitive. All purification steps must be completed at room temperature.

ADSL Compound Screen

The Library of Pharmacologically Active Compounds (LOPAC)-1280 was acquired through the Johns Hopkins Medical Institute. Recombinant ADSL (1 uM) was mixed with 10 uM compound resuspended in DMSO and 20 uM

adenylosuccinate in buffer (20 mM HEPES pH 7.4, 150 mM NaCl, 1 mM DTT, 1 mM EDTA). The absorbance at 280 nm was monitored for one hour using the Tecan Infinity.

ADSL Activity Assays

Recombinant ADSL (0.5-1 uM) was mixed with 0-50 uM compound resuspended in water and 0-60 uM adenylosuccinate in buffer (20 mM HEPES pH 7.4, 150 mM NaCl, 1 mM DTT, 1 mM EDTA). The absorbance at 280 nm was monitored for one hour using the Tecan Infinity.

Cell Culture

HeLa and H1299 cells were maintained in Dulbecco's Modified Eagle Medium (DMEM) supplemented with FBS and pencillin/streptomycin at 5% CO_2, 37°C, and 80% humidity.

Cell Proliferation

HeLa or H1299 cells were plated in a six-well dish, 2.5X10E5 cells per well. Cells were incubated in Dulbecco's Modified Eagle Medium (DMEM) supplemented with dialyzed FBS and pencillin/streptomycin for 24 hours. Compound 1 (resuspended in DMSO) was added to each well and incubated for 24 hours. Cells were trypsinized and counted using a Moxi Z counter.

REFERENCES

Batova A, Diccianni MB, Omura-Minamisawa M, Yu J, Carrera C, Bridgeman L, Kung F, Pullen J, Amylon, M, and Yu, A. (1999) *Cancer Res 59*, 1492-7.

Casey, P. J., and Lowenstein, J. M. (1987) *Biochem Pharmacol 36*, 705-9.

Keller K, Tan I, and Lee YS. (2012) SAICAR stimulates pyruvate kinase isoform M2 and promotes cancer cell survival in glucose-limited conditions. *Science 338*, 1069-1072

Keller K, Doctor Z, Dwyer Z, and Lee YS. (2014) SAICAR Induces Protein Kinase Activity of PKM2 that is Necessary for Sustained Proliferative Signaling of Cancer Cells. *Mol. Cell* 53, 700-709

Lee P, Colman RF (2007). "Expression, purification, and characterization of stable, recombinant human adenylosuccinate lyase". *Protein Expr. Purif.* **51** (2): 227–34.

Spiegel EK, Colman RF, Patterson D (2006). "Adenylosuccinate lyase deficiency". *Mol. Genet. Metab.* **89** (1–2): 19–31

Tyagi A, and Cooney DA. (1980) *Cancer Res 40*, 4390-7.

APPENDIX 2.

LOCALIZATION OF THE GLUCOSE TRANSPORTER GLUT1 IS AFFECTED BY SAICAR

*The findings of this appendix reflect the work of both Danielle Meyer (Johns Hopkins REU, 2012) and Kirstie Keller.

INTRODUCTION

Cancer cells undergo a metabolic reprogramming event called the Warburg effect (Hanahan et al 2011). The Warburg effect is characterized by an increase in glucose uptake and oxygen-independent lactate fermentation. Several proteins have been implicated as important in this metabolic reprogramming, including pyruvate kinase M2 (PKM2). Recently, we identified that the cellular metabolite SAICAR, a nucleotide biosynthesis intermediate, accumulates upon glucose deprivation in cancer cells (Keller et al. 2012). We also found that SAICAR activates PKM2, and may help cells to balance energy production when the anabolic demand is overwhelming (Keller et al. 2012). To test the effect of SAICAR on different cellular processes, cell lines were created that knocked down the PAICS, the SAICAR synthetase, or ADSL, the SAICAR cleavage enzyme. The resultant cells had artificially altered SAICAR levels: constitutively elevated *(adsl-kd)* or depleted (*paics-kd*), regardless of glucose conditions (Keller et al. 2012). We found that cancer cells with non-inducible SAICAR levels (*paics-kd*) have decreased glucose consumption in glucose-limited conditions. Our findings indicate that SAICAR may affect glucose uptake in cancer cells, either directly or indirectly.

Glucose transporter 1, or GLUT1, facilitates glucose transport across the plasma membrane of cells and is thought to be responsible for the basal rate of glucose uptake (Mueckler et al. 1985). GLUT1, also known as solute carrier family 2 member 1 (SLCA1), is a transmembrane protein; however it is constantly

recycled between the plasma membrane and vesicles within the cytoplasm, depending on the needs of the cell (Olson et al. 2008). In glucose-limited conditions, GLUT1 is recruited to the plasma membrane to optimize the uptake of glucose, by facilitating diffusion through the membrane at a rate over 50,000 times greater than uncatalyzed glucose diffusion (Nelson et al. 2008). Thus, GLUT1 is a highly relevant protein in maintaining homeostasis within the cell in rapidly changing environments.

Although GLUT1 is expressed in nearly every tissue of the human body, the expression is the most prevalent in the placenta, fetal tissues, and other tissues with high turnover rates, such as skin and lung (Gen Bank, Human Protein Atlas, Uhen et al. 2008). Additionally, GLUT1 is highly expressed in a number of cancer types and is currently classified as a potential cancer biomarker (Human Protein Atlas, Uhen et al. 2008). Furthermore, high expression of GLUT1 is associated with pancreatic carcinogenesis, poor prognosis of breast and oral squamous cell cancers, and hepatocellular carcinoma (Agmann et al. 2009, Eckert et. al 2008, Pizzi et al. 2009).

As cellular SAICAR appears required for increased glucose uptake in nutrient-limited conditions, we hypothesized that SAICAR may influence GLUT1 localization. Here, we report that the GLUT1 expression is increased in cells with high levels of SAICAR, while appearing diminished in cells with non-inducible SAICAR (paics-kd). GLUT1 localization appears altered in cells with non-inducible SAICAR, although in an unexpected manner. We found that GLUT1

primarily localizes to the nucleus in *paics-kd* cells. However, we also found that cells with a disrupted PKM2-SAICAR interaction exhibited exclusion of GLUT1 from the nucleus. Finally, we determined that PKM2 and Glut1 interact either directly or indirectly *in vivo*. These findings represent the first instance of an interaction between GLUT1 localization and PKM2, although the overall mechanism or importance of this interaction remains unclear.

RESULTS AND DISCUSSION

To establish the localization of Glut1 protein in HeLa cells and those with altered cellular SAICAR levels, we monitored Glut1 in cells treated with no glucose media over a short time course. Unexpectedly, we found that Glut1 primarily localized to the nucleus prior to glucose starvation. Despite the surprise, the result was very reproducible. After glucose starvation, Glut1 was found in the cytoplasm and noticeably in punctae within the cell (Figure A2-1). In cells with high levels of SAICAR, Glut1 protein appeared elevated in all conditions tested (Figure A2-2). Additionally, Glut1 was found throughout the cell, regardless of condition, although glucose starvation lead to more pronounced punctae (Figure A2-2). In contrast, cells with non-inducible cellular SAICAR showed decreased Glut1 expression (Figure A2-3). After starving cells of glucose over time, Glut1 expression rose and then fell, to nearly imperceptible levels (Figure A2-3). Glut1 also appeared localized primarily to the region of membrane making contact with a nearby cell. After glucose starvation, the protein appeared to enter the cell cytoplasm (Figure A2-3).

To further establish a role of SAICAR in Glut1 localization, we utilized a cell line in which the SAICAR synthetase PAICS was overexpressed (CMV-PAICS). Glut1 was evenly distributed throughout the cell (Figure A2-4A). After thirty minutes of glucose starvation, Glut1 retained localization throughout the cell and appeared to be present in large punctae, possibly endosomes. As PKM2 is activated by SAICAR and is important for the Warburg effect in cancer cells, we

wanted to test the possibility that PKM2 is involved in Glut1 localization. For this purpose, we utilized a cell line where the endogenous copy of PKM2 has been replaced by the SAICAR-insensitive mutant, PKM2 Q393K, in HeLa cells. Interestingly, we found that Glut1 was robustly excluded from the nucleus regardless of condition (Figure A2-4B). These data suggest that SAICAR influences Glut1 trafficking either directly or indirectly, and potentially through PKM2.

Due to the apparent change in expression found in the immunofluorescence experiments, we next confirmed these results using Western blots. Extracts of HeLa cells, adsl-kd, and paics-kd cells, before and after glucose starvation for thirty minutes, were tested for Glut1 protein level. In accordance with the immunofluorescence data, Glut1 protein was elevated in adsl-kd cells prior to glucose starvation, while it became elevated in all cell types after glucose withdrawal (Figure A2-5A). However, this was less pronounced in CMV-PAICS cells (Figure A2-5B). Finally, to determine if Glut1 and PKM2 interact, we performed a co-IP on cells exposed to high or no glucose. We found that PKM2 and Glut1 interact upon glucose starvation (Figure A2-5C).

This study presents a novel finding that SAICAR-PKM2 influences Glut1 localization. The interaction between SAICAR, PKM2, and Glut1 may provide insight into the mechanism by which cancer cells have altered glucose uptake and other metabolic abnormalities.

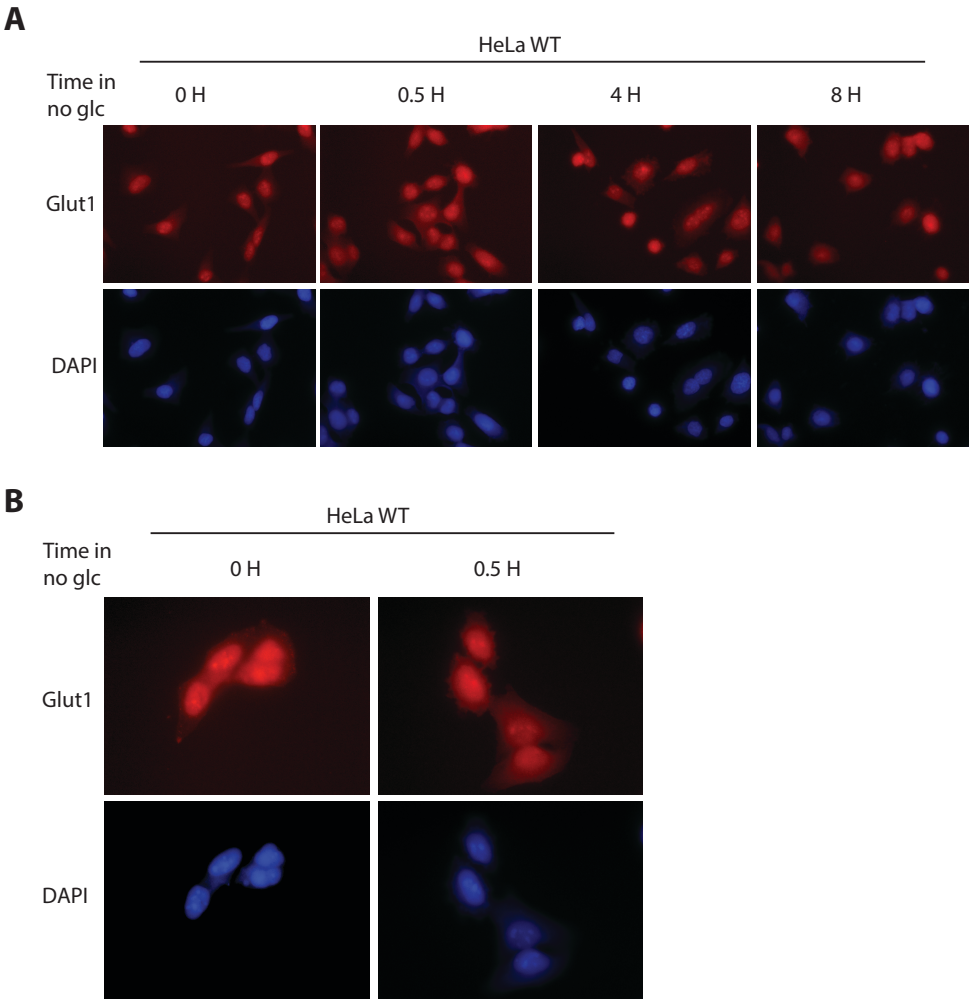

Figure A2-1. Glut1 localization changes upon glucose starvation in HeLa cells. A) HeLa cells were subjected to treatment in no glucose media for 0, 0.5, 4, or 8 hours and Glut1 localization was monitored by immunofluorescence. Prior to glucose starvation, Glut1 localized primarily to the nucleus. Upon starvation, Glut1 was more evenly spread throughout the cell and also became punctate. The images were taken at 40X. B) Glut1 localization was monitored in HeLa cells after 0 and 0.5 hours of glucose starvation, at 63X.

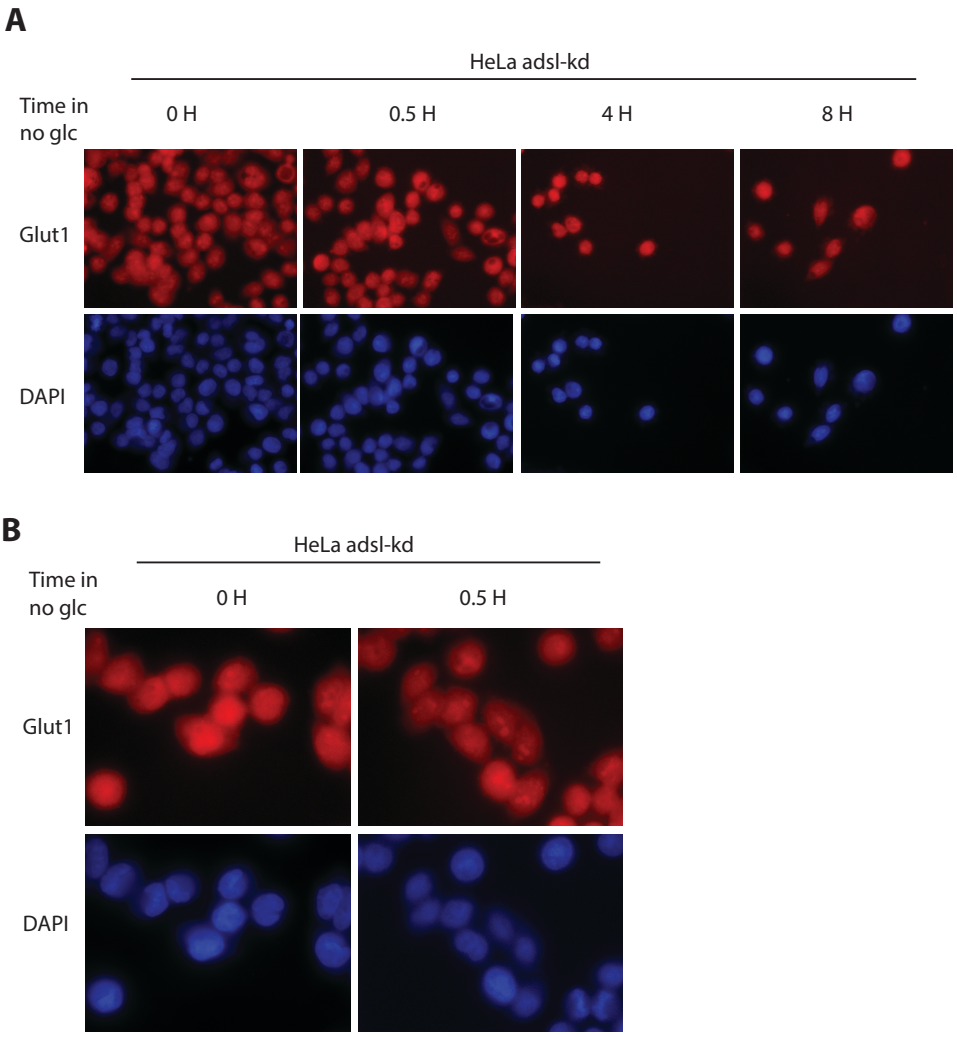

Figure A2-2. Glut1 localization is altered in SAICAR-accumulating (adsl-kd) HeLa cells. A) Adsl-kd cells were starved of glucose for 0, 0.5, 4, or 8 hours and Glut1 localization was monitored by immunofluorescence. Regardless of glucose treatment, Glut1 localized throughout the cell, although large punctae were noticeable. The images were taken at 40X. B) Glut1 localization was monitored in adsl-kd cells after 0 and 0.5 hours of glucose starvation, at 63X.

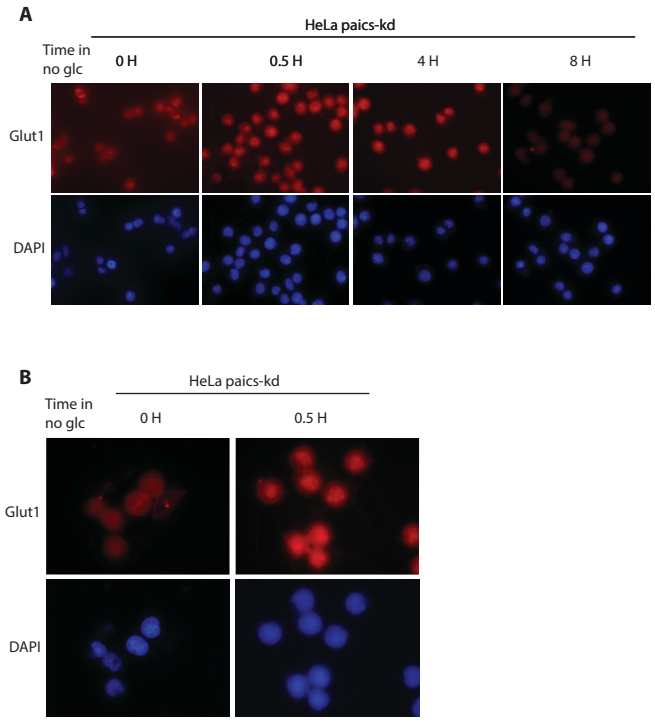

Figure A2-3. Glut1 localization and expression appears altered in HeLa cells with non-inducible SAICAR levels (paics-kd). A) Paics-kd cells were starved of glucose for 0, 0.5, 4, or 8 hours and Glut1 localization was monitored. Prior to glucose starvation, paics-kd cells appeared to have lower overall levels of Glut1 and Glut1 appeared localized to cell-cell contacts. After starvation, Glut1 levels increase and then decrease, while the protein itself became internalized. The images were taken at 40X. B) Glut1 localization was monitored in adsl-kd cells after 0 and 0.5 hours of glucose starvation, at 63X.

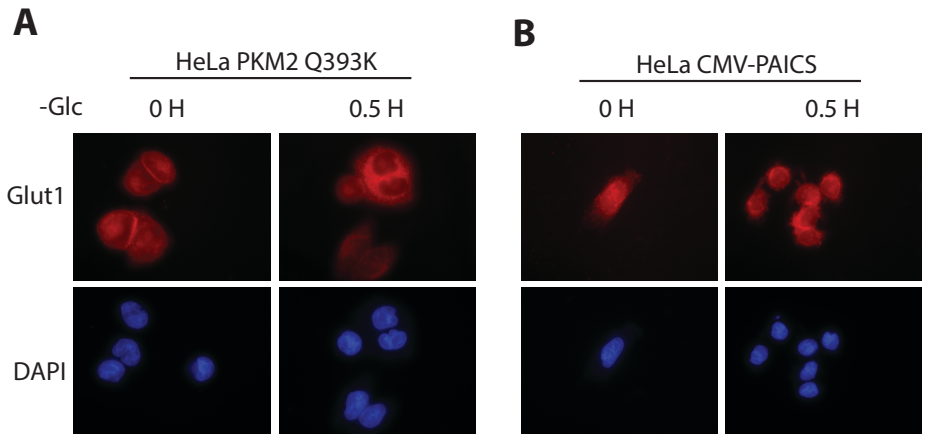

Figure A2-4. Glut1 localization and expression appears altered in HeLa cells with the SAICAR-PKM2 interaction disrupted or increased SAICAR. HeLa cells transfected with a SAICAR-insensitive PKM2 (Q393K) or an overexpression vector of PAICS, the SAICAR synthetase, were starved of glucose for 0 or 0.5 hours. A) PKM2 Q393K cells showed exclusion of Glut1 from the nucleus, especially after glucose starvation. B) CMV-PAICS cells show Glut1 protein spread throughout the cell, which becomes localized more towards the plasma membrane upon glucose starvation.

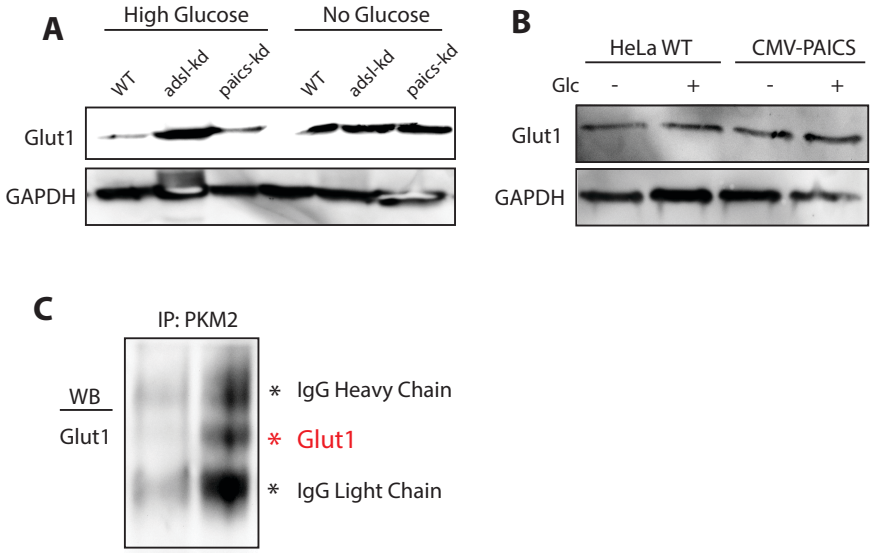

Figure A2-5. Glut1 expression is increased upon glucose starvation and interacts with PKM2. A) Glut1 levels were measured in HeLa, adsl-kd, and paics-kd cells that were incubated either in high glucose or no glucose media for thirty minutes. B) Glut1 levels were measured in HeLa or CMV-PAICS cells that were incubated either in high glucose or no glucose media for thirty minutes. C) HeLa cells were lysed after treatment in high glucose (lane 1) or no glucose (lane 2) media. PKM2 was immunoprecipitated and the blot was probed for Glut1 protein. Glut1 co-immunoprecipitated with PKM2 in no glucose conditions.

MATERIALS AND METHODS

Cell Culture

HeLa cells and their derivatives were maintained in Dulbecco's Modified Eagle Medium supplemented with 10% fetal bovine serum (FBS), penicillin, and streptomycin. Cells were incubated at 37°C, 5% CO_2, and 85% humidity. In glucose starvation assays, cells were incubated in DMEM with dialyzed FBS for at least 8 hours prior to the experiment and during the experiment.

Glut1 Localization via Immunofluorescence

HeLa cells were grown in 6-well dishes with coverslips. After treatment with high glucose or no glucose media for 0, 0.5, 4, or 8 hours, cells were washed with PBS, fixed with 4% paraformaldehyde, and permeabilized with 0.01% Triton X-100 in PBS. Cells were then incubated in 5% goat serum in PBS for 1 hour and stained with mouse anti-Glut1 antibody (1:100, Cell Signaling Technologies) for two hours. Coverslips were washed with PBS, incubated with DAPI, and then with a TRITC-conjugated secondary antibody (1:400, Sigma). Microscopic images were obtained using a Zeiss AxioVert 200 fluorescence microscope (Integrated Imaging Center, JHU, 40 or 63x optical zoom).

Western Blot

HeLa cells were lysed in ice-cold non-denaturing buffer (20 mM Tris HCl, pH 8, 137 mM NaCl, 1% NP-40, 2 mM EDTA) supplemented with 1 mM

phenylmethylsulfonyl fluoride and 5 mM sodium fluoride, and protein concentration using a Pierce 660 kit (Thermo Scientific). SDS-PAGE gels were run with 10 ug of protein. Membranes were probed with primary antibody (mouse anti-Glut1 or rabbit anti-GAPDH) overnight at 4^{o}C diluted in 5% BSA. Membranes were probed with horseradish peroxidase (HRP) conjugated goat anti-rabbit IgG or goat anti-mouse IgG secondary antibodies (Bio-Rad). HRP-conjugated secondary antibodies were then detected using a commercial chemiluminescence substrate kit (Pierce). Chemiluminescence images were acquired using a FluorChem M FM0455 imager.

Co-Immunoprecipitation

HeLa cells were lysed in ice-cold non-denaturing buffer (20 mM Tris HCl, pH 8, 137 mM NaCl, 1% NP-40, 2 mM EDTA) supplemented with 1 mM phenylmethylsulfonyl fluoride and 5 mM sodium fluoride. Cell lysates (500 ug) were mixed with rabbit anti-PKM2 (1:100, Sigma) overnight at 4^{o}C. Cell lysates were mixed with magnetic Protein A/G beads (Pierce) for 1 hour at room temperature. Beads were cleared, washed several times in buffer, and protein was eluted of beads using SDS loading dye at 95^{o}C. A western blot was then performed.

REFERENCES

Amann T1, Maegdefrau U, Hartmann A, Agaimy A, Marienhagen J, Weiss TS, Stoeltzing O, Warnecke C, Schölmerich J, Oefner PJ, Kreutz M, Bosserhoff AK, Hellerbrand C. (2009). GLUT1 expression is increased in hepatocellular carcinoma and promotes tumorigenesis. *Am J Pathol*. 2009 Apr;174(4):1544-52.

Hanahan D, Weinberg, RA. (2011). Hallmarks of cancer: the next generation. *Cell* 144(5), 646.

Eckert AW1, Lautner MH, Taubert H, Schubert J, Bilkenroth U. Expression of Glut-1 is a prognostic marker for oral squamous cell carcinoma patients. *Oncol Rep*. 2008 Dec;20(6):1381-5.

Keller K, Tan I, and Lee YS. (2012) SAICAR stimulates pyruvate kinase isoform M2 and promotes cancer cell survival in glucose-limited conditions. *Science 338*, 1069-1072

Mueckler M, Caruso C, Baldwin SA, Panico M, Blench I, Morris HR, Allard WJ, Lienhard GE, Lodish HF (September 1985). "Sequence and structure of a human glucose transporter". *Science* 229 (4717): 941–5..

Nelson DL, Cox MM (2008). Lehninger, Principles of Biochemistry. W. H. Freeman and Company. ISBN 978-0-7167-7108-1.

Olson AL, Pessin JE (1996). "Structure, function, and regulation of the mammalian facilitative glucose transporter gene family". *Annu. Rev. Nutr.* **16**: 235–56.

Pizzi S1, Porzionato A, Pasquali C, Guidolin D, Sperti C, Fogar P, Macchi V, De Caro R, Pedrazzoli S, Parenti A (2009). Glucose transporter-1 expression and prognostic significance in pancreatic carcinogenesis. *Histol Histopathol*. 24(2):175-85.

Uhlen M, Oksvold P, Fagerberg L, Lundberg E, Jonasson K, Forsberg M, Zwahlen M, Kampf C, Wester K, Hober S, Wernerus H, Björling L, Ponten F (2010). Towards a knowledge-based Human Protein Atlas. *Nat Biotechnol*. 28(12):1248-50.

APPENDIX 3.

PKM2 IS STIMULATED BY AN UNKNOWN COMPOUND IN YEAST EXTRACTS

INTRODUCTION

Allosteric regulation of enzymes is a major mechanism by which cells can respond to their environment. Pyruvate kinase M2 (PKM2) is a glycolytic enzyme responsible for catalyzing the reaction from phosphoenol pyruvate (PEP) and ADP to pyruvate and ATP. Regulators of PKM2 have been well characterized and are known to both activate and inhibit pyruvate kinase activity. PKM2 is activated by the upstream glycolytic intermediate fructose 1,6-bisphosphate (FBP), by lowering the K_m for its substrate PEP by stabilizing the tetrameric active form (Kung at al. 2012). Serine is also an activator of PKM2. Additionally, our lab identified SAICAR, a *de novo* purine biosynthesis intermediate, as an activator of PKM2 (Keller et al. 2012). Thyroid hormone (T3), alternatively, is an inhibitor of PKM2 and acts by disrupting the quaternary structure and promoting formation of the inactive monomer (Ashizama et al. 1991). Peptide aptamers also inhibit PKM2, leading to dimerization of the protein and decreased activity (Spoden at al. 2009). PKM2 has been shown to be important for cancer cell proliferation and survival. Thus, identifying compounds that bind and regulate PKM2 activity *in vivo* is ideal for drug development.

In this study, we report that a metabolite in yeast activates PKM2 pyruvate kinase activity by lowering its K_m for substrate and also increasing the catalytic efficiency. Through several biochemical tests, we were able to partially purify this compound and are awaiting confirmation of its identity.

RESULTS AND DISCUSSION

To identify PKM2 regulating compounds, *Saccharomyces cerevisiae* cells were grown in high and low glucose conditions and cellular metabolites were extracted. PKM2, Cdc19, and Pyk2 (yeast homologs of pyruvate kinase) activity was tested in the presence and absence of yeast cell extracts. We found that yeast cell extract activated PKM2, but not Cdc19 or Pyk2, in a glucose-dependent manner (Figure A3-1A). The effect of high glucose yeast extract on PKM2 activity was tested (Figure A3-1B). Also, the effect of the yeast extract on PEP binding to PKM2 was also tested (Figure A3-1C). A Lineweaver-Burke plot revealed that the binding affinity of PEP to PKM2 was lowered from 80 mM to 3.5 mM PEP and the k_{cat} was increased from 0.07 to 0.49 uM/sec (Figure A3-1D-E). These data suggest that the PKM2 stimulating factor (P2SF) is a previously undiscovered metabolite, as no known stimulator increases the k_{cat} of PKM2.

To further characterize P2SF, we performed a battery of biochemical assays. First, we separated P2SF using a size exclusion centrifugal filter. The metabolite that activated PKM2 was less than 3 kDa (data not shown). The P2SF was rotary evaporated and resuspended in water, and the activating effect of PKM2 was confirmed using resuspended lysate, indicating that the compound is non-volatile and water-soluble. Next, we examined the spectrum of the P2SF in the presence or absence of 0.02% formic acid. P2SF absorbs at 202 nm; formic acid shifts the absorbance maximum to 215 nm. Next, we ran the P2SF over a coarse anion exchange column and each fraction was added to PKM2 and

the effect on its activity was measured (Figure A3-2A). P2SF did not bind to the column, indicating that is not strongly ionic. Then, P2SF was run over a coarse cation exchange column and tested against PKM2 activity (Figure A3-2B). Again, P2SF did not bind the column strongly, indicating that the factor is weakly cationic (Figure A3-2B).

Next, we subjected the P2SF to a reverse phase column and measured the effect of each fraction on PKM2 activity (Figure A3-3A). Fractions that activated and were in a similar location in the elution plate were pooled. Pooled fractions were incubated with PKM2 and the activity was measured (Figure A3-3B). Pooled fraction 4 activated PKM2 robustly and was utilized in all subsequent steps of purification (Figure A3-3B). The pooled fraction was run over a reverse phase column for a second time, however this time using an acetonitrile and carbonic acid gradient, and the effect of PKM2 activity was monitored (Figure A3-4). The P2SF did not appear to be polar at low pH (Figure A3-4). The fractions that activated PKM2 were pooled.

The P2SF was then dried and resuspended in several rounds with either water or methanol and each fraction was tested for an effect on PKM2 activity (Figure A3-5A). P2SF appears soluble in methanol. Fraction 4 and 5 were subsequently tested on PKM2 activity and both appeared to stimulate PKM2 activity (Figure A3-5B). Fractions 4 and 5 were pooled together and used in subsequent steps. A subset of the P2SF was dried and resuspended in acetone several times and each fraction was tested on PKM2. P2SF did not appear to be

as soluble in acetone as it was in methanol or water (Figure A3-6A). Next, P2SF dissolved in water, acetone, treated with 0.02% formic acid or 0.5 mM TCEP (tris(2-carboxyethyl)phosphine) was incubated with PKM2 and each sample was tested for its effect on PKM2 activity (Figure A3-6B). The P2SF appears sensitive to oxidation, as addition of the reducing agent TCEP, increased the stimulation of PKM2 (Figure A3-6B).

Finally, P2SF was dried and resuspended in water and 0.1% formic acid and subjected to MS/MS using a Waters Q-TOF. The principle ion was 615.3 m/z. A peak at 637.3 m/z was also identified, and is likely due to the addition of one sodium ion (Na^+). The first round of MS/MS, at 18% collision energy, revealed the appearance of a peak at 597.3 m/z (M-18) and the principal ion was still present. Likely, this peak is due to the loss of H_2O. The second round of MS/MS showed the appearance of a peak at 579.2 (M-36; potentially loss of 2 H_2O), 561.2 (M-54; potentially loss of butadiene), and 430.2 (M-185) m/z. Though searches of databases, including the Scripps Metabolomics Database, the Human Metabolomics Database, and the Yeast Metabolomics Database, yielded many results, the atomic mass unit obtained through mass spectrometry data was not exact enough to obtain an identity with certainty.

The metabolite purified in this studied represents a new allosteric activator of PKM2, by increasing the protein's catalytic efficiency. As of now, no known compounds activate PKM2 in this manner; most increase the binding affinity for the substrate PEP. This result in itself makes the findings in this study unique.

From the various biochemical tests, we predict that the metabolite of interest is likely a non-aromatic, polar compound. We believe that this metabolite potentially helps make PKM2 suitable for high glycolytic flux, i.e. when PEP levels are high. The effect of this metabolite must be tested on the three other human isoforms to determine if it is isozyme specific. Additionally, more sensitive mass spectrometry much be used in order to obtain the identity of this compound, as the Q-TOF utilized in this study only has accuracy to the tenth decimal place. Once identified, the effect of this compound on cancer cell proliferation, PKM2 structure, and localization must be tested. As PKM2 is a viable target for the treatment of cancer, the metabolite discovered in this study may represent a different class of activators that could potentially be utilized in drug design of anti-cancer drugs.

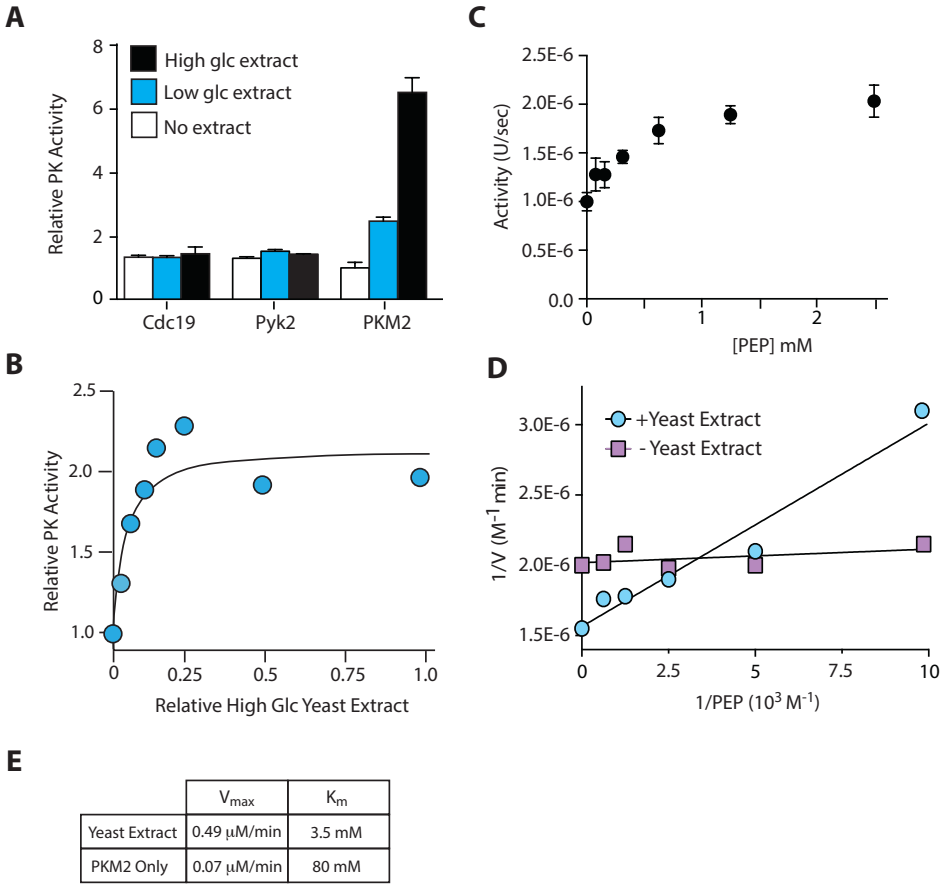

E

	V_{max}	K_m
Yeast Extract	0.49 μM/min	3.5 mM
PKM2 Only	0.07 μM/min	80 mM

Figure A3-1. A yeast metabolite present in cells incubated in high glucose media activates PKM2 activity. A) Yeast extracts grown in either high or no glucose media were tested on scCdc19, scPyk2, or huPKM2 to determine their effect on pyruvate kinase activity. High glucose yeast extracts activated PKM2. B) The effect of high glucose yeast extract on pyruvate kinase activity was measured. C) PKM2 activity was monitored while titrating PEP in the presence of high glucose yeast extract. D) Lineweaver-Burke plot of PKM2 activity in the presence and absence of high glucose yeast extract while titrating PEP. E) A table of the extracted kinetic parameters in the presence and absence of yeast extract.

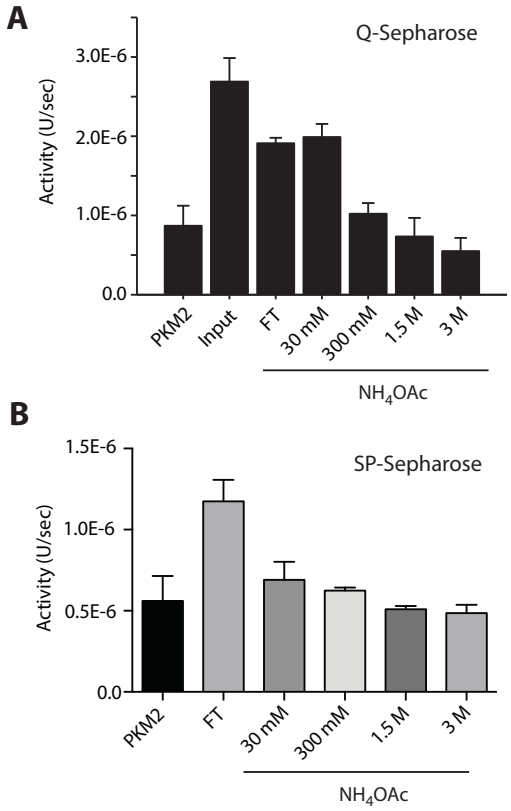

Figure A3-2. PKM2 stimulating factor is weakly anionic. A) P2SF was run over a batch anion exchange Q-Sepharose FF column using a stepwise gradient of NH_4OAc. The fractions were mixed with PKM2 and the activity was monitored. P2SF did not bind well to the column indicating that the compound is weakly anionic. B) P2SF was run over a batch cation exchange SP-Sepharose FF column using a stepwise gradient of NH_4OAc. The fractions were mixed with PKM2 and the activity was monitored. P2SF did not bind to the column indicating that the compound is not cationic.

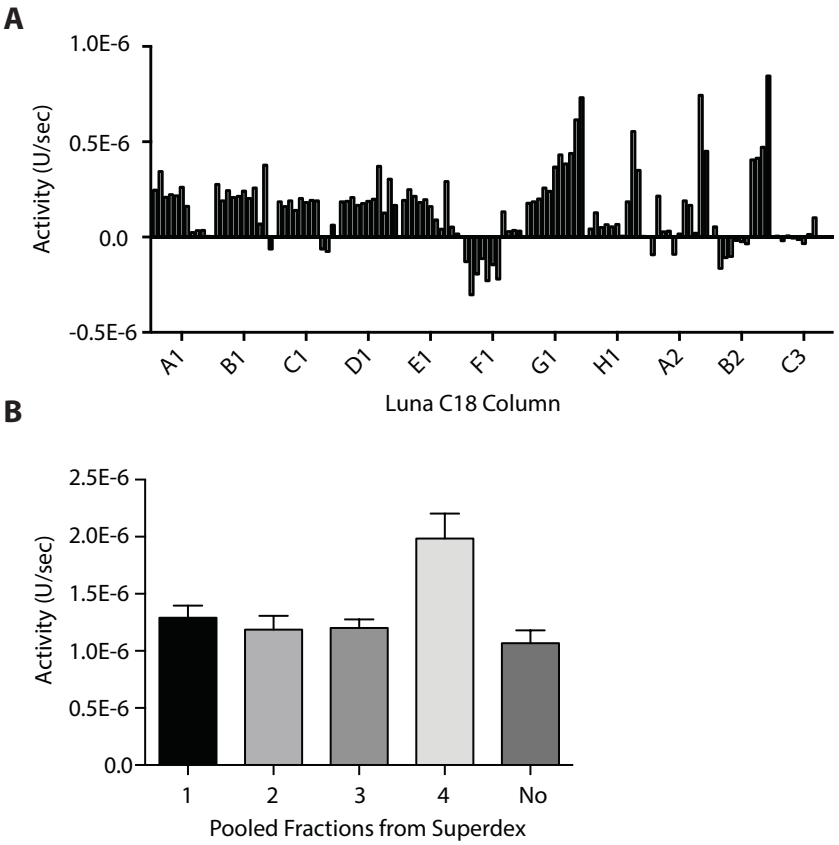

Figure A3-3. PKM2 stimulating factor is not polar at pH 7.0. A) P2SF was separated using a Luna C18 column with a MeOH and ammonium acetate gradient and each fraction was tested with PKM2 and the activity was measured. B) Fractions from the similar part of the elution plate and also activated PKM2 were pooled (i.e. G7-12), and the fraction's effect on PKM2 activity was measured.

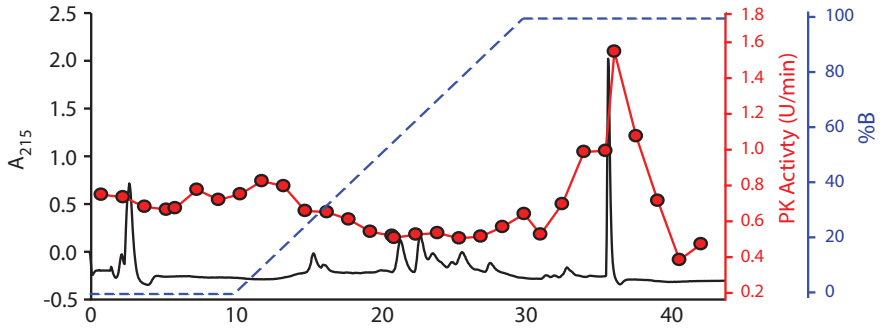

Figure A3-4. PKM2 stimulating factor is not polar at pH 3.0. P2SF was separated using a Luna C18 column with an acetonitrile and HCO_3H gradient (blue) and the effect of each fraction on PKM2 activity (red) was measured. The chromatogram is shown in black. The compound of interest absorbs at 215 nm.

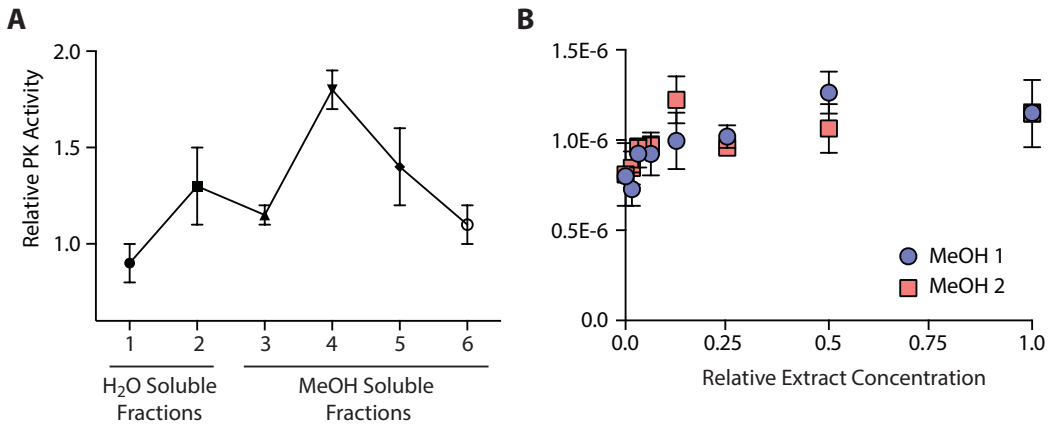

Figure A3-5. The PKM2 stimulating factor is methanol soluble. A) P2SF water-soluble fractions and methanol-soluble fractions were tested on PKM2 to determine their effect on activity. B) The methanol fractions identified as PKM2 activators (fraction 4 and 5) were titrated and PKM2 activity was measured.

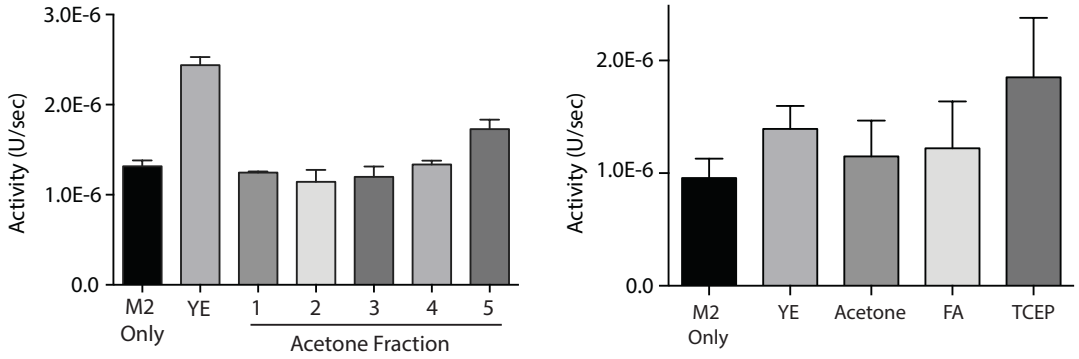

Figure A3-6. PKM2 stimulating factor is very soluble in acetone and is sensitive to oxidation. A) P2SF acetone-soluble fractions were tested on PKM2 activity, as well as PKM2 alone or mixed with untreated P2SF (YE). P2SF is not as soluble in acetone as it appeared to be in methanol. B) PKM2 was incubated alone, with P2SF (YE), P2SF mixed with acetone, 0.1% formic acid (FA), or 0.5 mM TCEP.

MATERIALS AND METHODS

PKM2 Purification and Activity Assays

PKM2 was purified as previously described (Keller et al. 2012, Keller et al. 2014). The activity of PKM2 was measured as previously described (Keller et al. 2012). In brief, 10 nM recombinant PKM2 was incubated with 1 mM ADP, 2 mM NADH, 150 uM PEP, and 5 U/mL lactate dehydrogenase in buffer (20 mM HEPES pH 7.4, 100 mM KCl, 6.6 mM $MgSO_4$). The change in absorbance at 340 nm was monitored for fifteen minutes.

Yeast Extract Preparation

Wild type *Saccharomyces cerevisiae* was grown overnight in synthetic dextrose media at 30°C while shaking. After overnight growth, a fresh culture was inoculated and grown to OD_{600} of between 0.6-0.8. For the initial screen, 5 mL cultures were grown in 20 g/L or 2 g/L glucose. For any subsequent steps, 1.5 L cultures were grown in 20 g/L glucose. Cells were centrifuged at 3000xg for one hour, lysed in Yeast Protein Extraction Reagent (YPER), supplemented with 1 mM DTT, 1 mM phenylmethylsulfonyl fluoride (PMSF), and 0.5 mM EDTA. Lysates were then centrifuged at 13000 RPM for 10 minutes and the supernatant was taken. The supernatant was then filtered through a centrifuge filter (MWCO 3 kDa) and rotary evaporated. The extract was resuspended in water, methanol, or acetone.

Metabolite Purification

For anion exchange, a Q-Sepharose FF 5 mL column and a stepwise gradient of ammonium acetate was utilized (30 mM, 300 mM, 1.5 M, and 3 M); for cation exchange, a SP-Sepharose FF 5 mL column and a stepwise gradient of ammonium acetate was also utilized (30 mM, 300 mM, 1.5 M, and 3 M). All reverse-phase FPLC purification were performed using a Phenomenex Luna C18 (2) column (4.6x150 mm, 3 um beads) at 4^{o}C at 0.5 mL/min; 1.5 mL fractions were collected. The first round of purification was at neutral pH using a linear gradient of water to methanol, in 10 mM ammonium acetate. The second round of purification was performed at a pH of 3 using a linear gradient of acetonitrile to carbonic acid.

Biochemical Characterization

The PKM2 stimulating factor spectrum was measured using a Beckman UV-Vis Spectrometer in the presence or absence of 0.02% formic acid (v/v). P2SF was treated with 50% acetone, 0.1% formic acid, or 0.5 mM TCEP for activity assays with PKM2.

REFERENCES

Ashizawa K, McPhie P, Lin KH, Cheng SY (1991). An in vitro novel mechanism of regulating the activity of pyruvate kinase M2 by thyroid hormone and fructose 1, 6-bisphosphate. Biochemistry. 23;30 (29):7105-11.

Keller K, Tan I, and Lee YS. (2012) SAICAR stimulates pyruvate kinase isoform M2 and promotes cancer cell survival in glucose-limited conditions. *Science 338*, 1069-1072

Kung C1, Hixon J, Choe S, Marks K, Gross S, Murphy E, DeLaBarre B, Cianchetta G, Sethumadhavan S, Wang X, Yan S, Gao Y, Fang C, Wei W, Jiang F, Wang S, Qian K, Saunders J, Driggers E, Woo HK, Kunii K, Murray S, Yang H, Yen K, Liu W, Cantley LC, Vander Heiden MG, Su SM, Jin S, Salituro FG, Dang L (2012). Small molecule activation of PKM2 in cancer cells induces serine auxotrophy. Chem Biol. 19(9):1187-98.

Spoden GA1, Rostek U, Lechner S, Mitterberger M, Mazurek S, Zwerschke W (2009). Pyruvate kinase isoenzyme M2 is a glycolytic sensor differentially regulating cell proliferation, cell size and apoptotic cell death dependent on glucose supply. *Exp Cell Res*. 2009 Oct 1;315(16):2765-74

APPENDIX 4.

EFFECT OF LIGAND BINDING AND POINT MUTATIONS ON THE QUATERNARY STRUCTURE OF PKM2

INTRODUCTION

Pyruvate kinases catalyze the final step of glycolysis, from phosphoenol pyruvate (PEP) to pyruvate. In humans, there are four isoforms of pyruvate kinase: PKM1, PKM2, PKR, and PKL. Biochemically, the isoforms have different activities and different regulatory elements. Structurally, all four isomers exist as a homotetramer, and this is thought to be the fully functional form of a pyruvate kinase. The homeotetramer is actually a dimer of homodimers, and pyruvate kinases can transition between all three structural forms: tetramer, dimer, and monomer. The dimer and monomer are generally regarded as the inactive form of pyruvate kinase, as the K_m for its substrate PEP is much higher than physiological conditions. Of the pyruvate kinase isoforms, PKM2 has been shown to exist both as a tetramer and dimer in cells. Interestingly, this isoform has also been shown to be important in cancer cell metabolism, proliferation, and survival in stress conditions.

Previous work has suggested that PKM2's role in cancer comes from the quaternary structure transition from a tetramer to a homodimer (Landt et al. 2010, Mazurek et al. 2002, and Zwerschke et al. 1999). As a tumor progresses to malignancy, PKM2 quaternary structure shifts from a tetramer towards a dimer (Landt et al. 2010, Mazurek et al. 2002, and Zwerschke et al. 1999). Additionally, PKM2 has been shown become a protein kinase in the dimeric state, and is capable of phosphorylating a number of cellular targets leading to expression of

target genes (Keller et al. 2104). We recently identified SAICAR, a *de novo* purine biosynthesis intermediate, as an activator of PKM2 protein kinase activity (Keller et al., 2014). The activation of PKM2 by SAICAR is distinct from the previous known PKM2 activator, fructose 1, 6-bisphosphate (FBP), as a combination of both activators inhibits protein kinase activity (Keller et al. 2014). This is likely due to the fact that FBP is known to shift the equilibrium of PKM2 quaternary structure towards the tetrameric form, which is diminished in late stage cancer cells (Landt et al. 2010, Mazurek et al. 2002, and Zwerschke et al. 1999). Furthermore, because FBP levels are decreased in conditions similar to a tumor microenvironment (i.e. hypoxia and glucose starvation), and because PKL, which is also activated by FBP, is unable to support tumor growth, it is unlikely that FBP is relevant to the role of PKM2 in tumor growth. Thus, it appears that SAICAR is likely the most relevant factor in the regulation of PKM2 in malignant cancer cells.

Here, we report that SAICAR activates the dimeric form of PKM2, although it does not shift the equilibrium of PKM2 quaternary structure significantly. Additionally, PKM2 mutants were shown to have altered quaternary structure. Specifically, the SAICAR hypersensitive mutant R399V exists primarily as a dimer, while the wild type protein and SAICAR insensitive mutant is mostly a tetramer. Our data indicate that SAICAR may bind and activate the dimer of PKM2, activating the pyruvate kinase and protein kinase activity of the protein.

RESULTS AND DISCUSSION

As quaternary structure appears important for PKM2 activity and cancer cell proliferation, we decided to probe the effect of the PKM2 activator SAICAR on the quaternary structure. To test this, we incubated recombinant PKM2 in the presence or absence of the known PKM2-binding ligands fructose 1,6-bisphosphate (FBP), thyroid hormone (T3), or SAICAR and separated PKM2 based on size by gel filtration chromatography. As expected, FBP shifted PKM2 structure towards the tetramer, while T3 shifted towards the dimer and monomer (Figure A4-1). The addition of SAICAR did not substantially alter the quaternary structure, although there was a slight shift towards the dimer (Figure A4-1). Next, we tested the activity of fractions corresponding to the tetramer, dimer, and monomer after incubation with no ligand, FBP, or SAICAR and separation through size exclusion chromatography. As expected, most pyruvate kinase activity was observed in tetramer fractions for both untreated and with added FBP (Figure A4-2). In contrast, most activity was observed in the dimer peaks upon the addition of SAICAR (Figure A4-2). These data indicated that SAICAR likely activates the dimer and possibly stabilizes the dimer.

To further validate this finding, we separated recombinant PKM2 into the tetramer, dimer, and monomer by size exclusion chromatography. Although there is the possibility that the protein can equilibrate, the assumption in this experiment is that the equilibration occurs slowly. The activity of each fraction was monitored in the presence SAICAR at two concentrations of the substrate

PEP (Figure A4-3). In both conditions, SAICAR activated the dimer specifically, while having no effect on the tetramer or monomer.

In an effort to establish a connection between SAICAR sensitivity and PKM2 structure, we examined the quaternary structure of various PKM2 mutants. Recombinant PKM2, PKM2 R399V, PKM2 Q393K, and PKM2 K433E were subjected to size exclusion chromatography and the overall quaternary structure was quantified (Figure A4-4). Wild type PKM2 and the SAICAR insensitive PKM2 mutant Q393K existed primarily as a tetramer (Figure A4-4). The hypersensitive mutant PKM2 R399V exists primarily as a dimer (Figure A4-4). Interestingly, the FBP-insensitive K433E mutant appears to be equally distributed between tetramer, dimer, and monomer (Figure A4-4). These data suggest that the hypersensitivity of PKM2 to SAICAR may be due to the increased dimerization of the protein.

Overall, our findings indicate that SAICAR binds and activates the dimeric form of PKM2. As PKM2 exists primarily as a dimer in cancer cells, our data suggest that SAICAR may be a relevant activator in malignant tumor cells. Thus, the quaternary structure of PKM2 could be a viable therapeutic target for anti-cancer drugs.

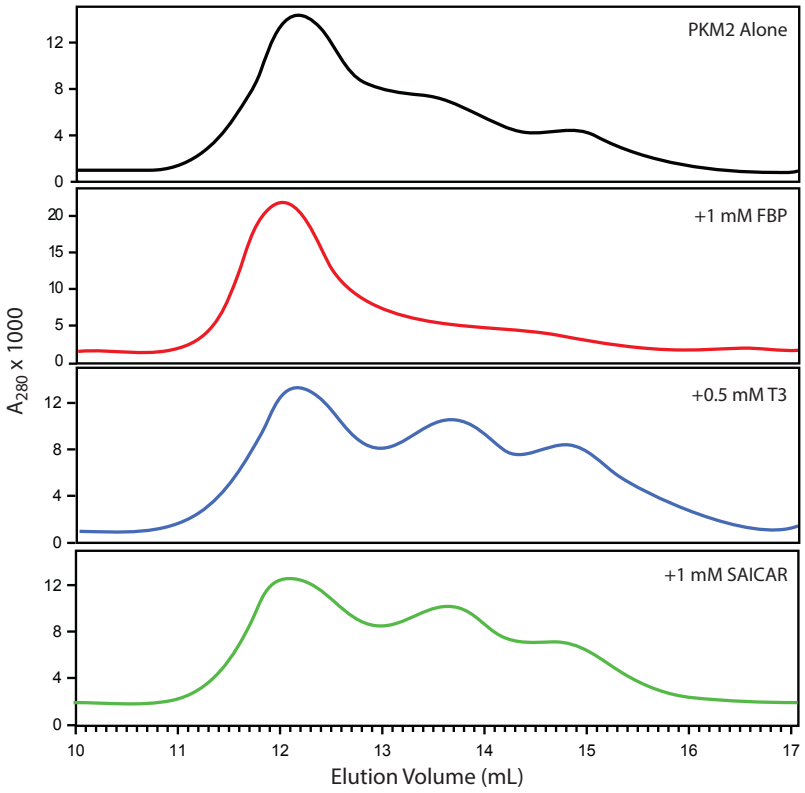

Figure A4-1. Ligands affect the quaternary structure of PKM2.

Recombinant PKM2 was subjected to gel filtration in the absence or presence of ligands (1 mM FBP, 0.5 mM T3, or 1 mM SAICAR) for 37°C for thirty minutes. The first peak corresponds to the tetramer, second to the dimer, and third to the monomer. As expected, FBP shifted PKM2 quaternary structure to the tetramer, while T3 shifted the structure towards a dimer and monomer. The addition of SAICAR mildly shifted the structure of PKM2 towards the dimer.

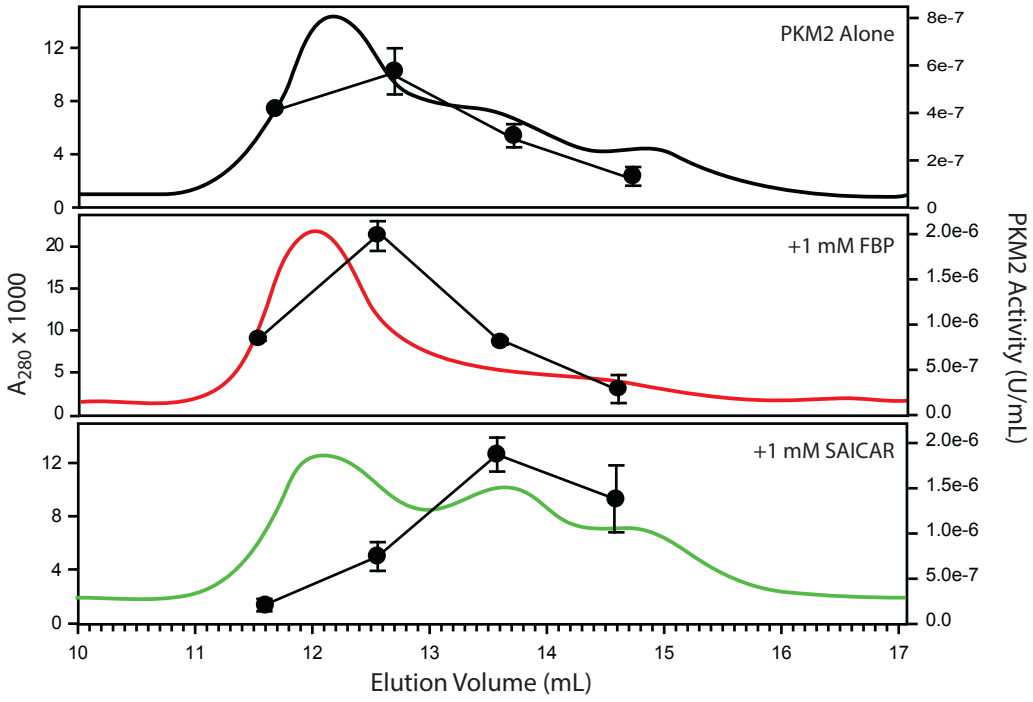

Figure A4-2. Ligands affect the activity of PKM2 differentially. Recombinant PKM2 was subjected to gel filtration in the absence or presence of 1 mM FBP or 1 mM SAICAR. The spectrum of each assay is depicted with a chromatogram trace. Fractions were collected and the activity of PKM2 was assessed and is depicted by the circles and straight-line connectors.

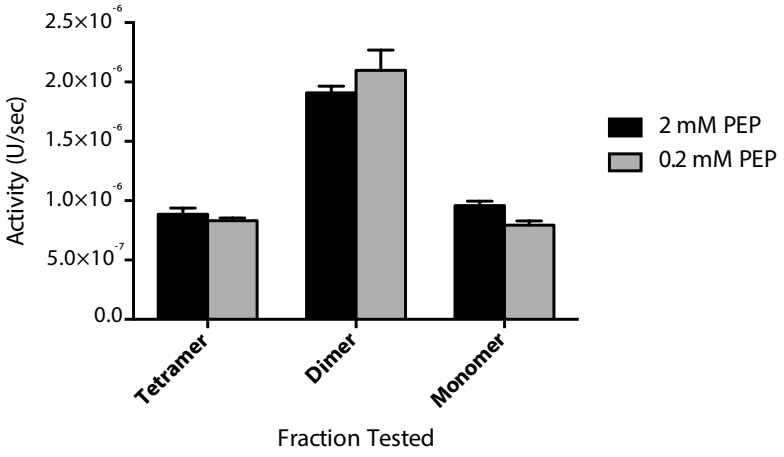

Figure A4-3. SAICAR activates the PKM2 dimer. Recombinant PKM2 (1 mM) was subjected to gel filtration and fractions were collected. Fractions were mixed with 1 mM SAICAR in the presence of 0.2 or 2 mM PEP, and the activity of PKM2 was measured. The activity was normalized to the area of the corresponding peak of the chromatogram of the size exclusion column. SAICAR activated the dimer peak specifically, while the tetramer and monomer were not.

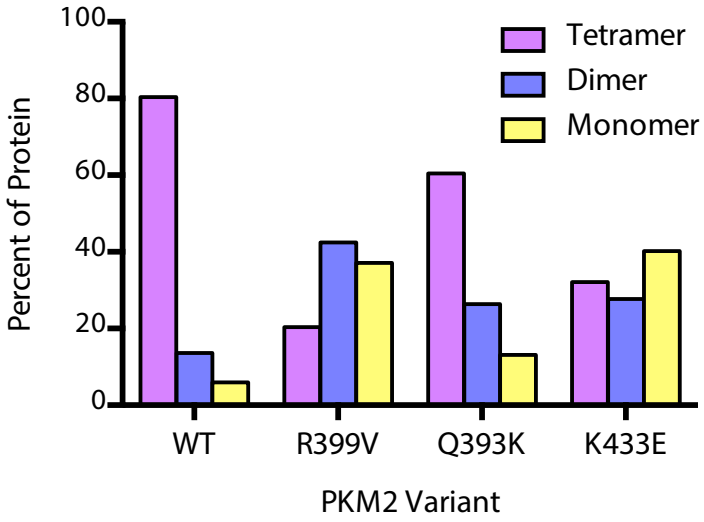

Figure A4-4. Point mutations of PKM2 lead to a change in quaternary structure. Recombinant PKM2, PKM2 R399V, PKM2 Q393K, and PKM2 K433E were subjected to gel filtration chromatography. The chromatogram peaks corresponding to the tetramer, dimer, and monomer were integrated and the data are presented as a percent of the total protein peak. The SAICAR hypersensitive R399V protein appears to exist primarily as a dimer, while wild type and the SAICAR-insensitive Q393K mutant exist primarily as a tetramer. FBP-insensitive K433E mutant appears to be equally distributed.

MATERIALS AND METHODS

PKM2 Purification and Activity Assays

The purification of PKM2 and its variants were performed as previously described (Keller et al. 2012). Subsequent activity assays used 10 uL of fraction from size exclusion chromatography were utilized in the activity assay, instead of 2-10 nM protein.

Size Exclusion Chromatography

Recombinant PKM2 (1 mL of 10 uM protein) was injected into a Superdex 10/300 column (flow rate: 5 mL/min) and 1 mL fractions were collected. Tetramer peak was identified by the PKM2 and FBP peak, which is known to shift the equilibrium to a tetramer.

REFERENCES

Keller K, Tan I, and Lee YS. (2012) SAICAR stimulates pyruvate kinase isoform M2 and promotes cancer cell survival in glucose-limited conditions. *Science 338*, 1069-1072

Keller K, Doctor Z, Dwyer Z, and Lee YS. (2014) SAICAR Induces Protein Kinase Activity of PKM2 that is Necessary for Sustained Proliferative Signaling of Cancer Cells. *Mol. Cell* 53, 700-709

Landt S, Jeschke S, Koeninger A, Thomas A, Heusner T, Korlach S, et al. Tumor-specific correlation of tumor M2 pyruvate kinase in pre-invasive, invasive and recurrent cervical cancer. Anticancer Res. 2010;30(2):375-81.

Mazurek S, Zwerschke W, Jansen-Durr P, Eigenbrodt E. Effects of the human papilloma virus HPV-16 E7 oncoprotein on glycolysis and glutaminolysis: role of pyruvate kinase type M2 and the glycolytic-enzyme complex. Biochem J. 2001;356(Pt 1):247-56. PMCID: 1221834.

Zwerschke W, Mazurek S, Massimi P, Banks L, Eigenbrodt E, Jansen-Durr P. Modulation of type M2 pyruvate kinase activity by the human papillomavirus type 16 E7 oncoprotein. Proc Natl Acad Sci U S A. 1999;96(4):1291-6. PMCID: 15456.

Kirstie E. Keller

Department of Biology
Johns Hopkins University
Baltimore, MD 21218
kkeller6@jhu.edu

EDUCATION

2010-2014 Johns Hopkins University, Baltimore, MD
Cellular, Molecular, Developmental Biology and Biophysics (Ph.D)

2006-2010 Gonzaga University, Spokane, WA
B.S. in Biology with Research Option *Cum Laude*

PUBLICATIONS

1. **Keller KE**, Doctor Z, Dwyer Z, and Lee YS. (2014) SAICAR induces protein kinase activity of PKM2 that is necessary for sustained proliferative signaling of cancer cells. Molecular Cell. 53: 700-709

2. **Keller KE**, Tan IS, Lee YS. (2012) SAICAR stimulates pyruvate kinase isoform M2 and promotes cancer cell survival in glucose-limited conditions. Science 338: 1069-1072 (Faculty of 1000)

3. Anders K, Kurdna J, **Keller K**, Kingston B, Miller E, Pauw D, Peck A, Shellooe C, and Strong I. (2009) A strategy for constructing aneuploid yeast strains by transient nondisjunction of a target chromosome. BMC Genetics 10:36

AWARDS AND HONORS

2013 Finn Wold/Young Investigator's Protein Society Meeting travel award
2012 Selected Speaker, Dept of Biology Retreat, Johns Hopkins University
2011 Best Poster award, Dept of Biology Retreat, Johns Hopkins University
2010 Cum Laude, Gonzaga University
2009-2010 McDonald Award, Robert and Claire McDonald Work Award
2008-2009 Howard Hughes Medical Institute, Gonzaga University Undergraduate Research Award
2006-2010 Trustee Scholarship, Gonzaga University

RESEARCH EXPERIENCE

2009-2010 Research Assistant, Gonzaga University
Advisor: Jillian Cadwell, PhD; cadwellj@gonzaga.edu
Computational modeling of broadcast spawning systems

2009 Summer Research Intern, Fred Hutchinson Cancer Research Center Advisor: Robert Eisenman, PhD; eisenman@fhcrc.org Interaction between Myc and microtubules

2008-2010 Research Assistant, Gonzaga University Advisor: Kirk Anders, PhD; anders@gonzaga.edu Aneuploidy and gene dosage effects in *Saccharomyces cerevisiae*

TEACHING EXPERIENCE

2012 Teaching Assistant: Microbiology, Johns Hopkins University

2012 Teaching Assistant: General Biology II lab, Johns Hopkins University

2011 Teaching Assistant: Biochemistry lab, Johns Hopkins University

2011-2014 Research Mentoring, Johns Hopkins University. Mentored over ten students while performing research in Young-Sam Lee's laboratory.

2009-2010 Teaching Assistant: Physics II lab, Gonzaga University

2008 Teaching Assistant: General Biology lab, Gonzaga University

CERTIFICATIONS

2013 Agilent Mass Profiler Professional Training Certification

2013 Agilent Pathway Architect Training Certification

UNIVERSITY SERVICES

2010-2014 Biology Representative of CMDB Program, Johns Hopkins. Position requires organizing events for graduate students and serving as a liaison between faculty and students

2010-2012 Mentoring to Inspire Diversity in Science member, Johns Hopkins. Science mentoring at a local high school

2010 Science in Action volunteer, Gonzaga University. Taught science lectures to 1st grade students, Spokane, WA

2009-2010 Tutor for Gonzaga University Chemistry Department: Intro to Chemistry, Bioanalytical Chemistry and Organic Chemistry I and II

2009-2010 Founded Science Mentoring Program at Gonzaga University Program involved forming mentoring partnerships between students